

**A Comparative Analysis of the Neurochemical Properties of Olfactory Ensheathing Cells  
and their Biocompatibility in Various Biomatrices**

**By**

**Khalil S. Rawji**

A thesis submitted to the Graduate Program in Neuroscience  
in conformity with the requirements for the  
Degree of Master of Science

Queen's University  
Kingston, Ontario, Canada

July, 2012

Copyright © Khalil S. Rawji, 2012

## **ABSTRACT**

Olfactory ensheathing cells (OECs) are the chief glial population of the mammalian olfactory nervous system and are thought to be responsible for the successful directional growth of new olfactory axons throughout the life of adult mammals. Due to this unique property, OECs have been targeted as a potential cellular transplantation therapy for spinal cord injury. In order to effectively isolate OECs for intraspinal transplantation, more knowledge must be gained on their phenotypic properties. We investigated the neurochemical features of OECs in a variety of mammalian species (including hamsters, rabbits, monkeys, mice, and pigs) using three biomarkers: glial fibrillary acidic protein (GFAP), S100 $\beta$ , and  $\alpha$ -smooth muscle actin ( $\alpha$ SMA). In addition, we tested the ability of a few biomatrices to sustain and promote OEC growth and survival *in vitro*. The rationale for using biomatrices is to provide a supportive environment for glial and axonal growth in the spinal lesion. Here, we found that mucosal and bulbar OECs from all five of the aforementioned mammalian species express S100 $\beta$ . Expression of GFAP, however, was not consistent across the five species. Both mucosal and bulbar OECs of monkeys express  $\alpha$ SMA; only bulbar OECs of hamsters and only mucosal OECs of rabbits express  $\alpha$ SMA as well. Though  $\alpha$ SMA immunostaining was not detected in the OECs of adult mice, in adult mutant mice lacking  $\alpha$ SMA expression, OECs displayed perturbed ultrastructural morphology. None of the biomatrices used (methacrylated glycol chitosan, arginine-glycine-aspartic acid – grafted methacrylated glycol chitosan, and agarose) were able to promote OEC proliferation. Isolated strips of rodent olfactory lamina propria (the deep connective tissue layer in the olfactory mucosa containing primary sensory axons and OECs) showed sustained growth when cultured for 10 days.

In sum, these findings highlight the following points: the efficacy of S100 $\beta$  and  $\alpha$ SMA as biomarkers for mammalian OECs *in vivo*; the potential for isolated strips of lamina propria to provide a natural, supportive environment for OECs during intraspinal transplantation; the failure of methacrylated glycol chitosan and its derivatives, as well as agarose, to promote OEC proliferation.

## **CO-AUTHORSHIP**

The results for Chapter 3 were jointly obtained by Khalil Rawji, Shannon X. Zhang, Ying-Yu Tsai, and Laura J. Smithson. The immunostaining and photography for Figure 3 and Figure 5 were performed by Shannon X. Zhang. The immunostaining and photography for Figure 6 were performed by Ying-Yu Tsai. The photography for Figure 9 and Figure 10 was performed by Laura J. Smithson. All other experiments and photography for the rest of the results were performed by Khalil S. Rawji. Data analyses and the drafting of the paper were performed by Khalil S. Rawji. The final editorial recommendations and comments were provided by Dr. Michael D. Kawaja and Laura J. Smithson.

## **ACKNOWLEDGEMENTS**

First and foremost, I would like to thank my supervisor, Dr. Michael D. Kawaja, for his continuous inspiration, guidance, and mentorship. His passion for teaching and research has instilled in me a love for research in neuroscience and I am very grateful for having him as a supervisor.

Second, a big thank you to my colleagues: Laura J. Smithson for her advice and feedback, Verna Norkum for all her assistance with the sectioning of frozen tissues as well as with laboratory techniques, Anne-Marie Crotty for her help with genotyping and cell culturing, Casey Petrie for his insightful comments, and Vera Xu for her help with editing.

Third, I would like to thank Dr. Brian Amsden for providing the materials for the hydrogels. I would also like to offer thanks to Dr. Dale Marecak for teaching me the hydrogel fabrication techniques.

I would also like to express a sincere thank you to my parents, Sherali Rawji and Nazma Rawji, for their continuous support, patience, and motivation over the last two years. I would also like to express my deepest gratitude to Sabrina Dewji, for her unwavering love and endless motivation, support, and inspiration. A big thanks to Nayela Dewji, for her spiritual guidance over the last year, giving me the extra focus in the laboratory. As well as a thank you to Nizar Dewji and Naznin Dewji for providing me with a home away from home on weekends.

Last and most importantly, I wholeheartedly acknowledge my brother, Rahim Rawji. For without him, I would not have chosen to pursue research in regenerative neurobiology. For this, I dedicate this thesis to him.

## TABLE OF CONTENTS

Abstract.....	ii
Co-Authorship.....	iv
Acknowledgements.....	v
Table of Contents.....	vi
List of Figures.....	ix
List of Abbreviations.....	xii
<b>Chapter 1</b> General Introduction and Literature Review.....	1
Spinal Cord Injury and Cellular Transplantation.....	1
Anatomy of the Olfactory Nervous System.....	2
Olfactory Mucosa.....	3
Olfactory Bulb.....	4
Neurochemistry.....	5
Secreted Neurotrophins.....	5
Effect of Growth Factors on OECs.....	6
Secreted Neuregulins.....	7
Membrane Surface Antigens.....	7
Phenotypic Similarities between OECs and Schwann Cells.....	12
Various Biomatrices Used With Cellular Therapies for Spinal Cord Injury.....	14
Hydrogels and CNS Regeneration.....	14
Photopolymerized Hydrogels.....	15
Main Objectives and Rationale.....	17
Figures.....	18

<b>Chapter 2 A Comparative Examination of Biomarkers for Olfactory Ensheathing Cells</b>	
in Hamsters, Rabbits, Pigs, Monkeys, and Mice.....	21
Abstract.....	21
Introduction.....	22
Methods and Materials.....	25
Tissue Preparation.....	25
Immunohistochemistry.....	29
Results.....	31
Figures.....	37
Discussion.....	58
Acknowledgements.....	64
<b>Chapter 3 A Cellular Scaffolding Study for Olfactory Ensheathing Cells Using</b>	
<b>Methacrylated Glycol Chitosan, Agarose, and Isolated Rodent Olfactory Lamina</b>	
<b>Propria.....</b>	<b>65</b>
Abstract.....	65
Introduction.....	66
Methods and Materials.....	71
Synthesis of Agarose.....	71
Dissection and Preparation of Rodent Lamina Propria.....	71
OEC Cultures.....	72
Immunofluorescence.....	73
Nissl Staining.....	75
Results.....	75

Figures.....	81
Discussion.....	92
Acknowledgements.....	96
<b>Chapter 4 Conclusion.....</b>	<b>97</b>
<b>References.....</b>	<b>100</b>

## LIST OF FIGURES

Figure 1: Schematic of the olfactory nervous system.....	19
Figure 2: Immunostaining for glial fibrillary acidic protein (GFAP), S100 $\beta$ , and $\alpha$ -smooth muscle actin ( $\alpha$ SMA) in the olfactory mucosa (OM) and olfactory bulb (OB) of adult hamsters.....	38
Figure 3: Immunostaining for glial fibrillary acidic protein (GFAP), S100 $\beta$ , and $\alpha$ -smooth muscle actin $\alpha$ SMA in the olfactory mucosa (OM) and olfactory bulb (OB) of adult rabbits.....	40
Figure 4: Immunostaining for glial fibrillary acidic protein (GFAP), S100 $\beta$ , and $\alpha$ -smooth muscle actin ( $\alpha$ SMA) in the olfactory mucosa (OM) and olfactory bulb (OB) of adult monkeys.....	42
Figure 5: Immunostaining for glial fibrillary acidic protein (GFAP), S100 $\beta$ , and $\alpha$ -smooth muscle actin ( $\alpha$ SMA) in the olfactory mucosa (OM) and olfactory bulb (OB) of fetal pigs.....	44
Figure 6: Immunostaining for glial fibrillary acidic protein (GFAP), S100 $\beta$ , and $\alpha$ -smooth muscle actin ( $\alpha$ SMA) in the olfactory mucosa (OM) and olfactory bulb (OB) of adult mice.....	46
Figure 7: $\beta$ -Galactosidase histochemical staining of the descending colon and urinary bladder from $\alpha$ SMA-LacZ transgenic mice.....	48
Figure 8: Immunostaining for $\alpha$ -smooth muscle actin ( $\alpha$ SMA) of the descending colon and urinary bladder from wild type and homozygous mice lacking $\alpha$ SMA expression.....	50

Figure 9: Electron photomicrographs of olfactory nerves fascicles from the lamina propria of wild type and homozygous mice lacking $\alpha$ -smooth muscle actin ( $\alpha$ SMA) expression.....	52
Figure 10: Electron photomicrographs of OEC nuclei (N) from the olfactory nerve fiber layer of the olfactory bulb from wild type and homozygous mice lacking $\alpha$ -smooth muscle actin ( $\alpha$ SMA) expression.....	54
Figure 11: Immunostaining for glial fibrillary acidic protein (GFAP) and S100 $\beta$ , as well as controls for specific staining, in the olfactory mucosa (OM) of adult rabbits.....	56
Figure 12: Immunostaining assay for survival of olfactory ensheathing cells (OECs) encapsulated in methacrylated glycol chitosan - with an arginine-glycine-aspartic acid group attached – (MGC-RGD) biomatrices mixed with cell media or phosphate buffer saline (PBS).....	82
Figure 13: Immunostaining of rat lamina propria sections cultured for 3 days for growth associated protein-43 (GAP-43), glial fibrillary acidic protein (GFAP), S100 $\beta$ , $\alpha$ -smooth muscle actin ( $\alpha$ SMA), Iba1, and calponin.....	84
Figure 14: Immunostaining of rat lamina propria sections cultured for 4 days for growth associated protein-43 (GAP-43), glial fibrillary acidic protein (GFAP), S100 $\beta$ , $\alpha$ -smooth muscle actin ( $\alpha$ SMA), Iba1, and calponin.....	86
Figure 15: Immunostaining of rat lamina propria sections cultured for 5 days for growth associated protein-43 (GAP-43), glial fibrillary acidic protein (GFAP), S100 $\beta$ , $\alpha$ -smooth	

muscle actin ( $\alpha$ SMA), Iba1, and	
calponin.....	88
Figure 16: Immunostaining of rat lamina propria sections cultured for 8 ( <b>A, C, E</b> ) and 10	
( <b>B, E, F</b> ) days for glial fibrillary acidic protein (GFAP), S100 $\beta$ , $\alpha$ -smooth muscle actin	
( $\alpha$ SMA).....	90

## LIST OF ABBREVIATIONS

$\alpha$ SMA	$\alpha$ -Smooth muscle actin
BDNF	Brain-derived neurotrophic factor
cAMP	Cyclic adenosine monophosphate
CGRP	Calcitonin gene-related product
CNS	Central nervous system
CS	Methacrylated chondroitin sulfate
DAPI	4', 6-diamidino-2-phenylindole
ECM	Extracellular matrix
FGF1	Acidic fibroblast growth factor
FGF2	Basic fibroblast growth factor
FGFr1	Acidic fibroblast growth factor high affinity receptor
FITC	Fluorescein isothiocyanate
GAP-43	Growth associated protein-43
GDNF	Glial cell line-derived neurotrophic factor
GFAP	Glial fibrillary acidic protein
GGF2	Glial growth factor 2
IgG	Immunoglobulin G
L14	L14 lectin
MAGC	Methacrylate acrylamide glycol chitosan
MGC	Methacrylated glycol chitosan
N-CAM	Neural cell adhesion molecule
NDS	Normal donkey serum

NGF	Nerve growth factor
NGS	Normal goat serum
NPY	Neuropeptide tyrosine
OEC	Olfactory ensheathing cell
ONL	Olfactory nerve fiber layer
PDGF-B	Platelet-derived growth factor B chain
3PGDH	3-Phosphoglycerate dehydrogenase
PLL	Poly-L-lysine
PN-1	Protease nexin-1
PNS	Peripheral nervous system
p75NTR	p75 Neurotrophin receptor
RGD	Arginine-glycine-aspartic acid
Sema3A	Semaphorin 3A
TBS	Tris-buffered saline
TBX	Triton-X100
Trk B	High affinity receptor tyrosine kinase B

## **CHAPTER 1: GENERAL INTRODUCTION AND LITERATURE REVIEW**

### **SPINAL CORD INJURY AND CELLULAR TRANSPLANTATION**

Spinal cord injury is a debilitating event which is immensely costly for both the patient and society. Every year, around 400 000 people in the United States are affected (Hulsebosch, 2002). Victims are four times more likely to be male than female, and the most frequent causes of injury are vehicle accidents (50%), sports (25%), falls (10%), and violence (10%) (Hulsebosch, 2002). Spinal cord injuries usually result in the loss of motor and sensory conduction below the level of the injury. Autonomic functioning below the level of the lesion is also frequently lost. Cellular loss is a major outcome of trauma, leading to secondary injuries such as nerve demyelination and axon retraction. This secondary injury and Wallerian degeneration usually occurs in the weeks following the initial injury trauma. One of the challenges in promoting the repair and regeneration of axons in spinal cord injury is the presence of many intrinsic and extrinsic growth inhibitors at the site of injury (Pearse and Barakat, 2006). Currently, there are many approaches being used and studied in the therapy of spinal cord injury. A very promising approach is cellular transplantation.

Cellular transplantation has been shown to be somewhat successful in animal models (Reier, 2004; Bunge and Pearse, 2003; Blits et al., 2002). The method has been tested on both incomplete spinal cord injuries as well as complete spinal cord injuries with limited success (Pearse et al., 2004; Reier et al., 1988). There are four main objectives that are targeted by cellular transplantation: i.) providing physical support in the area of injury to help the growth of axons (Ramon-Cueto et al., 1998); ii.) stabilizing the area of injury to prevent secondary injury (Martin et al., 1996); iii.) replacing lost

cells (Cheng et al., 1996); iv.) remyelination of demyelinated axons (Sasaki et al., 2001). There are six prominent cellular strategies that have been tested in experimental models, and to some degree, in clinical settings. These strategies include stem cells and precursors, peripheral nerve tissue such as Schwann cells, olfactory ensheathing cells (OECs), activated macrophages, marrow stromal cells, and fetal central nervous system tissue. The research presented in this thesis discusses the neurochemical properties of OECs and examines their compatibility in various biomatrices for application in spinal cord injury.

## ANATOMY OF THE OLFACTORY NERVOUS SYSTEM

The primary olfactory nervous system is known for its capability to continuously regenerate primary olfactory neurons throughout adulthood (Graziadei and Graziadei, 1979a). Primary olfactory neurons have a turn-over rate of approximately 28 days (Graziadei and Graziadei, 1979b). Graziadei and Graziadei (1979b) observed that damage to the primary olfactory system increases the occurrence of olfactory neurogenesis. Olfactory neurogenesis occurs in the olfactory mucosa of the nasal cavity. Newly generated axons are guided by OECs and project from the lamina propria to the olfactory bulb (Figure 1). These glial cells are important in promoting the proper directional growth of the primary olfactory axons (Doucette, 1990). A single OEC extends long cytoplasmic processes to ensheath hundreds of olfactory axons (Boyd et al, 2003). These glial cells are found in both the peripheral and the central compartments of the first cranial nerve. The ability for OECs to promote axonal growth from the peripheral nervous system (PNS) to the central nervous system (CNS) makes it a very

popular potential therapeutic strategy for spinal cord injury. Injury to the spinal cord results in permanent neuronal loss, which leads to sensory and motor impairment. The potential of OECs to promote axonal regeneration in the spinal cord makes it important to understand their anatomical and neurochemical features. This section will review the anatomy of mammalian OECs in relation to their native olfactory environment, followed by a review of the various neurochemical features present in mammalian OECs, and then finally a review of tissue engineering applications of cellular therapies for spinal cord injury.

### ***Olfactory Mucosa***

The olfactory mucosa consists of the olfactory neuroepithelium and the lamina propria. The epithelium consists of primary olfactory neurons, basal cells, and supporting cells (Farbman, 1994). Between the lamina propria and the epithelium lies a basal lamina (Farbman, 1994). Mature primary olfactory neurons are found between the apical and basal sides of the neuroepithelium, and are bipolar neurons. Each primary olfactory neuron extends a dendritic process to the apical surface of the epithelium, where it expresses one receptor type to detect one type of odorant molecule. This apical surface is lined with cilia and mucous to assist in dissolving the odorant molecules. Separating the dendrites of the primary olfactory cells are sustentacular cells. In addition to the dendritic processes of the primary olfactory neurons, each neuron also projects an axon into the lamina propria of the olfactory mucosa. Once in the lamina propria, the primary olfactory axons continue to pass through the cribriform plate of the ethmoid bone. Once they have passed through the cribriform plate, they synapse with second-order neurons of

the olfactory bulb. In the lamina propria, the axons coalesce to form nerve fascicles. OECs extend cytoplasmic processes to compartmentalize and ensheath the olfactory axons into these separate fascicles, forming a 'tunnel'-like structure around the axons. Each of these OEC 'tunnels' contain hundreds of axons of various sizes (Franssen et al, 2007). In addition to compartmentalizing the axons into fascicles, OECs also extend cytoplasmic processes within these fascicles, separating each fascicle into smaller sections. Coating the surface of these olfactory fascicles is a basal lamina, consisting of collagen and perineurial fibroblasts (Li et al, 2005). In the lamina propria of rats and mice, the fascicles are surrounded by one to two loose layers of perineurial fibroblasts. In the lamina propria of cats and monkeys, the fascicles are surrounded by multiple layers of perineurial fibroblasts (Kawaja et al, 2009). The processes of these OECs are always observed ahead of the elongating axon terminals (Tennent and Chuah, 1996). Once the axons pass through the lamina propria, they enter the CNS to synapse in the olfactory bulb.

### ***Olfactory Bulb***

The olfactory bulb is part of the CNS and consists of six distinct cellular layers. From outermost to innermost, these layers are the olfactory nerve fiber layer (ONL), glomerular layer, external plexiform layer, mitral cell layer, internal plexiform layer, and the granule layer. Primary olfactory axons enter the olfactory bulb via the olfactory nerve fiber layer (ONL) (Franssen et al, 2007). The primary olfactory neurons synapse in the glomerular layer with secondary neurons, which then project to the olfactory cortex via the lateral olfactory stria of the olfactory tract (Farbman, 1994). Primary axons

expressing the same odorant receptor gene converge and target the same glomeruli in the olfactory bulb (Vincent et al, 2005). Unlike the lamina propria, the olfactory bulb contains clusters of OECs, with each cluster extending processes around groups of olfactory axons. This organization is fairly conserved between mice, rats, monkeys, and humans (Kawaja et al, 2009).

In the mammalian nervous system, the glia limitans marks the boundary between the PNS and the CNS. The formation of the glia limitans is normally carried out by astrocytes, but in the olfactory nervous system, OECs present in the ONL contribute to its formation as well (Doucette, 1991). The glia limitans is observed in the outer portion of the olfactory bulb.

## NEUROCHEMISTRY

### *Secreted Neurotrophins*

OECs have been reported to secrete many different neurotrophins. Chuah and colleagues (2000) showed, using reverse transcriptase-polymerase chain reaction experiments, that OECs isolated from neonatal rat olfactory bulbs synthesize nerve growth factor (NGF), brain-derived neurotrophic factor (BDNF), glial cell line-derived neurotrophic factor (GDNF), neurturin, as well as glial growth factor 2 (GGF2). NGF secretion has also been reported by Woodhall and colleagues (2001) in cultured OECs isolated from the olfactory bulbs of rats. This group also found that OECs secrete seven times more NGF than BDNF. Rat OECs have been found to synthesize acidic fibroblast growth factor (FGF1) and basic fibroblast growth factor (FGF2) (Chuah and Teague, 1999; Gall et al, 1994; Key et al, 1996). Chuah and Teague (1999) also found that rodent

OECs express the high affinity receptor for acidic fibroblast growth factor (FGFr1), possibly implying autocrine activity. Kott and colleagues (1994) observed rat OECs positively staining for the B-chain of platelet-derived growth factor (PDGF-B). Adding to these findings, Lipson and colleagues (2003) reported that in the adult olfactory bulb of rats, OECs express the RET receptor, a receptor tyrosine kinase involved in intracellular signal transduction. All findings considered, it is postulated that the neurotrophic properties of OECs may involve the secretion of neurotrophic molecules that aid in the guidance of newly-regenerating olfactory axons in the primary olfactory pathway.

### ***Effect of Growth Factors on OECs***

In addition to the observations of neurotrophins being secreted by OECs, various groups have observed the effect of different growth factors on OECs themselves. In 1999, Chuah and Teague showed that 10 ng/mL of bFGF *in vitro* increased the number of rodent OECs threefold over 18 hours. Pollock and colleagues (1999) showed that NDF $\beta$ 1, -2, and -3 (neuregulins) induce rat bulbar OECs to divide. The same group also showed that NDF $\beta$ 3 and NDF $\alpha$ 2 play a role in inhibiting OEC apoptosis. Chuah and colleagues (2000) showed that GGF2 (neuregulin) promotes OEC proliferation in rats. Another molecule found to enhance the proliferation of rodent OECs is forskolin (Yan et al, 2001). Altogether, growth factors influence the proliferation and survival of OECs and may play a role in regulating the equilibrium of OECs in the primary olfactory system.

### ***Secreted Neuregulins***

The neuregulins are a family of four structurally-related proteins that have diverse functions in the development of the nervous system, including Schwann cell and oligodendrocyte differentiation (Vartanian et al, 1999; Burden and Yarden, 1997). A small number of studies have found that OECs express a few neuregulins, yet their function is still unknown. Boruch and colleagues (2001) showed that rodent OECs express neuregulins *in vivo*. Perroteau and colleagues (1998) also reported that, in addition to being able to secrete neuregulins, murine OECs also express neuregulin receptors, specifically ErbB-3 and ErbB-4. These findings suggest that the secreted neuregulins may be acting in an autocrine manner. The expression of these various neuregulins and their receptors may play a role in the development of the OECs, in addition to impacting the development of the primary olfactory neurons.

### ***Membrane Surface Antigens***

OECs express a range of molecules on their membrane surfaces. Some of these antigens are used as biomarkers to identify OECs for isolation. As will become apparent in this section, Schwann cells and OECs express many of the same antigens, resulting in difficulties when attempting to isolate pure cultures of OECs. This section will describe some of the antigens found on the membrane surface of OECs.

A common antigen expressed by OECs is the p75 neurotrophin receptor (p75NTR). Turner and Perez-Polo (1992) demonstrated the expression of p75NTR on rat OECs in the olfactory nerve. Gong and colleagues (1994) showed p75NTR staining in both embryonic and adult rat OECs. In addition, this group also found that during the

migration of the OECs during embryonic development, they begin to express p75NTR on their surfaces. Doucette (1993), as well as Boyd and colleagues (2003), both proposed that p75NTR may be important in providing chemotactic guidance to the developing olfactory axons. It has been found that rodent OECs in the mucosa down-regulate their expression of p75NTR, whereas OECs in the glia limitans of the olfactory bulb maintain their levels of p75NTR expression (Gong et al, 1994; Vickland et al, 1991). Vincent and colleagues (2005) hypothesized that the expression of p75NTR is regulated by axonal contact based on the following finding: in co-culture with olfactory neurons, p75NTR-positive OECs isolated from rats ensheathed the neurites and subsequently lost their p75NTR in areas that were in direct contact with the neurites (Ramon-Cueto et al, 1993). To further support this hypothesis, Vickland and colleagues (1991) found that p75NTR was down-regulated on rodent OECs that were in contact with olfactory axons in the adult ONL, whereas OECs facing the pia mater were unaffected. Additionally, freshly dissociated cultures containing p75NTR-negative rat OECs, with axonal fragments adhering to their surfaces, started to become p75NTR-positive once the axonal fragments were phagocytosed (Wewetzer et al, 2005). This same group also found that OECs that did not have any adhering axonal fragments were p75NTR-positive from the outset. It is important to note that although p75NTR is widely present on OECs in the outer ONL, it has been reported to be absent in the inner ONL (Vincent et al, 2005).

Two other molecules found to be commonly expressed by OECs are glial fibrillary acidic protein (GFAP) and S100 $\beta$ . GFAP is an intermediate-sized cytoskeletal protein that is commonly used as a marker for astrocytes. Barber and Lindsay (1982) found that rat OECs in the inner olfactory nerve layer express GFAP. Additionally,

Doucette and Devon (1995) showed that GFAP expression on OECs isolated from the rodent olfactory system is regulated by intracellular levels of cyclic adenosine monophosphate (cAMP). On the other hand, S100 $\beta$  is a calcium-binding protein that is involved in the regulation of many different intracellular processes, including protein phosphorylation, proliferation, and differentiation. This protein is commonly expressed in Schwann cells and astrocytes (Donato, 1999). Takahashi and colleagues (1984) showed positive immunostaining for S100 $\beta$  in human OECs. Also, unlike p75NTR, rat OECs were found to express S100 $\beta$  throughout the ONL (Franssen et al, 2007). For both GFAP and S100 $\beta$ , there is a gradient in their expression between the inner and outer sublaminae of the ONL. During embryogenesis, both antigens are restricted to the outer nerve layer. However, at birth, S100 $\beta$  starts to appear in the inner ONL. GFAP does not begin to appear in the inner ONL until postnatal day 7 to 20 (Vincent et al, 2005). Vincent and colleagues (2005) stated that this delayed glial maturation in the inner ONL may be to allow prolonged neuroplasticity of major innervation to the olfactory bulb during development. In summary, there is a general consensus that OECs co-express p75NTR, GFAP, and S100 $\beta$  (Kawaja et al, 2009).

Another molecule commonly observed on the membrane surface of OECs is oligodendrocyte marker O4 (O4). This antigen is frequently used to identify oligodendrocyte progenitor cells (Sommer and Schachner, 1981). Barnett and colleagues (1993) demonstrated that rat OECs react to antibodies against O4. These investigators also found that O4 reactivity was present throughout the ONL and glomerular layer. Vincent and colleagues (2005) reported that O4 is prominent in OECs throughout development but decreases in the adult rat. These findings are controversial however

when considering the study conducted by Wewetzer and colleagues (2005). In this study, rodent OECs were found to be O4-immunopositive due to O4-positive axonal fragments adhering to the membrane surface. The investigators in this study propose that the OECs themselves do not actually express O4. In fact, in this same study, the authors reported that the O4-positive axonal fragments were phagocytosed by the OECs. This finding is supported by Chuah and colleagues (1995), who found phagosomes and cellular debris in the cytoplasm of murine OECs. Given these results, and the finding that OECs express genes that are commonly found in immune cells (such as Gro1, a neutrophil chemoattractant that is involved in the immune response and inflammation), Vincent and colleagues (2005) propose that OECs may also be contributors to the innate immune response in the olfactory system.

A few more antigens expressed on the surface of OECs are neuropeptide tyrosine (NPY), neural cell adhesion molecule (N-CAM), and L1. NPY is expressed in the Golgi apparatus of OECs, surrounding the nerves from the epithelium to the bulb in both embryonic and adult rats. It is expressed in the ONL at embryonic day 15, before the olfactory bulb differentiates into distinct laminae. In adult rats, NPY is present in the inner ONL, but not in the glomerular layer (Ubink et al, 1994; Ubink and Hokfelt, 2000). These investigators suggest that NPY may play an important role in neuronal differentiation, axonal growth, or axonal guidance in the olfactory system. Furthermore, Miragall and colleagues (1988) showed that adult mouse OECs stain positive for neural cell adhesion molecule (N-CAM) as well as the L1 cell adhesion molecule. N-CAM and L1 are thought to allow the OECs to guide the growing olfactory axons from the epithelium to the bulb by providing an adhesive surface (Doucette, 1993; Boyd et al,

2003). These molecules begin to appear on the surface of mouse OECs as they enter the mesenchyme in between the placode and the telencephalic vesicle (Miragall et al, 1989). In addition to expressing these cell adhesion molecules, rat OECs have also been reported to express extracellular matrix (ECM) molecules such as fibronectin, laminin, and collagen type IV (Doucette, 1996).

Adding to the list of antigens already mentioned, OECs also express proteins that are involved in axonal guidance. A few of these molecules are semaphorin 3A (Sema3A), L14 lectin (L14), P(0), 3-phosphoglycerate dehydrogenase (3PGDH), and protease nexin-1 (PN-1). Sema3A is a membrane-associated secreted protein that has been shown to have chemorepulsive properties for neuropilin-1, an antigen present on olfactory axons (Rohm et al, 2000; Schwarting et al, 2000). Schwarting and colleagues (2000) showed that Sema3A knock-out mice have aberrant axonal trajectories in the ONL. L14 is a divalent, lactosamine-binding lectin that has been shown to be expressed on rat OECs during fetal development (Zhou and Cummings, 1993; Mahanthappa et al, 1994; Boyd et al, 2003). Mahanthappa and colleagues (1994) showed that, in rats, L14 is important in adhering olfactory neurons to laminin as well as promoting intercellular adhesion *in vitro*. Based on these findings, it was suggested that L14 may be important for axonal adhesion to the extracellular matrix, as well as axon fasciculation *in vivo*. P(0) is a PNS-specific myelin protein that has a major structural role in Schwann cell myelin. Lee and colleagues (2001) found it expressed on rodent OECs from embryonic day 13 throughout adulthood. At present, the functional significance of this protein on OECs is unknown, but it is speculated that it is involved in facilitating interactions between growing nerve fibers and glial cells during embryogenesis (Boyd et al, 2003). 3PGDH is

an intermediate enzyme in the biosynthesis of L-serine. L-serine is involved in the synthesis of proteins, membrane lipids, and nucleotides. Yamasaki and colleagues (2001) demonstrated the expression of 3PGDH on murine OECs and astrocytes and speculated that this enzyme is involved in assisting membrane synthesis in developing olfactory neurons. PN-1 is a factor released by glial cells and has been shown to act as a chemotropic agent for neurites *in vitro* (Monard et al, 1973). Reinhard and colleagues (1988) demonstrated the expression of this protein by rodent OECs in the ONL. It is thought that the presence of this protein in the olfactory system may be correlated to the continuous regeneration of olfactory axons.

In summary, OECs express a variety of different antigens on their membrane surface, although the functions of most of these proteins remain unknown. Elucidating these functions will allow us to gain a better understanding of the regenerative-promoting properties of this fascinating glial population.

### ***Phenotypic Similarities between OECs and Schwann Cells***

One of the biggest challenges facing OEC research is that these glial cells express many of the same phenotypic markers as Schwann cells, including p75<sup>NTR</sup>, S100 $\beta$ , and GFAP. Attempts to isolate pure cultures of OECs based on these markers are prone to Schwann cell contamination, especially since Schwann cells are also found in sensory and sympathetic axons in the lamina propria of the olfactory mucosa (Rizek and Kawaja, 2006). This phenotypic similarity results in difficulties isolating pure cultures of OECs for intraspinal implantation as well as for *in vitro* studies. Due to this problem in isolating pure cultures of OECs, there is confusion as to whether or not OECs have the

ability to myelinate central axons after implantation into the injured spinal cords of adult rats (Franklin et al, 1996; Barnett et al, 2000; Smith et al, 2001). All of these studies have reported myelination of central axons after intraspinal implantation of rodent or human OEC cultures. It should be noted however that rat OECs have not been observed to myelinate olfactory axons in the olfactory system (Rizek and Kawaja, 2006).

Ultrastructurally, these ‘myelinating’ OECs appear almost identical to Schwann cells. Rizek and Kawaja (2006), as well as Jahed and colleagues (2007), suggest that the idea of OECs transforming into Schwann cell-like cells after intraspinal implantation should be seriously reconsidered, as isolated OEC cultures may be contaminated with Schwann cells. Rizek and Kawaja (2006) propose that the remyelination of central axons in the injured spinal cord after OEC implantation is due to the presence of either contaminating Schwann cells in the isolated OEC cultures or from the invasion of host Schwann cells into the site of injury. This confusion as to whether or not OECs have the ability to myelinate axons has led to the quest for phenotypic markers that are expressed solely on OECs, and not on Schwann cells. The first of such a marker was discovered by Boyd and colleagues (2006) in a proteomic analysis of embryonic rat bulbar OECs. These investigators found that OECs exclusively express the actin-binding protein calponin, which was not expressed by Schwann cells isolated from adult rat sciatic nerve. In 2007, Jahed and colleagues then found that embryonic rat bulbar OECs also strongly express  $\alpha$ -smooth muscle actin ( $\alpha$ SMA), as well as many other actin-binding proteins (caldesmon [light isoform], smooth muscle tropomyosin, and transgelin), all of which were not found in adult rat sciatic nerve Schwann cells. Boyd and colleagues (2004, 2006) used LacZ- and calponin-positive rodent OECs to show that these cells create tunnel structures

through which LacZ- and calponin-negative Schwann cells pass through. The advent of these new phenotypic biomarkers for OECs provides a way to distinguish this glial cell from the otherwise phenotypically similar Schwann cells, allowing us to better understand whether or not OECs possess the ability to remyelinate central axons.

## VARIOUS BIOMATRICES USED WITH CELLULAR THERAPIES FOR SPINAL CORD INJURY

### *Hydrogels and CNS Regeneration*

Hydrogels (natural or synthetic polymers in which water is the dispersion medium) are used in the injured spinal cord to provide a supportive framework for axonal regeneration as well as to provide a protective biomatrix for the proliferation of transplanted cells. It has been suggested that the lack of nerve regeneration in the CNS may be due to a lack of an ordered basal lamina (Vracko, 1974). After an injury to the PNS, some axons will normally regrow in an orderly pattern, following the tracts of old axons. This orderly growth is thought to be due to the consistent basal lamina found in the PNS. This basal lamina, which is surrounded by bands of collagen fibers, forms a tube which encases peripheral nerve fibers (axons and Schwann cells). This organized framework may be a reason for the neural regeneration seen in the PNS. In the CNS, however, nerves are not surrounded by distinct basal lamina tubes. Instead, these nerve fibers (axons and oligodendrocytes) are in immediate apposition to glial cells. This feature of the CNS is one reason why OECs are so remarkable. They are able to guide olfactory axons within the CNS where there is a disorderly basal lamina. In all parenchymal tissue, if a framework is lost, healing normally results in the formation of

scar tissue. In the CNS, this scar is represented by an infiltration of astrocytes (Vracko, 1974). Woerly (2000) commented that the cellular and molecular regeneration in spinal cord injury is actively inhibited due to a lack of support matrix at the lesion. They suggested that the incorporation of a synthetic support matrix at the site of the lesion would allow the wound-healing cells as well as any axonal outgrowth to be directed and organized. Woerly (2000) also noted that tissue extracellular matrix is made up of cross-linked macromolecules and are highly hydrated gel-like structures. Therefore, the implantation of synthetic hydrogels is thought to be an adequate replacement for the extracellular matrix, hopefully promoting tissue regeneration in the CNS.

### ***Photopolymerized Hydrogels***

A common method employed in the creation of hydrogels for cell encapsulation is photopolymerization (Nguyen and West, 2002). In this process, light is used to initiate a cross-linking reaction between reactive groups of different multifunctional monomers. A molecule that is very reactive to light is a photoinitiator and is usually included to initiate the cross-linking reaction (a free radical reaction). This process presents many advantages. One such advantage is the ability to encapsulate living cells. If living cells are injected into the reaction mixture prior to photoinitiation, they can be rapidly entrapped within the biogel upon photoinitiation. Another advantage of this process is in its ability to produce scaffolds of varying shapes and sizes. This capability is achieved by simply altering the geometry of the reaction vessel (Amsden et al., 2007; Davis et al., 2003).

One requirement for the successful implantation of a hydrogel is biocompatibility with the tissue of interest. Bryant and colleagues (2000) did a study in which several photoinitiators were observed to be biocompatible with cultured chondrocytes. Chondrocytes were encapsulated within hydrogels that were photocrosslinked with the photoinitiator Darocur 2959 and were shown to survive. One reason for this biocompatibility (in addition to its high water content) may be due to the observation that the photopolymerization reaction releases less heat than traditional redox initiation reactions seen in traditional hydrogels, preventing excessive necrosis at the site of implantation (Davis et al., 2003).

Another study concluded that there is a high degree of control over the final properties of photocrosslinkable hydrogels (Bryant and Anseth, 2002). These hydrogels demonstrate greater temporal and spatial control. Temporal control refers to the rate of polymerization and is easily controlled through the manipulation of four variables: i. Altering the choice as well as the concentration of photoinitiator; ii. Altering the concentration of reactive double bonds in the reactants; iii. Using different wavelengths of the light source (either UV or visible); iv. Altering the intensity of the light. This flexibility in adjusting the reaction rate would prove practical in a surgical setting. It also allows the hydrogel to be partially cured before implantation and completely cured after implantation, yielding more time for the material to be altered. Spatial control refers to the physical geometry of the hydrogel and as mentioned above, can be easily controlled by the geometry of the reaction vessel (Davis et al., 2003).

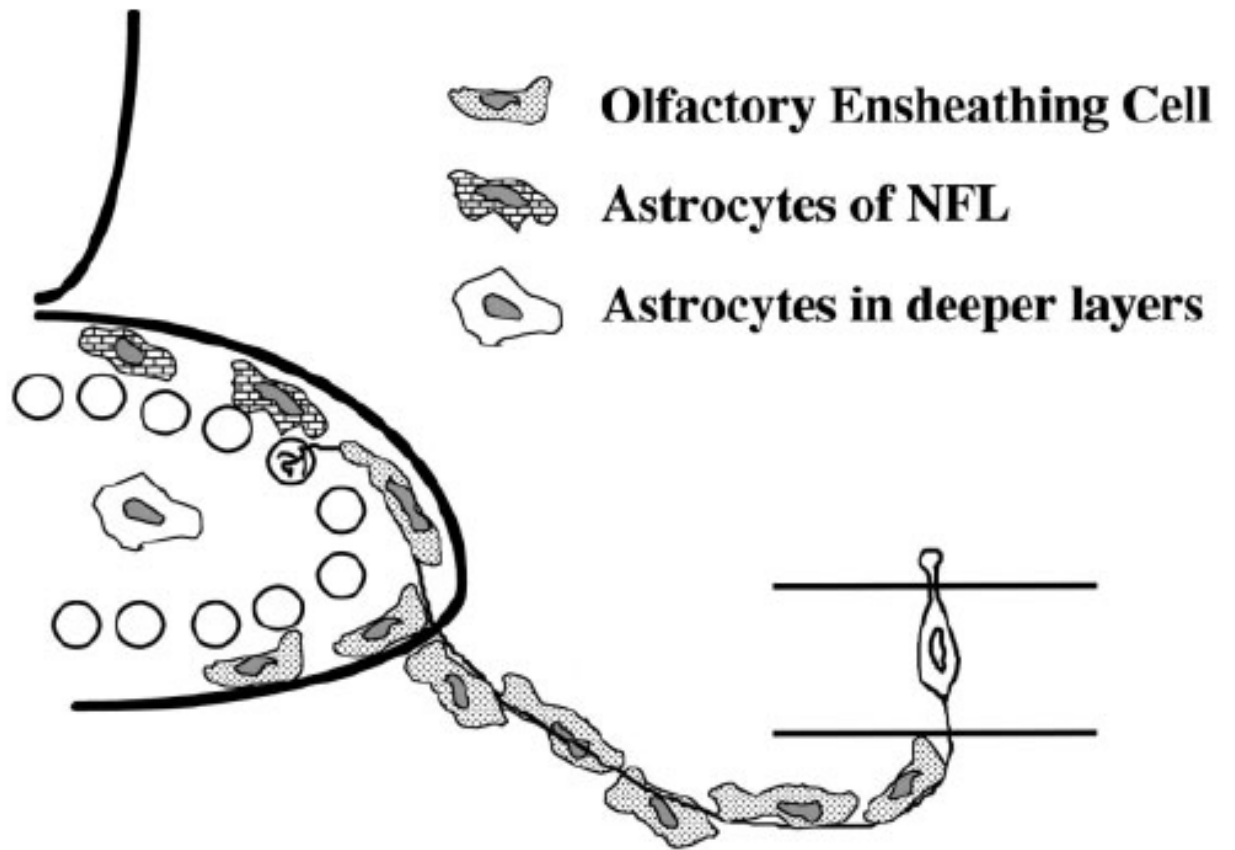
### ***Main Objectives and Rationale***

The first objective of the research presented in this thesis is to comparatively analyse the expression of GFAP, S100 $\beta$ , and  $\alpha$ SMA on OECs isolated from adult hamsters, rabbits, monkeys, and mice, as well as fetal pigs. The purpose of this examination is to identify a common phenotypic marker that can be used to reliably identify OECs when attempting to isolate them for *in vitro* studies, as well as for intraspinal implantation. In addition, it is important to have unique biomarkers for OECs in order to be able to identify and study their functional activity in the injured spinal cord.

The second objective of this thesis is to identify a biocompatible polymer that is capable of supporting OEC survival and proliferation *in vitro*. The rationale behind this idea is to find a biomatrix that can be used to implant OECs into the spinal cord, providing them with a protective, three-dimensional environment to promote axonal regeneration.

## **FIGURES**

**Figure 1:** Schematic of the olfactory nervous system. Olfactory ensheathing cells (OECs) form a ‘tunnel’-like structure around primary olfactory axons from the olfactory epithelium in the olfactory mucosa (lower right) to their synapses with secondary neurons within the glomeruli (open circles) of the olfactory bulb. Together with astrocytes, OECs form the glia limitans at the pial surface of the olfactory bulb. Figure taken Boyd and colleagues (2003).



**CHAPTER 2: A Comparative Examination of Biomarkers for Olfactory  
Ensheathing Cells in Hamsters, Rabbits, Pigs, Monkeys, and Mice**

**Khalil S. Rawji<sup>1</sup>, Shannon X. Zhang<sup>2</sup>, Ying-Yu Tsai<sup>2</sup>, Laura J. Smithson<sup>1</sup>, and  
Michael D. Kawaja<sup>1,2</sup>**

<sup>1</sup>Centre for Neuroscience Studies and <sup>2</sup>Department of Biomedical and Molecular  
Sciences  
Queen's University  
Kingston ON  
CANADA K7L 3N6

**ABSTRACT**

Olfactory ensheathing cells (OECs) are the chief glial population of the mammalian olfactory nervous system, residing in the olfactory mucosa and at the surface of the olfactory bulb. We investigated the neurochemical features of OECs in a variety of mammalian species (including hamsters, rabbits, monkeys, mice, and pigs) using three biomarkers, glial fibrillary acidic protein (GFAP), S100 $\beta$ , and  $\alpha$ -smooth muscle actin ( $\alpha$ SMA). Mucosal and bulbar OECs from all five of the aforementioned mammalian species express S100 $\beta$ . Mucosal OECs, but not bulbar OECs, also express GFAP in adult hamsters and monkeys; adult mice, by comparison, have only a sparse population of OECs expressing GFAP. Both mucosal and bulbar OECs of monkeys express  $\alpha$ SMA; only bulbar OECs of hamsters and only mucosal OECs of rabbits express  $\alpha$ SMA as well. Though  $\alpha$ SMA immunostaining was not detected in the OECs of adult mice, we postulated that this structural protein may be expressed at earlier developmental periods.

In adult mutant mice lacking  $\alpha$ SMA expression, mucosal OECs displayed fewer cytoplasmic processes extending among the hundreds of olfactory axons in the olfactory nerve fascicles, and many bulbar OECs had perturbed nuclear morphology. In sum, these findings (and our previous findings in rats, guinea pigs, and cats) highlight the efficacy of S100 $\beta$  and  $\alpha$ SMA as biomarkers for mammalian OECs *in vivo*. In addition, this study emphasizes the importance of empirically testing these and other biomarkers when assessing mucosal and bulbar OECs from various mammalian species.

## INTRODUCTION

The mammalian olfactory nervous system is known for its ability to continually generate new primary olfactory neurons throughout adulthood (Monti Graziadei and Graziadei, 1978). This neurogenesis occurs in the neuroepithelium, where the cell bodies of primary olfactory neurons and their basal stem cells are located. The olfactory mucosa is composed of this superficial avascular neuroepithelium and a deeper (and highly vascularized) layer referred to as the lamina propria. The primary olfactory neurons extend small unmyelinated axons (0.1-0.4  $\mu$ m in diameter) through the lamina propria toward the olfactory bulbs. Specialized glial cells known as olfactory ensheathing cells (OECs) protect the olfactory axons in the lamina propria by creating tunnel-like structures that surround dozens to hundreds of fibres simultaneously (Doucette, 1990). These OEC fascicles, with the ensheathed olfactory axons, continue through the cribriform plate and terminate at the surface of the olfactory bulbs, where they form the olfactory nerve fiber layer. Rather than clearly-defined fascicles, OECs in the olfactory

nerve fiber layer cluster together to surround crisscrossing bundles of olfactory axons; these axons extend into the olfactory bulbs where they synapse with the dendritic processes of the second-order olfactory mitral, periglomerular, and tufted neurons in the glomerular layer (Franssen et al, 2007; Valverde et al., 1992).

OECs can be isolated from both the peripheral lamina propria of the olfactory mucosa and the central olfactory nerve fiber layer of the olfactory bulbs (Au and Roskams, 2003; Ramon-Cueto et al, 1993; Rubio et al, 2008). In culture, mucosal and bulbar OECs share the expression of three antigenic markers: the p75 neurotrophin receptor (p75NTR), the calcium-binding protein S100 $\beta$ , and glial fibrillary acidic protein (GFAP) (Barber and Lindsay, 1982; Devon and Doucette, 1992; Gong et al, 1994). Though thought to be identical cell types, it is apparent that mucosal and bulbar OECs display some degree of variance in their cellular morphology and phenotypic characteristics *in vitro* (Chuah and Au, 1991; Doucette, 1993). Using a proteomic strategy to examine the phenotypes of rat bulbar OECs, our group has shown that both mucosal and bulbar OECs from rats express certain structural proteins, including calponin and  $\alpha$ -smooth muscle actin ( $\alpha$ SMA) *in vivo* and *in vitro* (Boyd et al., 2006; Jahed et al., 2007; Kawaja et al., 2009; Rizek and Kawaja, 2006). That OECs express  $\alpha$ SMA has been validated by revealing similar expression in OECs from other mammalian species, including guinea pigs and cats (Smithson and Kawaja, 2009).

While the expression of glial biomarkers such as S100 $\beta$  and GFAP by mammalian OECs *in situ* has been widely accepted, it seems quite unexpected that OECs from rats, guinea pigs, and cats would also express a structural protein like  $\alpha$ SMA. We

have speculated that  $\alpha$ SMA confers some degree of structural plasticity to OECs as they ensheath variable numbers of olfactory axons from the most distal olfactory mucosa to the olfactory nerve fiber layer around the olfactory bulb. Unlike non-myelinating Schwann cells that associate with a dozen or so small-diameter sensory or autonomic axons, OECs can be seen ensheathing a great range of olfactory axon numbers – from a few dozen to many hundreds. Moreover, while the numbers of unmyelinated peripheral axons associated with each Schwann cell remains relatively static throughout life, the numbers of unmyelinated olfactory axons associated with each OEC is constantly changing due to the degeneration and generation of new olfactory neurons. In this study, we sought to assess whether mucosal and/or bulbar OECs identified in a variety of mammalian species display a unifying phenotype characterized by the expression of S100 $\beta$ , GFAP, and  $\alpha$ SMA *in vivo*. Here we examined the neurochemical features of OECs in adult hamsters, adult rabbits, adult monkeys, and adult mice, as well as in fetal pigs. Both mucosal and bulbar OECs in all species express S100 $\beta$ ; GFAP, on the other hand, display variable levels of expression among these five mammalian species. Adult hamsters, rabbits, and monkeys (but not adult mice) have OECs that express  $\alpha$ SMA. By in large, these results regarding all three biomarkers support our previous findings in adult rats, guinea pigs, and cats (Jahed et al, 2007; Smithson and Kawaja, 2009). In this study we also show that OECs in adult mice lack positive immunostaining for  $\alpha$ SMA; this paucity of expression was confirmed in transgenic mice that express the reporter gene LacZ under control of the  $\alpha$ SMA promoter. This is an important distinction between mice and the other mammalian species we have examined to date. As further validation that murine OECs do not express  $\alpha$ SMA, we assessed the neurochemical and

structural features of mucosal and bulbar OECs in mice lacking functional  $\alpha$ SMA. Though the patterns of immunostaining for S100 $\beta$  and GFAP are unaffected, these adult mice that lack  $\alpha$ SMA do display several morphological features of defective and/or degenerating OECs. Our new observations provide further anatomical evidence that mammalian OECs express  $\alpha$ SMA and that the lack of this structural protein can have a negative impact on the physical association between these olfactory glial cells and the olfactory axons which they ensheath.

## **METHODS AND MATERIALS**

### ***Tissue preparation***

All experiments were performed according to the guidelines of the Canadian Council for Animal Care and under the approval of the Queen's University Animal Care Committee. Olfactory tissues were obtained from adult golden hamsters (*Mesocricetus auratus*; n=5; 150 g), adult New Zealand white rabbits (*Oryctolagus cuniculus*; n=2; 2 kg), adult monkeys (*Macaca fascicularis*; n=3; 4-6 kg), and adult C57Bl/6 mice (*Mus musculus*; n=20; 30 g). Hamsters and mice were anesthetized with sodium pentobarbital (12 mg/hamster and 8 mg/mouse, i.p.), rabbits were anesthetized with Ketamine (80 mg/rabbit, i.p.) and Xylazine (20 mg/rabbit, i.p.), and adult monkeys were anesthetised with a cocktail of Ketamine (15 mg/primate, i.m.), medetomidine (0.75 mg/primate, i.m.), and sodium pentobarbital (125 mg/primate, i.v.). Under deep anesthesia, the animals were perfused transcardially with 4% paraformaldehyde in 0.1M phosphate buffer (pH 7.4). The olfactory mucosa and bulbs were removed from these animals, post-fixed in

the same fixative for 48 hours, and then cryoprotected in phosphate-buffered 30% sucrose for 2-3 days. Adult North American pregnant gilts (*Sus scrofa*; n=3) were sacrificed at 50 to 60 days gestation; the uteri were removed and the fetal pigs (n=20) were decapitated. The heads were immersion-fixed in phosphate-buffered 4% paraformaldehyde (pH 7.4) for 1 week and then cryoprotected in phosphate-buffered 30% sucrose for 2-3 days. All tissues were embedded in Cryomatrix™ (Thermo Fisher Scientific, Ottawa, ON) and frozen in -20°C 2-methylbutane for sectioning with a cryostat. The olfactory tissues from all species were sectioned at 20 µm thickness; the tissues were directly mounted onto Superfrost/Plus slides (Thermo Fisher Scientific).

Two adult male  $\alpha$ SMA-LacZ mice (i.e., reporter mice expressing the bacterial gene LacZ under the control of the  $\alpha$ SMA promoter) were obtained from Dr. Gary Owens (University of Virginia). These males were bred with C57Bl/6 females, yielding progeny from postnatal day 1 to 3 months of age that were genotyped by polymerase chain reaction (KAPA Mouse Genotyping Kit; Boston, MA). Briefly, DNA isolated from tails (between the ages of postnatal days 1-14) and from ear punches (between the ages of postnatal day 16 and 3 months) were amplified with the following primers to detect the transgene LacZ (5': 5'-GTTGCAGTGCACGGCAGATACT TGCTGA; 3': 5'-GCCACTGGTGTGGGCCATAAT TCAATTCGC). Both transgenic and non-transgenic siblings (between the ages of postnatal day 16 and 3 months) were deeply anesthetised with sodium pentobarbital (8.2 mg/ mouse, i.p.) and sacrificed by transcardial perfusion with phosphate-buffered 0.5% glutaraldehyde (pH 7.4) plus 2mM MgCl<sub>2</sub>; mice between the ages of postnatal days 1 and 14 were sacrificed by decapitation, and the heads were immersion-fixed in this fixative for 3 days. The olfactory nervous system (mucosa and

bulbs), descending colon, and urinary bladder were removed from each mouse. These whole tissues were processed for histochemical localization of the reporter gene product,  $\beta$ -galactosidase, using the LacZ Staining Kit following the manufacturer's instructions (InvivoGen; San Diego, CA). After staining, these tissues were cryoprotected in phosphate-buffered 30% sucrose (pH 7.4) for 2 days. Tissues were embedded in Cryomatrix™ (Thermo Fisher Scientific) and frozen in -20°C 2-methylbutane for sectioning with a cryostat. The descending colons, urinary bladders, and olfactory tissues were sectioned at 20  $\mu$ m thickness; all sections were directly mounted onto Superfrost/Plus slides (Thermo Fisher Scientific). The histochemical reaction products were viewed and photographed under bright-field optics with a Zeiss microscope. Images were captured using a Zeiss AxioCam high resolution scanning digital camera with Axiovision software (version 4.2). After adjusting the images for brightness and contrast, these images were converted to .tif files and used to generate figures with Adobe Illustrator CS5.

Two adult  $\alpha$ SMA heterozygous mice (i.e., mutant mice with a Pol II promoter neomycin hybrid gene inserted into the  $\alpha$ SMA gene locus at the +1 cap site) were obtained from Dr. James Tomasek (University of Oklahoma), with permission from Dr. Robert Schwartz (University of Houston). The founder male and female mice were bred to yield wild type, heterozygous, and homozygous progeny. Briefly, DNA isolated from ear punches of the resulting F1 progeny and subsequent generations were amplified with the following primers to detect the mutated alleles by polymerase chain reaction (KAPA Mouse Genotyping Kit; Boston, MA): wild type, (5': 5'-TTGTTCTGAGGGCTTAGGATGTT; 3': 5'-CTTTTCCAGTAAATCAAGCGTTGTT),

yielding a 521-bp product; and, mutant (5': 5'-TTGGGCAACACAGGCTGGTTAATC; 3': 5'-ATTGGAAGTAGCCGTTATTAGTGGA), yielding a 701-bp product. Wild type, heterozygous, and homozygous male siblings (n=6 mice per genotype; 2-3 months of age) were deeply anesthetised with sodium pentobarbital (8.2 mg/ mouse, i.p.) and sacrificed by transcardial perfusion with 4% paraformaldehyde in 0.1M phosphate buffer (pH 7.4). The descending colon, urinary bladder, olfactory mucosa, and olfactory bulbs were removed from these mice, post-fixed in the same fixative for 48 hours, and then cryoprotected in phosphate-buffered 30% sucrose for 2-3 days. All tissues were embedded in Cryomatrix™ (Thermo Fisher Scientific) and frozen in -20°C 2-methylbutane for sectioning with a cryostat. The tissues were sectioned at 20 µm thickness; the tissues were directly mounted onto Superfrost/Plus slides (Thermo Fisher Scientific). For ultrastructural examination, other wild type and homozygous male siblings (n=4 mice per genotype; 2-3 months of age) were deeply anesthetised with sodium pentobarbital (8.2 mg/ mouse, i.p.) and sacrificed by transcardial perfusion with 2% paraformaldehyde and 2% glutaraldehyde in 0.1M phosphate buffer (pH 7.4). The olfactory mucosa and olfactory bulbs were removed from these mice, trimmed, and then post-fixed overnight in phosphate-buffered 1% osmium tetroxide (pH 7.4). The tissues were subsequently dehydrated and embedded in Epon. Semithin sections (~ 1 µm thickness) were cut and stained with toluidine blue. Ultrathin olfactory sections (cut on a RMC microtome and stained with uranyl acetate and lead citrate) were viewed using a Hitachi 7000 transmission electron microscope.

### ***Immunohistochemistry***

Frozen sections of the olfactory mucosa and olfactory bulbs were allowed to thaw for 5 minutes before commencing immunostaining procedures at room temperature. The sections were treated with 4% phosphate-buffered paraformaldehyde (pH 7.4) for 15 minutes (this improves the adherence of the tissues to the slides) and rinsed in 0.1M tris-buffered saline (TBS; pH 7.4) for 5 minutes; this rinsing step was repeated after each treatment. Those sections to be immunostained for the localization of  $\alpha$ SMA were pretreated with 0.008% proteinase K for 15-30 minutes (this step was often required to reveal antigenic sites in OECs). After treatment with 10% normal donkey serum (NDS) in 0.1M TBS plus 0.25% Triton-X100 (TBX) for 1 hour, sections were incubated for 24 hours with one of the following primary antibodies: mouse anti-synthetic  $\alpha$ SMA IgG (1:1000 dilution; Sigma-Aldrich, Oakville, ON) for detection in hamsters, rabbits, pigs, and monkeys; rabbit anti-synthetic  $\alpha$ SMA IgG (1:1000; Abcam, Cambridge, MA) for detection in mice and pigs; rabbit anti-bovine S100 $\beta$  IgG (1:500; Dako, Burlington, ON) for detection in all five mammalian species; and, rabbit anti-bovine GFAP IgG (1:250; Dako) for detection in all five mammalian species; and goat anti-human GFAP IgG (1:250; Santa Cruz). These antibodies were diluted in a final solution containing 3% NDS in 0.25% TBX. After rinsing, the sections were then incubated for 2 hours with the appropriate secondary antibodies: FITC-conjugated donkey anti-mouse IgG (1:100; for the detection of non-murine  $\alpha$ SMA), FITC-conjugated donkey anti-rabbit IgG (1:100; for the detection of murine  $\alpha$ SMA, porcine  $\alpha$ SMA, S100 $\beta$  and GFAP), and FITC-conjugated donkey anti-goat IgG (1:100; for the detection of rabbit GFAP). Secondary antibodies (Cedarlane, Burlington, ON) were diluted in a solution containing 3% NDS with 0.25%

TBX. Sections were coverslipped with DAPI-conjugated mounting media (Vector Laboratories, Burlington, ON). The immunofluorescence was viewed and photographed with a Zeiss microscope. Images were captured using a Zeiss AxioCam high resolution scanning digital camera with Axiovision software (version 4.2). After adjusting the images for brightness and contrast, these images were converted to .tif files and used to generate figures with Adobe Illustrator CS5.

Those sections to be immunostained for the localization of  $\alpha$ -SMA in  $\alpha$ SMA-deficient mice and their wild type siblings (i.e. descending colon and urinary bladder) were first treated with 4% phosphate-buffered paraformaldehyde (pH 7.4) for 15 minutes. Sections were rinsed in 0.1M TBS for 5 minutes; this rinsing step was repeated after each treatment. Once sections were blocked with 0.3% hydrogen peroxide in 0.1M TBS for 1 hour followed by treatment with 3% normal goat serum (NGS) in 0.1M TBS plus 0.25% TBX for 1 hour at room temperature, the sections were then treated with consecutive incubations of avidin and biotin solutions in 3% NGS in 0.25% TBX (Vector Laboratories; as per manufacturer's specifications). Sections were then incubated for 24 hours with a monoclonal mouse anti-synthetic  $\alpha$ SMA IgG conjugated to fluorescein (1:500; Sigma-Aldrich), followed by rabbit anti-fluorescein IgG (1:1000; Invitrogen, Eugene, OR) for 3 hours. After rinsing, the sections were subsequently incubated with biotinylated goat-anti rabbit IgG (1:500; Vector Laboratories) for 2 hours, and then incubated with avidin-biotin complex (Vector Laboratories) for another 2 hours. Sections of descending colon and urinary bladder were reacted in a solution containing 0.05% diaminobenzidine tetrahydrochloride, 0.04% nickel chloride, and 0.015% hydrogen peroxide in 0.1M TBS. Sections were dehydrated through a grade series of ethanols,

cleared, and coverslipped with Permount (Thermo Fisher Scientific). The chromogenic immunoreaction products were viewed and photographed under bright-field optics with a Zeiss microscope. Images were captured using a Zeiss AxioCam high resolution scanning digital camera with Axiovision software (version 4.2). After adjusting the images for brightness and contrast, these images were converted to .tif files and used to generate figures with Adobe Illustrator CS5.

## **RESULTS**

The basic anatomical organization of the adult hamster, rabbit, monkey, and mouse (as well as fetal pig) olfactory nervous systems is quite similar to that of the adult rat, guinea pig, and cat. The olfactory mucosa has olfactory nerve fascicles within the lamina propria layer that increase in size as they near the olfactory bulbs. These olfactory nerve fascicles are composed of OECs wrapping around variable numbers of olfactory axons. Though the exact morphological arrangement between OECs and olfactory axons varies among mammalian species (see Kawaja et al., 2009), it is clear that the primary function of OECs is to ensheath dozens (if not hundreds) of olfactory axons. Each fascicle is bound by a layer of perineurial fibroblasts, and in certain species, the larger olfactory nerve fascicles contain a single arteriole. At the olfactory nerve fiber layer, the fascicular arrangement of OECs and olfactory axons is replaced by clusters of OECs that surround bundles of criss-crossing olfactory fibres.

In the olfactory mucosa of adult hamsters, the cytoplasmic processes of OECs in olfactory nerve fascicles displayed positive immunostaining for both GFAP and S100 $\beta$  (Figure 2). Though hamster bulbar OECs also had positive immunostaining for S100 $\beta$ ,

there was a pronounced lack of GFAP immunostaining among these cells. Positive immunostaining for GFAP (and S100 $\beta$ ) was, however, evident in the astrocytes of the olfactory bulb. Immunostaining for  $\alpha$ SMA of the hamster olfactory mucosa revealed vascular smooth muscle cells (VSMCs) of arterioles (some of which were present within the larger olfactory nerve fascicles) and perineurial fibroblasts; this positive immunostaining was seen without pretreatment with proteinase K. Perineurial fibroblasts (i.e., flattened cells surrounding the nerve fascicles) have been described in the olfactory mucosa of adult rats, cats, and guinea pigs (Jahed et al., 2007; Kawaja et al., 2009; Smithson and Kawaja, 2009). These cells are also immunopositive for  $\alpha$ SMA. With proteinase K pretreatment of the hamster olfactory tissues, bulbar OECs (but not mucosal OECs) displayed positive immunostaining for  $\alpha$ SMA. As with GFAP and S100 $\beta$ , astrocytes in the olfactory bulbs of hamsters had positive immunostaining for  $\alpha$ SMA; this has been reported in astrocytes of rats, cats, and guinea pigs as well (Lecain et al., 1991; Smithson and Kawaja, 2009).

As described in adult hamsters, mucosal OECs of adult rabbits were immunopositive for GFAP (Figure 3). However, unlike what was observed in hamsters, bulbar OECs of rabbits were also immunopositive for GFAP. Additionally, both mucosal and bulbar OECs displayed S100 $\beta$  immunostaining, revealing their fascicular appearance in the lamina propria (data not shown) and their scattered appearance in the olfactory nerve fiber layer (Figure 3). For both GFAP and S100 $\beta$ , we observed stronger immunostaining in mucosal OECs after pretreatment with proteinase K (Figure 11). Since the secondary antibody used for both GFAP and S100 $\beta$  immunostaining was an FITC-conjugated donkey anti-rabbit IgG, we anticipated there to be a large quantity of

non-specific staining in the rabbit tissue. To control for this, we repeated the immunostaining procedure on the rabbit tissue, leaving out the application of the primary antibody (i.e. only the FITC-conjugated donkey anti-rabbit IgG was applied). As seen in Figure 11, non-specific staining within the olfactory nerve fascicles was absent in this control. Immunostaining for  $\alpha$ SMA with proteinase K pretreatment revealed mucosal OECs (Figure 3) and bulbar OECs (data not shown) in addition to immunopositive VSMCs and perineurial fibroblasts. Astrocytes in the olfactory bulbs of adult rabbits displayed positive immunostaining for GFAP, S100 $\beta$ , and  $\alpha$ SMA.

The olfactory mucosa of monkeys displayed GFAP-immunopositive OECs within numerous olfactory nerve fascicles of the lamina propria (Figure 4). Again, as seen in the adult hamsters, bulbar OECs in these monkeys lacked positive immunostaining for GFAP. S100 $\beta$  immunostaining, on the other hand, was detected in both mucosal and bulbar OECs. Immunostaining for  $\alpha$ SMA with proteinase K pretreatment revealed positive mucosal and bulbar OECs, as well as VSMCs and perineurial fibroblasts. The positive immunostaining for  $\alpha$ SMA had a distinctive punctate appearance in the mucosal and bulbar OECs. Furthermore, the  $\alpha$ SMA-immunostaining was not as robust as the  $\alpha$ SMA-immunopositive staining seen in hamsters or rabbits. Astrocytes in the olfactory bulbs of monkeys had positive immunostaining for GFAP, S100 $\beta$ , and  $\alpha$ SMA.

Given the previous use of porcine OECs for spinal cord implantation (Imaizumi et al., 2000; Radtke et al., 2004; Radtke et al., 2010), we sought to determine the phenotypic features of these cells during embryonic development. Fetal pigs displayed positive GFAP- and S100 $\beta$ -immunostaining of mucosal OECs in the olfactory nerve fascicles

(Figure 5). These two antigens revealed the processes of OECs that wrap around the olfactory axons. In the porcine olfactory bulbs, both GFAP and S100 $\beta$  immunostaining yielded clusters of OECs seen in the developing olfactory nerve fiber layer.

Immunostaining for  $\alpha$ SMA with proteinase K pretreatment failed to reveal mucosal and bulbar OECs. Both monoclonal mouse anti-synthetic  $\alpha$ SMA and polyclonal rabbit anti-synthetic  $\alpha$ SMA primary antibodies failed to yield positive immunostaining for  $\alpha$ SMA in OECs. Only VSMCs and perineurial fibroblasts in the olfactory mucosa, as well as VSMCs in the olfactory nerve fiber layer of fetal pigs, displayed positive immunostaining for  $\alpha$ SMA.

In the olfactory mucosa of adult mice, only a small number of OECs in the olfactory nerve fascicles had positive immunostaining for GFAP (Figure 6), whereas many more mucosal OECs displayed positive immunostaining for S100 $\beta$ . Schwann cells found in peripheral nerves, which course through the lamina propria, were immunopositive for GFAP and S100 $\beta$ . Bulbar OECs in the mouse olfactory nerve fiber layer displayed poor immunostaining for GFAP but strong immunostaining for S100 $\beta$ . Immunostaining for  $\alpha$ SMA with proteinase K pretreatment yielded positive VSMCs and perineurial fibroblasts in the lamina propria, as well as VSMCs in the olfactory nerve fiber layer. Neither mucosal nor bulbar OECs displayed positive immunostaining for  $\alpha$ SMA in adult mice.

To further explore the temporal and spatial aspects of  $\alpha$ SMA promoter activity in the olfactory nervous system of postnatal and adult mice, we obtained transgenic mice expressing the reporter gene LacZ under the control of the  $\alpha$ SMA promoter (Gan et al.,

2007). An assessment of the temporal expression of LacZ (which translates the bacterial enzyme  $\beta$ -galactosidase) was conducted on these transgenic mice at ages ranging from postnatal day 1 to three months. No positive detection of  $\beta$ -galactosidase (by histochemical staining) was seen in OECs of the olfactory mucosa or olfactory nerve fiber layer of transgenic mice between these ages. Transgenic mice did, however, display positive  $\beta$ -galactosidase staining in the smooth muscle cells of the colonic muscularis externa and the urinary bladder detrusor muscle (Figure 7).

To determine whether an absence of  $\alpha$ SMA expression throughout murine life affects the structural and/or neurochemical features of OECs, we examined adult mice having one or two mutated alleles for  $\alpha$ SMA, as compared to wild type siblings (Schildmeyer et al., 2000). To provide direct evidence that homozygous mice lacked  $\alpha$ SMA expression, we performed immunostaining for  $\alpha$ SMA in the descending colon and urinary bladder of null mutant and wild type male siblings. Immunostaining for  $\alpha$ SMA was observed in the colonic muscularis externa and the urinary bladder detrusor muscle of wild type mice but not in these tissues of age-matched homozygous mice (Figure 8). No differences were observed in the staining intensity or localization for GFAP and S100 $\beta$  among the three genotypes of mice between 1 to 3 months of age (data not shown). That is, comparatively weak immunostaining for GFAP in both mucosal and bulbar OECs, and stronger immunostaining for S100 $\beta$  in both glial subpopulations. Ultrastructural examination of the olfactory mucosa and the olfactory bulbs from age-matched wild type and homozygous mice (n=4 mice per genotype) revealed several distinct perturbations in OEC morphology and organization among the null mutant mice; these observations were consistent among all sections (no fewer than 2 per tissue per

animal) examined by transmission electron microscopy. First, the mucosal OECs of wild type mice had several long cytoplasmic processes that interweave among the olfactory axons. Together, multiple OECs in one cross-sectional view of an olfactory nerve fascicle contribute to the complete ensheathment of the axons travelling within this nerve (Figure 9); this fascicular organization of murine OECs was previously described by Kawaja et al. (2009). In  $\alpha$ SMA-deficient mice, the mucosal OECs had fewer and shorter cytoplasmic processes, as compared to their wild type siblings. This paucity of OEC cytoplasmic processes resulted in a scarcity of intercellular connections that contribute to the ensheathment of the olfactory axons within each fascicle. Second, bulbar OECs of wild type mice uniformly had large, ovoid nuclei with condensed chromatin confined to the inner portion of the nuclear envelope (Figures 10A, B). By contrast, bulbar OECs of  $\alpha$ SMA-deficient mice displayed a greater variety of nuclear morphologies. For instance, many resembled those seen in the wild type siblings (Figure 10C). There were, however, other OECs in the olfactory nerve fiber layer that had more darkly-stained condensed chromatin confined to the inner portion of the nuclear envelope (Figure 10D), while yet other bulbar OECs displayed irregularly-shaped nuclei (i.e., shrunken and indented) .

## FIGURES

**Figure 2:** Immunostaining for glial fibrillary acidic protein (GFAP), S100 $\beta$ , and  $\alpha$ -smooth muscle actin ( $\alpha$ SMA) in the olfactory mucosa (OM) and olfactory bulb (OB) of adult hamsters. **A.** Populations of GFAP-immunopositive olfactory ensheathing cells (OECs) are found inside the olfactory nerve fascicles of the lamina propria (LP) (as seen in longitudinal sections). **B.** Though GFAP-immunopositive bulbar OECs are not evident in the olfactory nerve fiber layer (ONL), GFAP-immunopositive astrocytes are seen in the deeper layers of the OB. **C.** Populations of S100 $\beta$ -immunopositive OECs are also seen in the olfactory nerve fascicles in the LP (as seen in longitudinal sections). **D.** Robust immunostaining for S100 $\beta$  is seen in OECs located in the ONL. In the deeper layers of the OB, S100 $\beta$ -immunopositive astrocytes are evident as well. **E.** OECs in the olfactory nerve fascicles (FAS) lack positive immunostaining for  $\alpha$ SMA; adjacent perineurial fibroblasts surrounding the fascicles, however, do display positive immunostaining for  $\alpha$ SMA. **F.** In the OB, populations of  $\alpha$ SMA-immunopositive OECs are found; the inset shows bulbar OECs (with DAPI staining for nuclei) at a higher magnification. Sections in **A-E** have DAPI staining (blue) to reveal the individual nuclei. Staining for GFAP, S100 $\beta$ , and  $\alpha$ SMA is shown in green. OE, olfactory epithelium. Scale bars = 100  $\mu$ m (**A-E**) and 50  $\mu$ m (**F**).

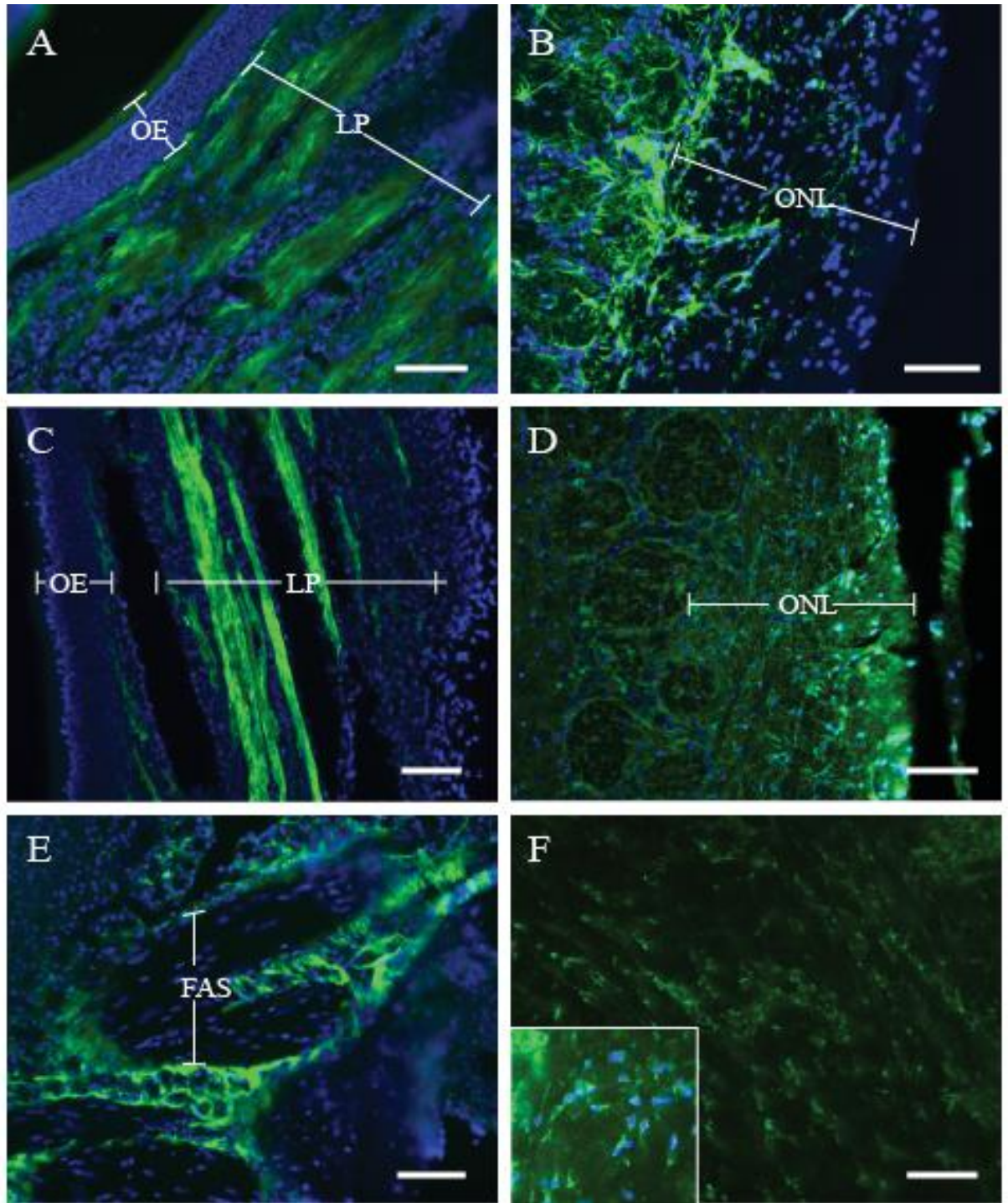


**Figure 3:** Immunostaining for glial fibrillary acidic protein (GFAP), S100 $\beta$ , and  $\alpha$ -smooth muscle actin  $\alpha$ SMA in the olfactory mucosa (OM) and olfactory bulb (OB) of adult rabbits. **A.** Populations of GFAP-immunopositive olfactory ensheathing cells (OECs) are found in the olfactory nerve fiber layer (ONL) of the OB. **B.** Robust immunostaining for S100 $\beta$  is seen in OECs located in the ONL. In the deeper layers of the OB, S100 $\beta$ -immunopositive astrocytes are evident as well. **C-E.** In the olfactory nerve fascicles (FAS) of the lamina propria (LP), populations of  $\alpha$ SMA-immunopositive OECs are found; adjacent perineurial fibroblasts (FB) as well as blood vessels (BV) also display positive immunostaining for  $\alpha$ -SMA (the image shown in **E** is a higher magnification of the olfactory nerve fascicle in **D**). Sections in **C** and **D** have DAPI staining (blue) to reveal the individual nuclei. Staining for GFAP, S100 $\beta$ , and  $\alpha$ SMA is shown in green. OE, olfactory epithelium. Scale bars = 40  $\mu$ m (**A**), 60  $\mu$ m (**B**, **D**), 130  $\mu$ m (**C**) and 20  $\mu$ m (**E**).

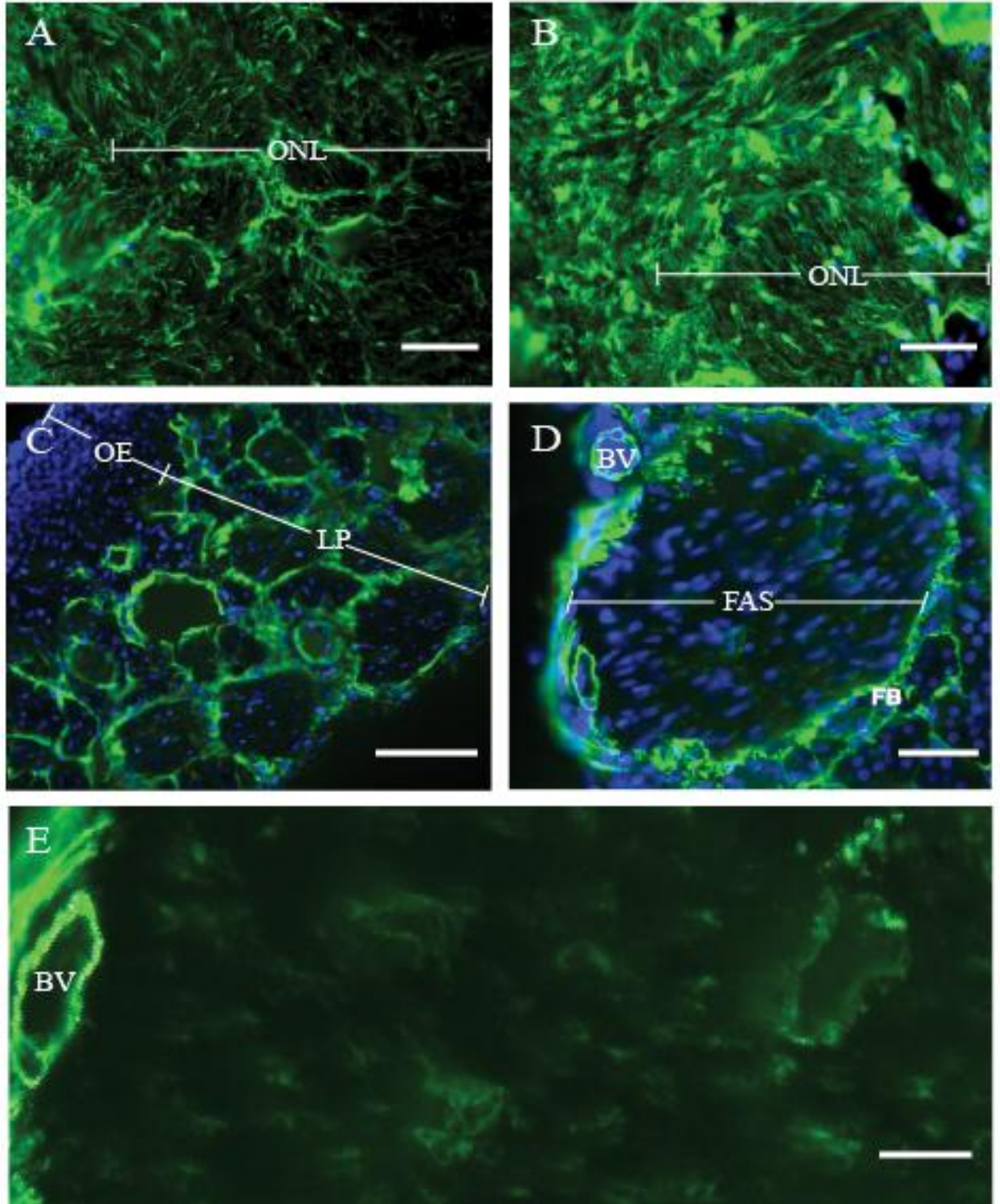


**Figure 4:** Immunostaining for glial fibrillary acidic protein (GFAP), S100 $\beta$ , and  $\alpha$ -smooth muscle actin ( $\alpha$ SMA) in the olfactory mucosa (OM) and olfactory bulb (OB) of adult monkeys. **A.** Populations of GFAP-immunopositive olfactory ensheathing cells (OECs) reside in the olfactory nerve fascicles (FAS) of the lamina propria (LP) (as seen in longitudinal sections). **B.** Though GFAP-immunopositive bulbar OECs are not evident in the olfactory nerve fiber layer (ONL), GFAP-immunopositive astrocytes are seen in the deeper layers of the OB, some of which extend processes into the ONL. **C.** Populations of S100 $\beta$ -immunopositive OECs are also seen in the olfactory nerve fascicles in the LP (as seen in longitudinal sections). **D.** Robust immunostaining for S100 $\beta$  is also seen in OECs located in the ONL. In the deeper layers of the OB, S100 $\beta$ -immunopositive astrocytes are evident as well. **E.** In the OM, populations of  $\alpha$ SMA-immunopositive OECs are found inside the olfactory nerve fascicles (FAS); immunopositive perineurial fibroblasts (FB) and blood vessels (BV) are also evident (as seen in longitudinal sections). **F.** Populations of  $\alpha$ SMA-immunopositive OECs and blood vessels are found in the ONL, whereas  $\alpha$ SMA-immunopositive astrocytes are evident in the deeper layers of the bulb. All sections have DAPI staining (blue) to reveal the individual nuclei. Staining for GFAP, S100 $\beta$ , and  $\alpha$ SMA is shown in green. Scale bars = 40  $\mu$ m (**A, D, E**), 200  $\mu$ m (**B**), 20 $\mu$ m (**C**) and 100  $\mu$ m (**F**).

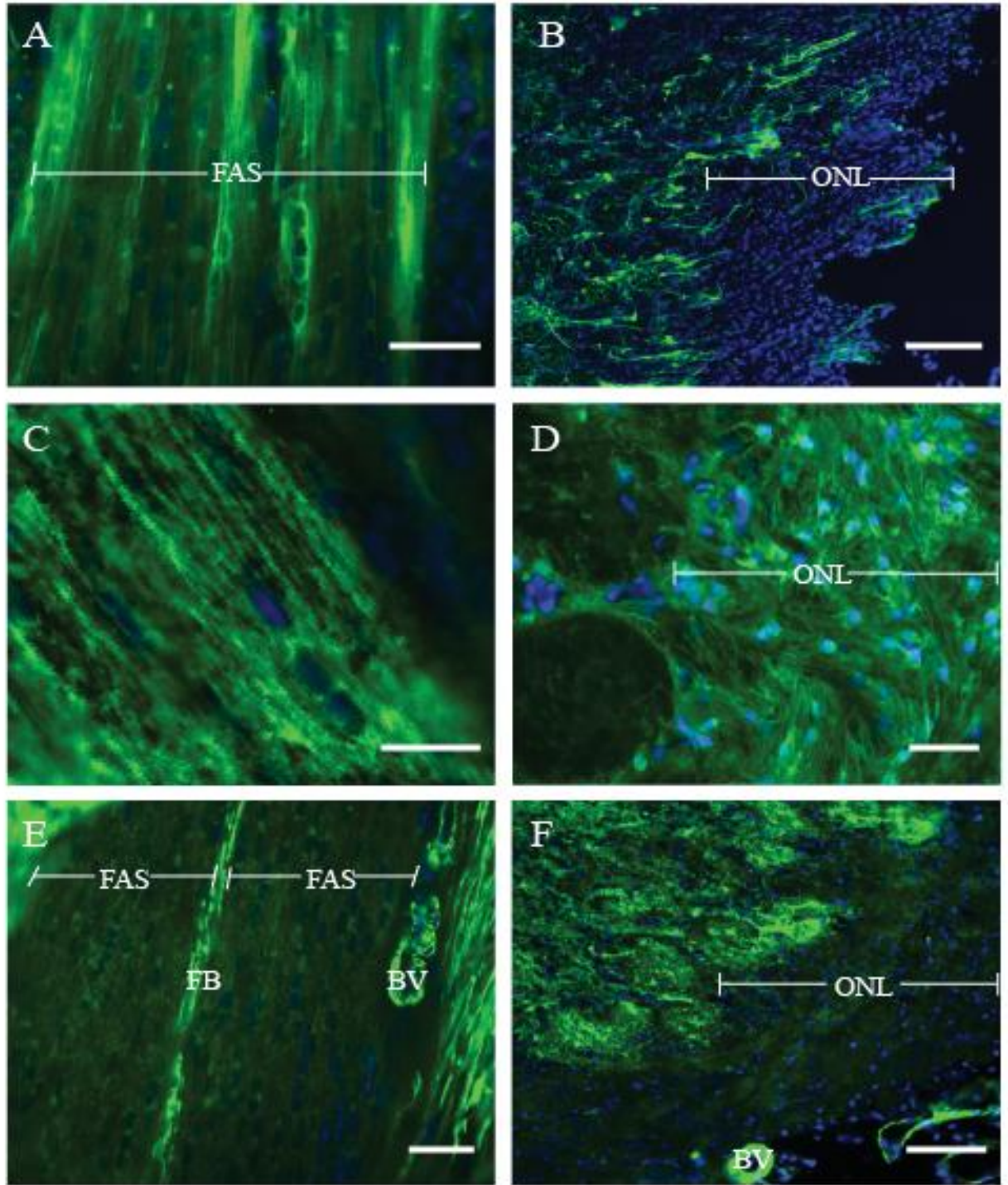


**Figure 5:** Immunostaining for glial fibrillary acidic protein (GFAP), S100 $\beta$ , and  $\alpha$ -smooth muscle actin ( $\alpha$ SMA) in the olfactory mucosa (OM) and olfactory bulb (OB) of fetal pigs. **A.** Populations of GFAP-immunopositive olfactory ensheathing cells (OECs) in numerous olfactory nerve fascicles are found in the OM (as seen in cross-sections). **B.** In the OB, individual olfactory nerve fascicles merge together near the developing olfactory nerve fiber layer (ONL), where clusters of GFAP-immunopositive OECs are evident. **C.** Populations of S100 $\beta$ -immunopositive OECs are also seen in the olfactory nerve fascicles (FAS) in the lamina propria (LP); the inset shows numerous olfactory nerve fascicles containing numerous S100 $\beta$ -immunopositive OECs (with DAPI staining for nuclei) (as seen in cross-sections). **D.** Immunostaining for S100 $\beta$  is seen in OECs located in the ONL. **E, F.** Though  $\alpha$ SMA-immunopositive OECs are not evident in the OM (**E**) and OB (**F**),  $\alpha$ SMA-immunopositive blood vessels are seen. Sections in **A, B, D, E,** and **F** have DAPI staining (blue) to reveal the individual nuclei. Staining for GFAP, S100 $\beta$ , and  $\alpha$ SMA is shown in green. OE, olfactory epithelium. NC, nasal cavity. Scale bars = 80  $\mu$ m (**A**), 100  $\mu$ m (**B, D, F**), 40  $\mu$ m (**C**), and 50  $\mu$ m (**E**).

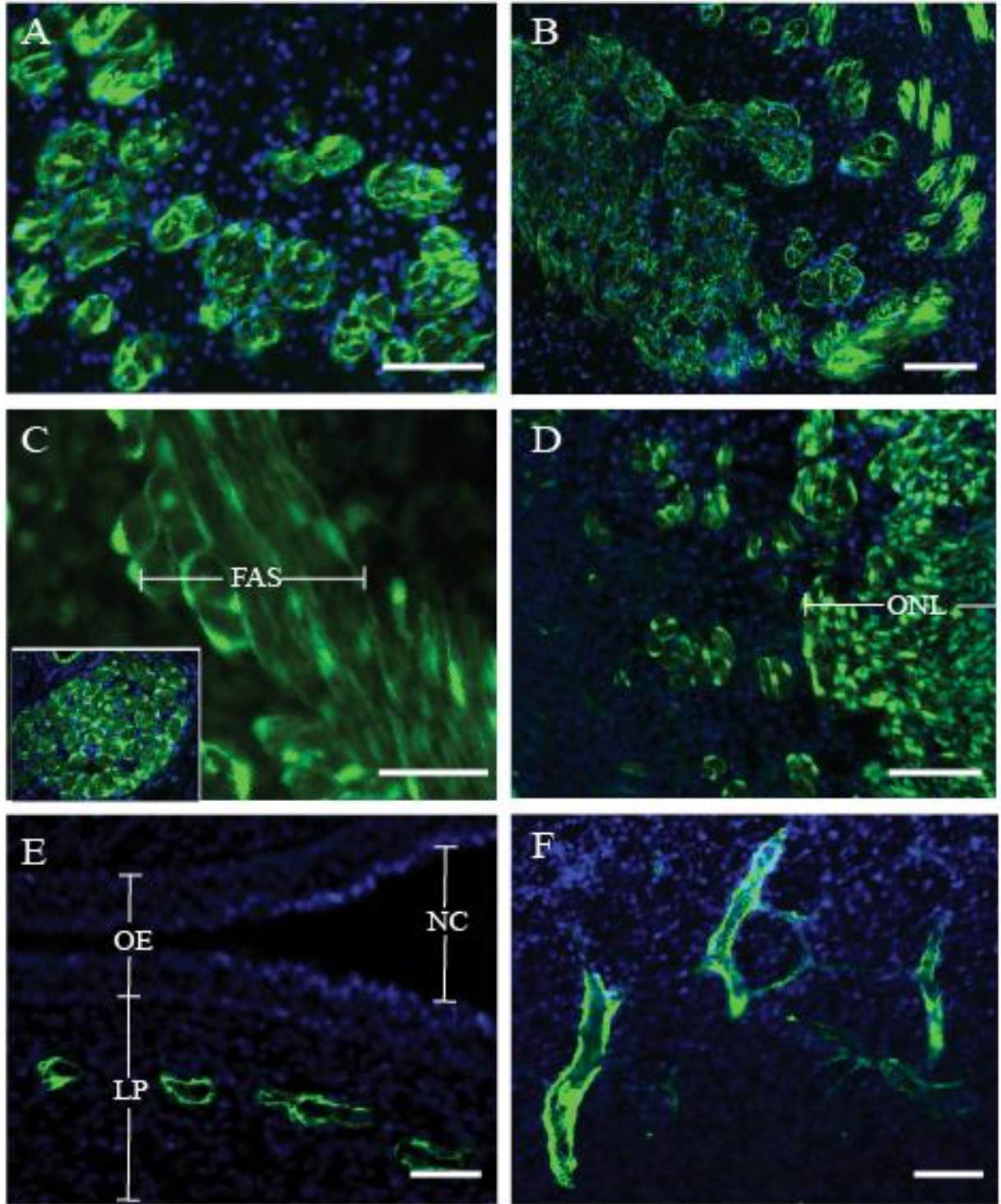


**Figure 6:** Immunostaining for glial fibrillary acidic protein (GFAP), S100 $\beta$ , and  $\alpha$ -smooth muscle actin ( $\alpha$ SMA) in the olfactory mucosa (OM) and olfactory bulb (OB) of adult mice. **A.** Sparse populations of GFAP-immunopositive olfactory ensheathing cells (OECs) are found in the lamina propria (LP); upper right inset shows GFAP immunolocalization in the thin cytoplasmic processes of an individual OEC, and lower left inset shows a GFAP-immunopositive peripheral nerve adjacent to a blood vessel (in cross-sections). **B.** Though GFAP-immunopositive OEC bulbar OECs are not evident in the olfactory nerve fiber layer (ONL), GFAP-immunopositive astrocytes are seen in the deeper layers of the OB. **C, D.** Populations of S100 $\beta$ -immunopositive OECs are found in the LP as well as in the ONL. **E.** OECs in the olfactory nerve fascicles (FAS) lack positive immunostaining for  $\alpha$ SMA; adjacent perineurial fibroblasts (FB) and blood vessels (BV), however, do display positive immunostaining for  $\alpha$ SMA (as seen in cross-sections). **F.** In the OB,  $\alpha$ SMA-immunopositive blood vessels, but not  $\alpha$ SMA-immunopositive OECs, are also evident. Sections in **B, D, E,** and **F** have DAPI staining (blue) to reveal the individual nuclei. Staining for GFAP, S100 $\beta$ , and  $\alpha$ SMA is shown in green. Scale bars = 50  $\mu$ m (**A, E**), 100  $\mu$ m (**B, D, F**), and 400  $\mu$ m (**C**).

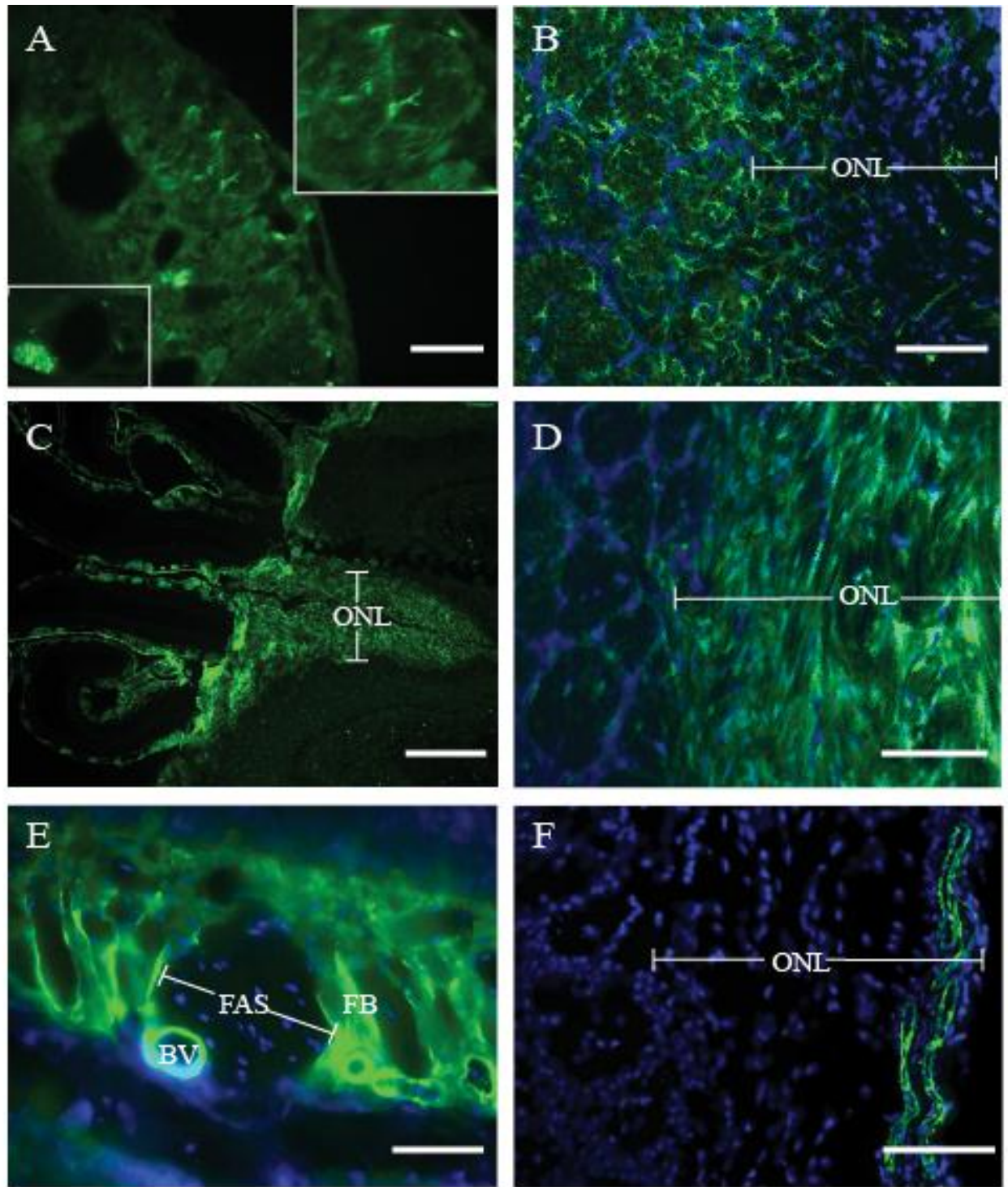


**Figure 7:**  $\beta$ -Galactosidase histochemical staining of the descending colon and urinary bladder from  $\alpha$ SMA-LacZ transgenic mice. **A, B.** Positive staining for  $\beta$ -galactosidase (blue) is seen in the smooth muscle cells of the muscularis externa (ME), as well as in the myofibroblasts located among the intestinal glands of the descending colon. **C.** In the urinary bladder, robust positive staining for LacZ (blue) is evident in the smooth muscle cells of the detrusor muscle. Mu, intestinal mucosa. Scale bars = 300  $\mu$ m (**A**), 200  $\mu$ m (**B**), and 100  $\mu$ m (**C**).

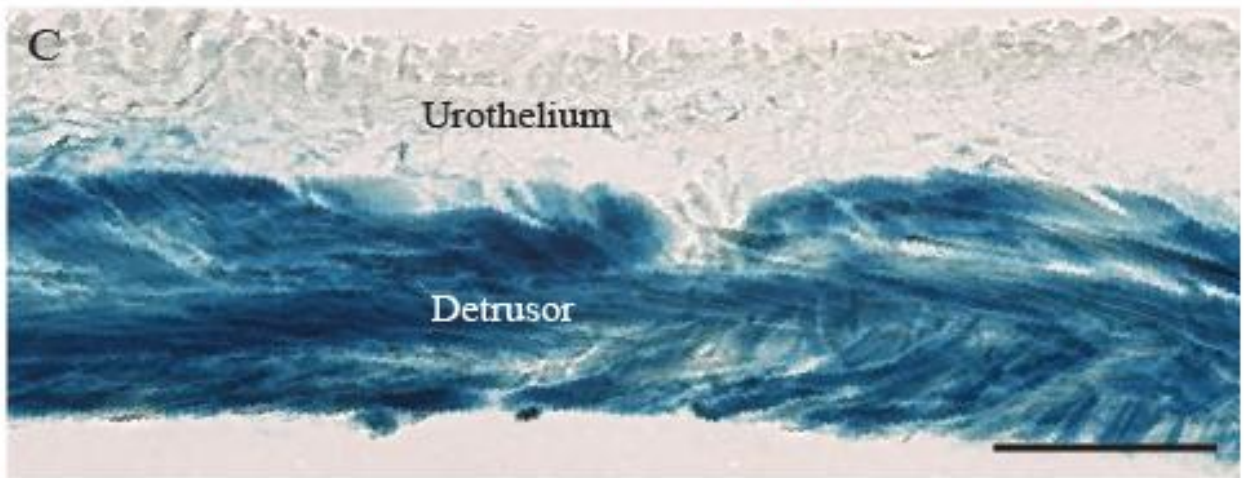
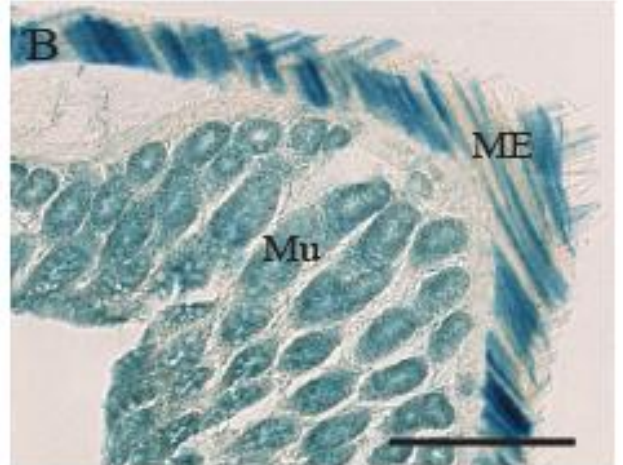
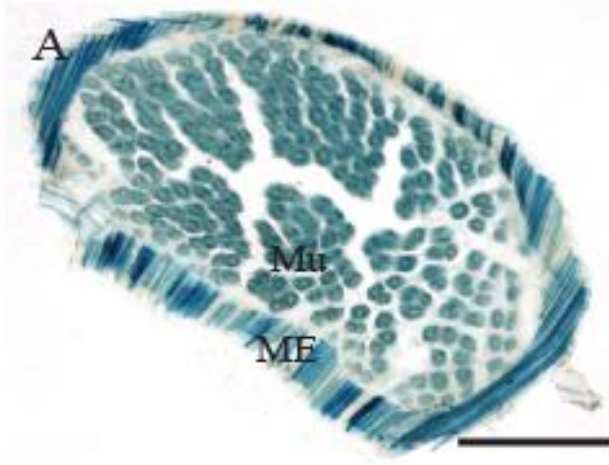


**Figure 8:** Immunostaining for  $\alpha$ -smooth muscle actin ( $\alpha$ SMA) of the descending colon and urinary bladder from wild type and homozygous mice lacking  $\alpha$ SMA expression. **A, B.** Positive staining for  $\alpha$ SMA (dark brown) is seen in the smooth muscle cells of the muscularis externa (ME) of the descending colon in wild type mice but not in homozygous mice. **C, D.** In the urinary bladder, positive staining for  $\alpha$ SMA (dark brown) is evident in the smooth muscle cells of the detrusor muscle in wild type mice but not in homozygous mice. Mu, intestinal mucosa. Scale bars = 100  $\mu$ m (**A, B**), and 60  $\mu$ m (**C, D**).

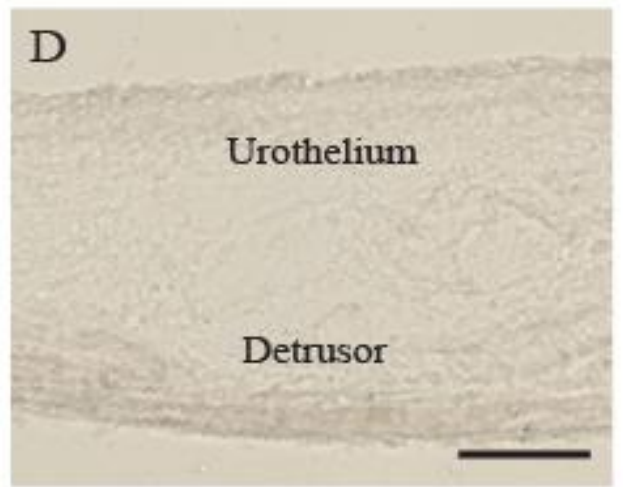
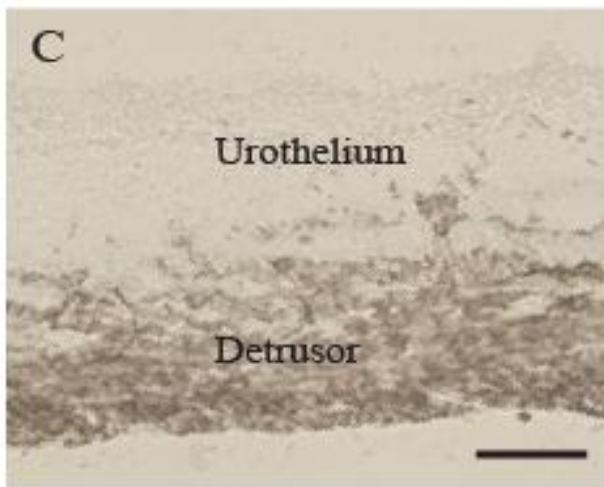
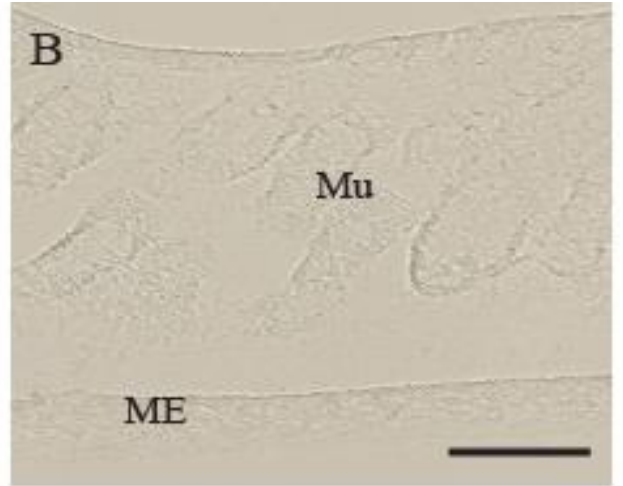
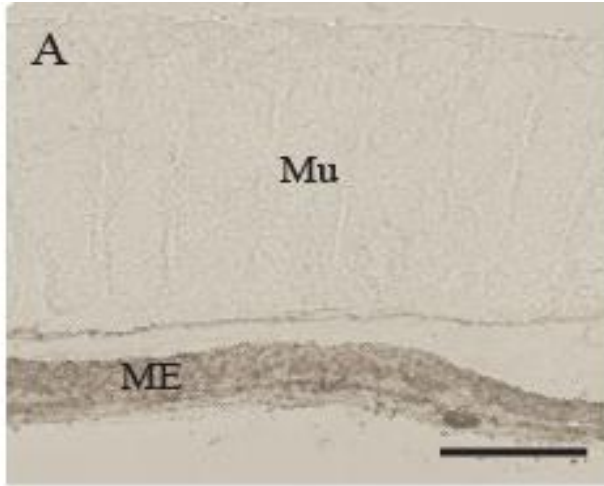


**Figure 9:** Electron photomicrographs of olfactory nerves fascicles from the lamina propria of wild type and homozygous mice lacking  $\alpha$ -smooth muscle actin ( $\alpha$ SMA) expression. **A.** Wild type mice have fascicles containing several OECs that surround hundreds of small-diameter unmyelinated olfactory axons. In this cross-sectional view, a single OEC (cell body with nucleus and numerous processes) is highlighted in blue. The adjacent OECs in this view (mostly processes) are highlighted in yellow. It is evident that murine mucosal OECs display extensive, long, and slender processes that contact each other to form a complete ensheathment of the olfactory axons. **B.** In homozygous mice, a single OEC (cell body with nucleus and processes) is highlighted in blue. These OECs in mice lacking  $\alpha$ SMA expression display swollen shorter processes, and there appears to be a paucity of contacts between OECs (highlighted in blue and yellow) in the one olfactory nerve fascicle. Scale bars = 2  $\mu$ m (**A**, **B**).

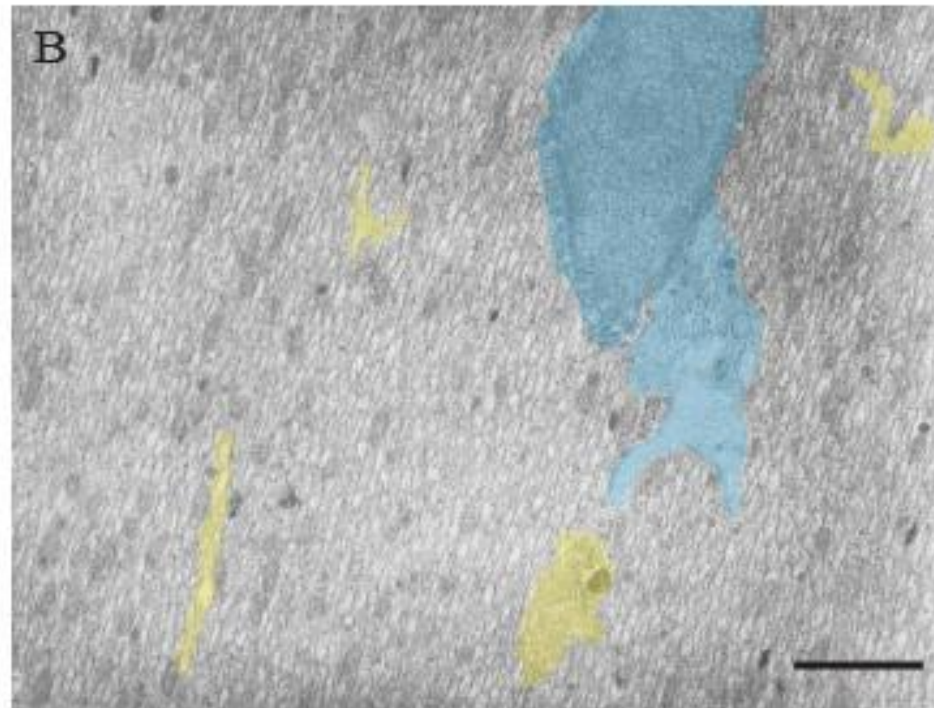
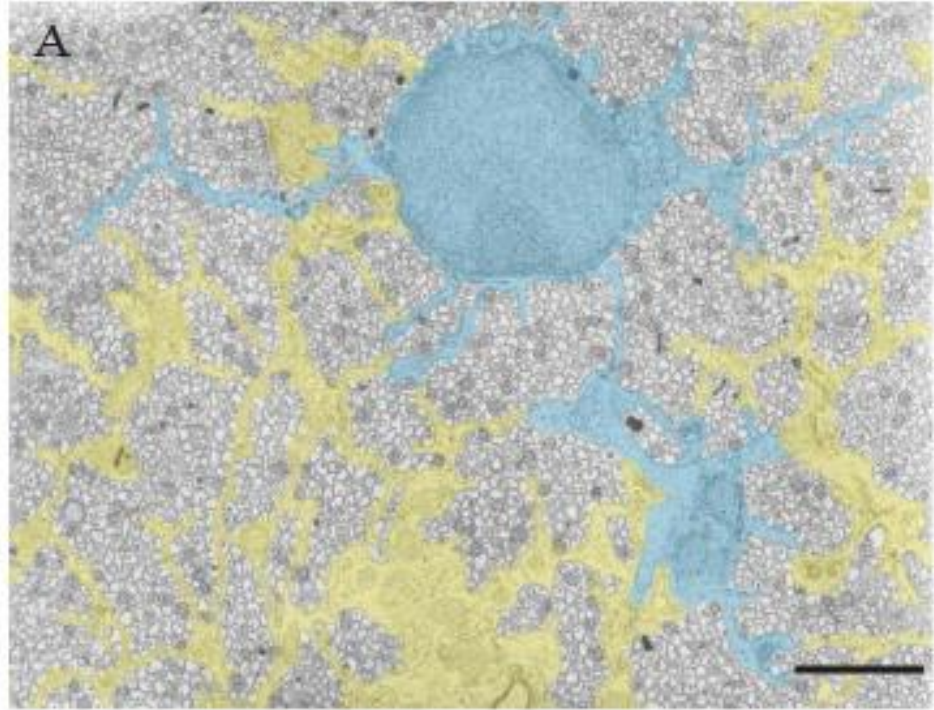


**Figure 10:** Electron photomicrographs of OEC nuclei (N) from the olfactory nerve fiber layer of the olfactory bulb from wild type and homozygous mice lacking  $\alpha$ -smooth muscle actin ( $\alpha$ SMA) expression. **A, B.** The large, round nuclei of OECs from wild type mice are surrounded by hundreds of crisscrossing small-diameter unmyelinated olfactory axons. The cytoplasm is predominantly translucent. **C-F.** The nuclei of OECs observed in homozygous mice are irregularly-shaped and contain condensed chromatin (electron-dense regions in nucleus). Scale bars = 2  $\mu$ m (**A-F**).

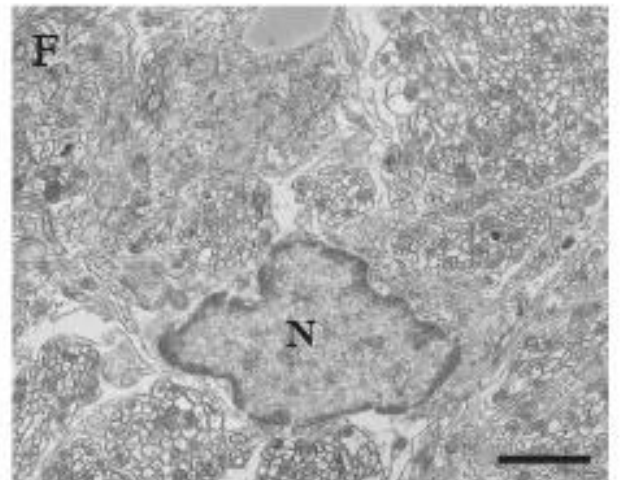
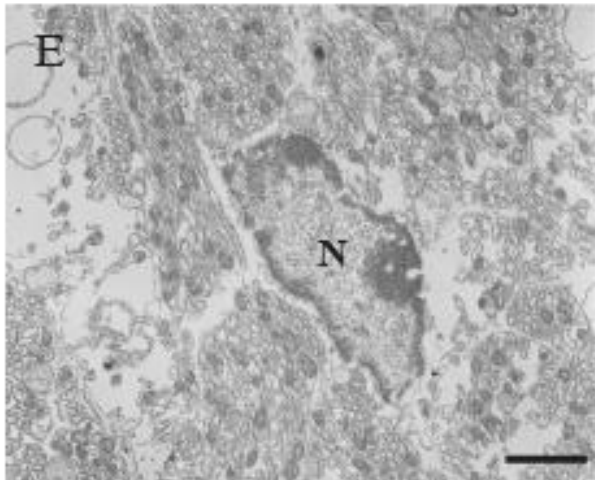
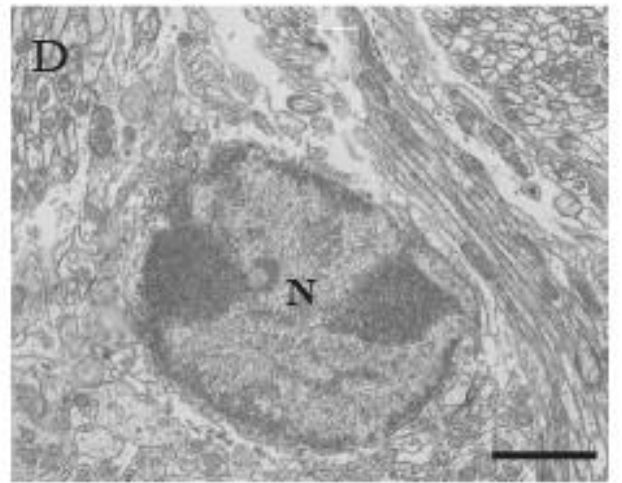
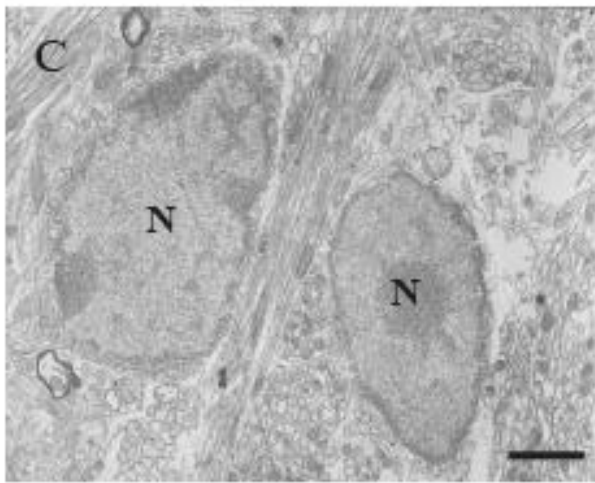
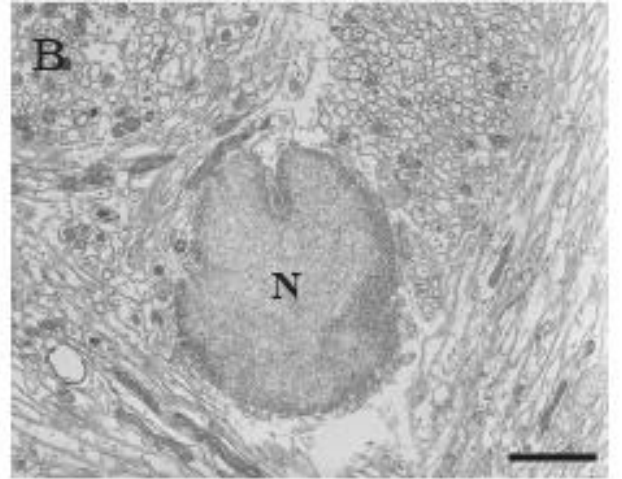
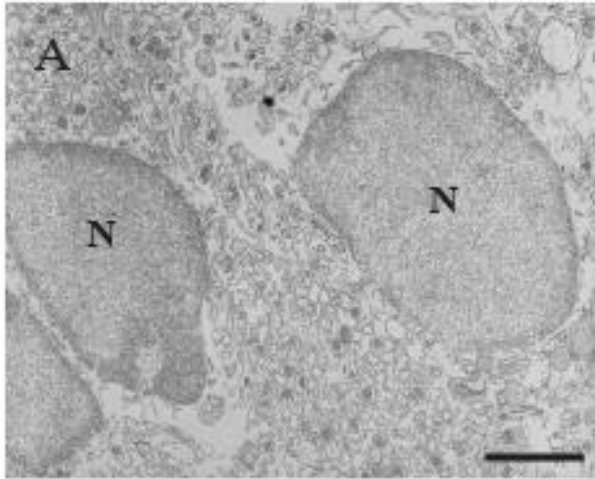
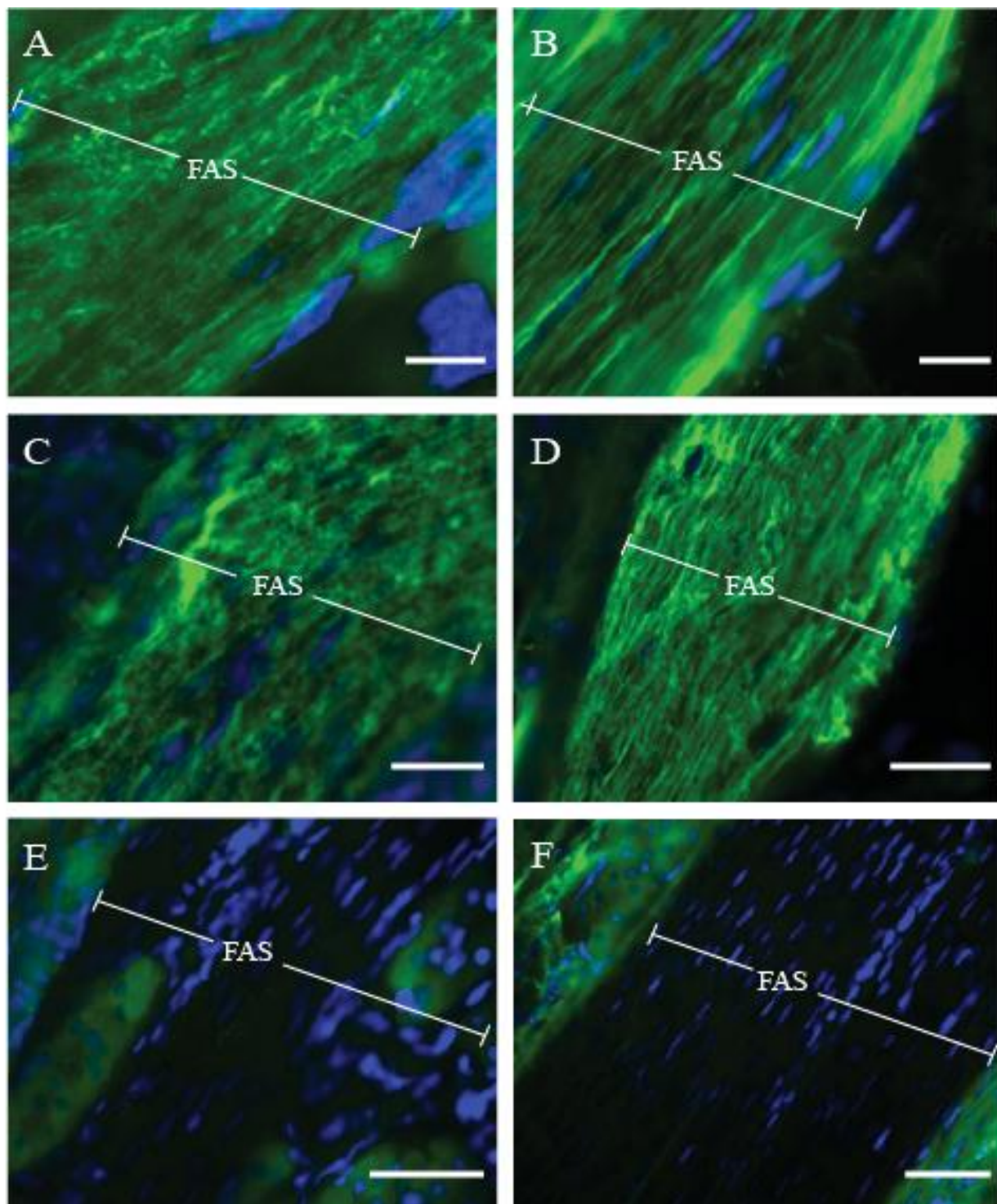


**Figure 11:** Immunostaining for glial fibrillary acidic protein (GFAP) and S100 $\beta$ , as well as controls for specific staining, in the olfactory mucosa (OM) of adult rabbits. **A, B.** Populations of GFAP-immunopositive olfactory ensheathing cells (OECs) are found inside an olfactory nerve fascicle (FAS) of the lamina propria (LP), without proteinase K pretreatment (**A**) and with proteinase K pretreatment (**B**) (as seen in longitudinal sections). **C, D.** Populations of S100 $\beta$ -immunopositive OECs are seen in an olfactory nerve fascicle of the LP without proteinase K pretreatment (**C**) and with proteinase K pretreatment (**D**) (as seen in longitudinal sections). **E.** No positive staining is observed in the olfactory nerve fascicle when the goat anti-human GFAP primary antibody was used. **F.** No specific staining is seen in an olfactory nerve fascicle when only the FITC-conjugated donkey anti-rabbit secondary antibody was applied as a control. Sections in **A, B, D, E,** and **F** have DAPI staining (blue) to reveal the individual nuclei. Staining for GFAP, S100 $\beta$ , and  $\alpha$ SMA is shown in green. Scale bars = 15  $\mu$ m (**A, B**), 40  $\mu$ m (**C, D**), and 60  $\mu$ m (**E, F**).



## DISCUSSION

In this study, we examined the neurochemical features of OECs from five mammalian species: adult hamsters, adult rabbits, adult monkeys, and adult mice, as well as fetal pigs. We assessed whether mucosal and/or bulbar OECs from these species have a unifying phenotype based on the expression of three biomarkers, namely S100 $\beta$ , GFAP, and  $\alpha$ SMA. Using immunofluorescence staining procedures, we found that while both mucosal and bulbar OECs from all species examined herein express S100 $\beta$ , the same is not true for GFAP. Likewise, OEC expression of  $\alpha$ SMA is variable among these mammals. Though the absence of  $\alpha$ SMA immunodetection in adult mice was validated in  $\alpha$ SMA-LacZ reporter mice, null mutant mice lacking  $\alpha$ SMA expression reveal pronounced defects of OEC morphology. Altogether, these results complement our previous neurochemical and ultrastructural studies on OECs from rats, guinea pigs, and cats (Jahed et al, 2007; Smithson and Kawaja, 2009).

The calcium binding protein S100 $\beta$  is found in mucosal and bulbar OECs of adult hamsters, rabbits, monkeys, and mice (as well as in fetal pigs). This observation is in agreement with our previous findings for mucosal and bulbar OECs of adult rats, cats, and guinea pigs (Jahed et al., 2007; Smithson and Kawaja, 2009). In all of these species, OECs display strong immunostaining for S100 $\beta$  as they ensheath the olfactory axons in the olfactory nerve fascicles. Though perineurial fibroblasts of these fascicles are also immunopositive for S100 $\beta$ , these cells are readily distinguishable from OECs by their location at the fascicular perimeter and by their flattened shape. In the olfactory nerve fiber layer, S100 $\beta$ -immunopositive OECs cluster together and extend long cytoplasmic processes around the interweaving bundles of olfactory axons. S100 $\beta$  is a member of a

multigenic family of calcium-binding proteins, and thus may serve several possible functions in OECs, such as cell signalling/growth/structure, regulation of metabolism, contraction, and intracellular signal transduction (Beharier et al., 2012). While the precise function(s) of S100 $\beta$  in mucosal and bulbar OECs has yet to be determined, it is clear that this protein is the most reliable biomarker for OECs *in vivo* among a wide variety of mammalian species examined to date.

GFAP is another biomarker that has been used to identify OECs *in vitro*, which have been isolated from mice, rats, dogs, and pigs (Au and Roskams, 2003; Jahed et al., 2007; Krudewig et al., 2006; Radtke et al., 2004; Techangamsuwan et al., 2009). Despite the consistent expression of GFAP by cultured OECs, immunodetection of this same structural protein among OECs *in vivo* has yielded variable results. For instance, our previous studies show that GFAP is expressed by mucosal and bulbar OECs in adult rats and cats but not by these populations in adult guinea pigs (Jahed et al., 2007; Smithson and Kawaja, 2009). Here we show that while mucosal OECs in adult hamsters and monkeys are GFAP-immunopositive, the bulbar OECs found in both these species are not. Both mucosal and bulbar OECs in fetal pigs and adult rabbits display strong immunostaining for GFAP, whereas these two cellular populations in adult mice have weak immunostaining for GFAP. Since the GFAP IgG used in our studies consistently labeled astrocytes in all mammalian species, we are confident that this antibody recognizes its epitope in a variety of cell types, including OECs. The presence versus absence of GFAP between mucosal and bulbar OECs from several mammalian species suggests that levels of expression may reflect glial functions in the two microenvironments of the olfactory nervous system (i.e., tight fascicular organization in

the olfactory nerves of the mucosa as compared to the loose dispersed organization in the olfactory nerve fiber layer). Given its expression patterns by mucosal and bulbar OECs in many mammalian species, it would seem that GFAP is a less reliable biomarker of OECs *in vivo* than is S100 $\beta$ . Though for OECs *in vitro*, both S100 $\beta$  and GFAP are expressed at sufficient levels for detection by immunostaining methods.

That rat OECs express the structural protein  $\alpha$ SMA arose from our comparison of the proteomes from cultured OECs (isolated from the olfactory bulbs of fetal rats) and cultured Schwann cells (isolated from the sciatic nerves of adult rats) (Jahed et al., 2007). We reported that the OEC proteome has detectable levels of  $\alpha$ SMA, whereas the Schwann cell proteome does not. This observation was validated by showing that rat OECs both *in vitro* and *in vivo* express  $\alpha$ SMA (as detected by immunofluorescence staining), whereas Schwann cells do not. We have already shown that both mucosal and bulbar OECs in adult guinea pigs and cats also express  $\alpha$ SMA (Smithson and Kawaja, 2009), and now in this study we provide new evidence that OECs from yet other mammalian species express this same structural protein. That is,  $\alpha$ SMA is detectable in both bulbar and mucosal OECs of adult monkeys, as well as in bulbar OECs of adult hamsters and mucosal OECs of adult rabbits. Neither monoclonal nor polyclonal antibodies against  $\alpha$ SMA reveal positive immunostaining in the OECs of fetal pigs. Though this absence of  $\alpha$ SMA immunodetection may reflect temporal patterns of expression in that species' olfactory development, our studies show that OECs in adult rats, guinea pigs, cats, hamsters, rabbits, and monkeys do express  $\alpha$ SMA, which is detectable by immunostaining methods (with proteinase K treatment to reveal antigenic sites) (Jahed et al., 2007; Smithson and Kawaja, 2009).

We employed two different strategies to assess whether OECs in mice express  $\alpha$ SMA, as we have detected in many other mammalian species. First, conventional immunostaining methods were used. Polyclonal antibodies against  $\alpha$ SMA fail to show expression of this structural protein in either mucosal or bulbar OECs of adult mice. The inability to detect  $\alpha$ SMA immunostaining may indicate either a *bona fide* lack of expression or protein expression below the levels of detectability by immunostaining procedures. In light of these two possibilities, we next used reporter mice that express the LacZ gene under the control of the  $\alpha$ SMA promoter. Mice from birth to 3 months of age were examined for the histochemical localization of  $\beta$ -galactosidase in the olfactory nervous system, as well as in other tissues populated with smooth muscle cells (e.g., the descending colon and urinary bladder). Though  $\beta$ -galactosidase-positive smooth muscle cells are detected in the descending colons and urinary bladders of the mice examined, no positive staining is evident in the olfactory nerve fascicles of the olfactory mucosa or in the olfactory nerve fiber layer of the olfactory bulb. We next postulated that  $\alpha$ SMA expression by OECs might occur during embryonic development, a period over which the unequivocal identification of OECs by immunostaining or LacZ expression is confounded by the immature nature of the olfactory nervous system. To test this idea we obtained heterozygous breeding pairs of mice that carry one mutated allele for  $\alpha$ SMA; we assessed their progeny both neurochemically and structurally. Neither the localization nor the intensity of S100 $\beta$  and GFAP immunostaining appears to be affected in the olfactory nerves and olfactory nerve fiber layer of null mutant mice at 2-3 months of age (i.e., those mice carrying two mutated alleles for  $\alpha$ SMA), as compared to their wild type siblings. Ultrastructural examination of these olfactory tissues, however, reveals several

pronounced features indicative of neural dysfunction in the null mutant mice. First, the olfactory nerve fascicles of  $\alpha$ SMA-deficient mice have OECs with only one or two cytoplasmic processes that are short and swollen. By contrast, the olfactory nerve fascicles of wild type siblings have several long cytoplasmic processes that connect with other OEC processes to form a continuous ensheathment around bundles of olfactory axons. Though the morphology of OECs in the nerve fascicles is perturbed in those mice lacking  $\alpha$ SMA expression, there does not appear to be any structural impairment to the olfactory axons. Second, the olfactory nerve fiber layer of  $\alpha$ SMA-deficient mice have OECs displaying a variety of nuclear morphologies, ranging from ovoid-shaped nuclei (as seen in wild type siblings) to irregular-shaped nuclei with indentations and darkly-stained condensed chromatin. Importantly, these irregular-shaped nuclei are not found in the olfactory nerve fiber layer of age-matched wild type mice. These dysfunctional features of the OECs in  $\alpha$ SMA-deficient mice, as viewed at the ultrastructural level, provide compelling evidence that murine OECs require this structural protein for their anatomical integrity and perhaps even for their survival. Though we were unable to detect  $\alpha$ SMA expression by OECs in postnatal and adult mice, these ultrastructural observations suggest that expression of this protein during embryogenesis may play an important role for determining the cellular structure and function of these glial cells into postnatal and adult life.

While other biomarkers of rat OECs have been reported, such as P0, O4, and neuropeptide Y (Barnett et al., 1993; Lee et al., 2001; Ubink and Hökfelt, 2000), there has been little evidence to suggest that these proteins are equally capable of OEC detection in non-rodent mammalian species. Like S100 $\beta$ , GFAP, and  $\alpha$ SMA, the p75

neurotrophin receptor (p75NTR) is expressed robustly by OECs *in vitro*. Numerous studies have shown that cultures of OECs obtained from rodent, murine, canine, and porcine olfactory tissues display positive immunostaining for p75NTR (Akiyama et al., 2004; Au and Roskams, 2003; Dunning et al., 2004; Imaizumi et al., 2000; Krudewig et al., 2006; Pearse et al., 2007; Radtke et al., 2004; Richter et al., 2008; Sasaki et al., 2004; Techangamsuwan et al., 2008, 2009). OECs *in vivo*, however, have variable levels of detectability among several mammalian species. For instance, we were unable to detect positive immunostaining for p75NTR in adult guinea pigs and cats (Smithson and Kawaja, 2009); a similar absence of immunostaining has been reported in adult dogs (Bock et al., 2007). For these reasons, we choose not to examine p75NTR immunostaining in the olfactory tissues of adult mice, hamsters, rabbits, monkeys, and fetal pigs in this study. The failure to detect p75NTR, a biomarker common to all cells of neural crest origin, is certainly interesting considering the recent findings that OECs are derived from the neural crest and not from the olfactory placode (Barraud et al., 2010).

In conclusion, we have examined both the similarities and differences in the expression patterns of GFAP, S100 $\beta$ , and  $\alpha$ SMA among mucosal and bulbar OECs of mice, hamsters, rabbits, pigs, and monkeys. Complementing our previous studies in rats, cats, and guinea pigs, it is evident that mammalian OECs express S100 $\beta$ . Though  $\alpha$ SMA expression in both mucosal and bulbar OECs is detected in several species (e.g., rats, guinea pigs, cats, and monkeys), it would seem that its reliability as an OEC biomarker is not universal for all mammals. The same can be said for GFAP as an OEC biomarker. Thus, the identification and characterization of OECs *in vivo* must meet several criteria, including anatomical location (i.e., within olfactory nerve fascicles and olfactory nerve

fiber layer) and neurochemical phenotype (i.e., positive immunostaining for S100 $\beta$  along with  $\alpha$ SMA and/or GFAP).

## **ACKNOWLEDGEMENTS**

This work was supported by a grant from the Botterell Foundation at Queen's University. Khalil S. Rawji is supported by an Ontario Graduate Scholarship and Laura J. Smithson is supported by a Banting and Best Scholarship from the Canadian Institutes of Health Research. We would like to thank Dr. Fredrick Kan for the hamster tissues, Dr. Chandra Tayade for the porcine tissues, Dr. Doug Munoz for the monkey tissues, and Ms. Debbie Harrington for the rabbit tissues, all of whom are at Queen's University. We would like to thank Dr. Gary Owens for the  $\alpha$ SMA-LacZ mice and Dr. James Tomasek (with permission from Dr. Robert Schwartz) for the  $\alpha$ SMA heterozygous mice. We would like to thank Ms. Verna Norkum for the preparation of tissues and sections for light and electron microscopic assessments, and Ms. Anne-Marie Crotty for the genotyping of the two mouse strains.

**CHAPTER 3: A Cellular Scaffolding Study for Olfactory Ensheathing Cells Using Methacrylated Glycol Chitosan, Agarose, and Isolated Rodent Olfactory Lamina Propria**

**Khalil S. Rawji<sup>1</sup> and Michael D. Kawaja<sup>1,2</sup>**

<sup>1</sup>Centre for Neuroscience Studies and <sup>2</sup>Department of Biomedical and Molecular Sciences  
Queen's University  
Kingston ON  
CANADA K7L 3N6

**ABSTRACT**

Olfactory ensheathing cells (OECs) are the chief glial population of the mammalian olfactory nervous system and are thought to be responsible for the successful directional growth of new olfactory axons throughout the life of adult mammals, making them a promising cellular transplantation strategy for spinal cord injury. We investigated the ability of various hydrogels to support and promote the growth of rodent OECs *in vitro*. We also examined the efficacy of lamina propria strips isolated from the rodent olfactory system in sustaining OECs in culture. OECs seeded onto methacrylated glycol chitosan (MGC) and its 2 variations, as well as agarose, did not survive after 4 to 6 days in culture. This observation provides new insight into developing biomatrices which display properties that may support cellular growth. Olfactory lamina propria strips isolated from the rodent olfactory system showed positive immunostaining for both GFAP and S100 $\beta$  between 3 to 10 days in culture, suggesting that OECs remained viable after this time

period. In addition, immunostaining for perineurial fibroblasts and microglia was evident between 3 to 10 days in culture, suggesting that the fascicular architecture and immune capabilities of these cultured lamina propria strips was maintained. In sum, these findings highlight the inability of MGC (and the variations used in this study), as well as agarose, to support OEC survival and proliferation for transplantation in spinal cord injury, while at the same time emphasizing the potential of using isolated olfactory lamina propria strips for autologous intraspinal transplantation.

## **INTRODUCTION**

The mammalian olfactory nervous system is known for its ability to continually generate new primary olfactory neurons throughout adulthood (Monti Graziadei and Graziadei, 1978). This neurogenesis occurs in the neuroepithelium, where the cell bodies of primary olfactory neurons and their basal stem cells are located. The olfactory mucosa is composed of this superficial avascular neuroepithelium and a deeper (and highly vascularized) layer referred to as the lamina propria. The primary olfactory neurons extend small unmyelinated axons (0.1-0.4  $\mu\text{m}$  in diameter) through the lamina propria toward the olfactory bulbs. Specialized glial cells known as olfactory ensheathing cells (OECs) protect the olfactory axons in the lamina propria by creating tunnel-like structures that surround dozens to hundreds of fibres simultaneously (Doucette, 1990). These OEC fascicles, with the ensheathed olfactory axons, continue through the cribriform plate and terminate at the surface of the olfactory bulbs, where they form the olfactory nerve fiber layer. Rather than clearly-defined fascicles, OECs in the olfactory

nerve fiber layer cluster together to surround crisscrossing bundles of olfactory axons; these axons extend into the olfactory bulbs where they synapse with the dendritic processes of the second-order olfactory mitral, periglomerular, and tufted neurons in the glomerular layer (Franssen et al, 2007; Valverde et al., 1992). It is thought that OECs are responsible for the successful directional growth of new olfactory axons throughout the life of adult mammals.

Due to this unique capability of promoting axonal regeneration in their native olfactory environment, OECs have become a very popular topic in spinal cord research in the last 15 years (Boyd et al, 2003). The transplantation of OECs into spinal cord injury models have resulted in regeneration of central nervous system (CNS) axons, particularly at the graft-host boundary (Imaizumi et al., 1998; Ramon-Cueto et al., 2000). Despite reported success, however, there have been many studies failing to show any axonal regrowth or functional improvements (Bretzner et al, 2008; Deumens et al, 2006; Lu et al, 2006; Ruitenberget al, 2003; Takami et al, 2002). In many cases, such results are due to the failure of OECs being able to survive in the graft after intraspinal transplantation.

One potential strategy to increase the efficacy of transplantations of OECs into the injured spinal cord is to encapsulate the cells within a biocompatible polymer matrix. Rather than transplanting glial cells directly into the lesioned spinal cord, synthetic pre-made biomatrices allow cells to be implanted within a controlled environment. This approach offers a few advantages: i.) Provides a carefully-controlled environment allowing axons to grow in response to the content of the matrix; ii.) Provides the transplanted cells and any in-growing axons a source of protection; iii.) Limits the

amount of scar tissue invasion; iv.) Promotes the appropriate exchange of factors that promote growth; v.) Allows the exchange of important nutrients; vi.) Allows the modification of the transplant through the addition or removal of various cellular and humoral constituents before implantation (Xu et al, 1995).

When using a biomatrix for cellular transplantation, three important points must be considered: i.) The polymer as well as its degradation products must be biocompatible to reduce the likelihood of an inflammatory or toxic response; ii.) The materials of the polymer must be conducive to cell growth; iii.) The materials of the polymer must be flexible enough to allow implantation into the spinal cord without causing any mechanical trauma to the tissue (Gautier et al, 1998).

Methacrylated glycol chitosan is an example of a biocompatible hydrogel. This gel has been demonstrated to provide consistent cell attachment and proliferation, promoting uniform tissue growth (Amsden et al., 2007). In addition, the relatively mild gelation conditions of this gel allow effective encapsulation of cells under physiological temperature and pH (Bryant and Anseth, 2002). Furthermore, since the polymerization reaction is initiated by the presence of light, precursors of this polymer can be readily injected into the lesioned spinal cord, allowing the cross-linking reaction to occur after transplantation. With this approach, oddly-shaped cavities can be more easily filled. In addition, this strategy prevents having to construct a gel outside the spinal cord and then transplant it into the lesioned spinal cord, thereby decreasing the surgical invasiveness (Davis et al., 2003).

Burdick and Anseth (2002) modified a photocrosslinkable hydrogel by adding an arginine-glycine-aspartic acid (RGD) group to the complex. This RGD-group is a

peptide that is commonly found in the cell-binding domains of extracellular matrix proteins. This peptide binds to integrins found on the surface of cells, enabling cells to adhere to surfaces that would not normally be adhesive. Therefore, it is thought that the inclusion of an RGD-group in a biomatrix would promote the adhesion of encapsulated cells. This research group also found that poly(ethylene glycol) hydrogels with RGD groups incorporated into their skeleton increased the attachment, spreading, and organization of the cytoskeleton of rat calvarial osteoblasts. This increased attachment was seen on polymer surfaces that would be otherwise non-adhesive. In addition, osteoblasts remained viable and formed a mineralized matrix.

Another substrate that has been used as a hydrogel is agarose. Agarose is a polysaccharide that has been shown to stimulate neurite extension from cultured dorsal root ganglia (Balgude et al, 2001). It is soluble in water at temperatures above 65°C and gels in the range of 17-40°C. Once agarose is a gel, it is stable and does not re-liquefy until heated to 65°C. Its ease of preparation as well as its biocompatibility with neurites makes it a promising candidate for biogel transplantations.

As an alternative to synthetic hydrogels for OEC transplantations, some research groups have isolated strips of olfactory mucosa and have transplanted this tissue immediately into the injured spinal cord cavity (Lu et al., 2001, 2002; Lima et al., 2006, 2010). Lu and colleagues (2001, 2002) used autografts from rats and observed a significant recovery in locomotor movement. Lima and colleagues (2006, 2010) performed pilot studies on human patients with complete spinal cord injury using autologous olfactory mucosal grafts and observed motor improvements in most of the

patients. Autologous olfactory mucosal grafts are advantageous in that they do not carry the risk of biological incompatibility within the spinal cord lesion. In addition, the connective tissue scaffold surrounding the olfactory nerve fascicles provides a natural, supportive framework for OECs to promote axonal regeneration in the spinal cord lesion. Furthermore, isolating olfactory mucosa is a minimally invasive procedure where the isolated tissue can be immediately transplanted into the injured spinal cord (providing an alternative to waiting days to weeks to produce cultures of OECs ready to implant within a biocompatible polymer gel).

In this study, we sought to assess whether various biomatrices would promote and sustain the growth of rat OECs *in vitro*. Though methacrylated glycol chitosan and agarose were not able to sustain or promote any viable cell growth, this observation provides new insight into developing biomatrices which display properties that may support cellular growth. In addition to testing synthetically-prepared biogels, we investigated whether strips of lamina propria isolated from the rodent olfactory system would be able to sustain OECs in culture. After ten days in culture, immunostaining for glial fibrillary acidic protein (GFAP) and S100 $\beta$  (both common biomarkers for OECs) was evident in the isolated lamina propria, suggesting that OECs remained viable after this time period. Immunostaining for these biomarkers after fifteen days in culture, however, was not seen. This observation provides further validation that isolated olfactory lamina propria can be sustained in culture for up to ten days. This result is important as it suggests that instead of transplanting the tissue into the spinal cord lesion immediately after dissection from the olfactory nervous system, it can be cultured for a short period of time, providing more flexibility in the implantation procedure.

## **METHODS AND MATERIALS**

The 2% methacrylated glycol chitosan (MGC), 2% methacrylated chondroitin sulfate-methacrylated glycol chitosan (MGC-CS), and 2% arginine-glycine-aspartic acid (RGD) - grafted methacrylated glycol chitosan was given to us by Dr. Brian Amsden (Queen's University) and prepared by Dr. Dale Marecak (Queen's University).

### ***Synthesis of agarose***

Agarose is a polysaccharide with alternating copolymers of 1,4-linked 3,6-anhydro- $\alpha$ -L-galactose and 1,3-linked  $\beta$ -D-galactose. Agarose is soluble in water at temperatures above 65°C and depending upon the degree of hydroxyethyl substitutions on its side chains, it gels in a range of 17-40°C. Once agarose gels, it is stable and does not swell at constant temperature or re-liquify until heated to 65°C. SeaPrep® agarose is commercially available and does not swell at constant temperature and forms an optically clear gel at 17°C. Agarose gels were fabricated as 1%, 2%, and 4% gels (wt/vol), by dissolving powdered agarose in sterile saline.

### ***Dissection and preparation of rodent lamina propria***

Adult rats which were already killed by decapitation were obtained from Dr. Dave Andrew (Queen's University). The nasal septum was freed by removal of the lower jaw, the upper teeth and the turbinates. The two olfactory mucosae lining the posterior part of

the nasal septum and two pieces of the respiratory mucosa lining the anterior portion of the septum were dissected and placed immediately onto poly-L-lysine (PLL)-coated plates (Sigma-Aldrich), fed Dulbecco's modified Eagle medium/ Ham's F12 (DMEM/F12; Sigma-Aldrich), 10% fetal bovine serum (Sigma-Aldrich), 2% penicillin/streptomycin (Sigma-Aldrich), 1% amphotericin B (Sigma-Aldrich) and maintained under standard culture conditions at 37°C in 5% CO<sub>2</sub>. The cell medium was changed every 2 days with fresh medium. The isolated lamina propria was maintained for 3, 4, 5, 8, and 10 days *in vitro*, and subsequently fixed with 4% paraformaldehyde in 0.1 M phosphate buffer (PB, pH 7.4), and then cryoprotected in phosphate-buffered 30% sucrose for 2-3 days. All tissues were embedded in Cryomatrix™ (Thermo Fisher Scientific) and frozen in -20°C 2-methylbutane for section with a cryostat. All tissues were sectioned at 20 µm thickness; the tissues were directly mounted onto Superfrost/Plus slides (Thermo Fisher Scientific), and immunofluorescence was commenced (see below).

### ***OEC cultures***

Frozen OECs obtained from rat olfactory tissue were thawed at 37°C and then transferred to culture plates (Sigma-Aldrich) with DMEM/ Ham's F-12, 10% fetal bovine serum (Sigma-Aldrich), 2% penicillin/streptomycin (Sigma-Aldrich), 1% amphotericin B (Sigma-Aldrich), and maintained under standard culture conditions at 37°C in 5% CO<sub>2</sub>. The cell medium was changed every 2 days with fresh medium. When the cells reached 90% confluence, they were lifted with 0.05% trypsin-EDTA (Sigma-Aldrich) and

replated. The OECs were passaged three times, at which point they were trypsinized and plated onto the hydrogels (methacrylated glycol chitosan, methacrylated glycol chitosan with RGD group attached, methacrylated chondroitin sulfate-methacrylated glycol chitosan, and agarose). The cell-seeded hydrogels were fed with culture medium, which was changed every 2 days. The cell-seeded hydrogels were maintained *in vitro* for 4 days (2% methacrylated glycol chitosan, 2% methacrylated chondroitin sulfate - methacrylated glycol chitosan, 1% agarose, and 2% agarose), 5 days (methacrylated glycol chitosan with RGD group attached), and 6 days (4% agarose). The hydrogels were subsequently fixed with 4% paraformaldehyde in 0.1 M phosphate buffer (PB, pH 7.4), and then cryoprotected in phosphate-buffered 30% sucrose for 2-3 days. All tissues were embedded in Cryomatrix™ (Thermo Fisher Scientific) and frozen in -20°C 2-methylbutane for sectioning with a cryostat. The hydrogel-cell suspensions were sectioned at 20 µm thickness; the tissues were directly mounted onto Superfrost/Plus slides (Thermo Fisher Scientific), and immunofluorescence was commenced. All experiments were repeated three times.

### ***Immunofluorescence***

Frozen sections of the rodent lamina propria and hydrogel-OEC matrices were allowed to thaw for 5 minutes before commencing immunostaining procedures at room temperature. The sections were treated with 4% phosphate-buffered paraformaldehyde (pH 7.4) for 15 minutes (this improves the adherence of the tissues to the slides) and rinsed in 0.1 M tris-buffered saline (TBS; pH 7.4) for 5 minutes; this rinsing step was repeated after each treatment. Those sections to be immunostained for the localization of

$\alpha$ SMA and calponin were pretreated with 0.008% proteinase K for 15-30 minutes (this step was often required to reveal antigenic sites in OECs). After treatment with 10% normal donkey serum (NDS) in 0.1M TBS plus 0.25% Triton-X100 (TBX) for 1 hour, sections were incubated for 24 hours with one of the following primary antibodies: mouse anti-synthetic  $\alpha$ SMA IgG (1:1000 dilution; Sigma-Aldrich) for detection in rat lamina propria sections; rabbit anti-bovine S100 $\beta$  IgG (1:500; Dako, Burlington, ON) for detection in all sections; rabbit anti-bovine GFAP IgG (1:250; Dako) for detection in all sections; rabbit anti-recombinant rat growth associated protein-43 (GAP-43) IgG (1:1000; Millipore, Etobicoke, ON) for detection in rat lamina propria sections; goat anti-human calponin IgG (1:500; Santa Cruz, Santa Cruz, CA) for detection in rat lamina propria sections; and, rabbit anti-synthetic Iba1 IgG (1:400; Wako, Richmond, VA) for detection in rat lamina propria sections. These antibodies were diluted in a final solution containing 3% NDS in 0.25% TBX. After rinsing, the sections were then incubated for 2 hours with the appropriate secondary antibodies: FITC-conjugated donkey anti-mouse IgG (1:100; for the detection of  $\alpha$ SMA), FITC-conjugated donkey anti-rabbit IgG (1:100; for the detection of S100 $\beta$ , GFAP, GAP-43, and Iba1), and FITC-conjugated donkey anti-goat IgG (1:100; for the detection of calponin). Secondary antibodies (Cedarlane) were diluted in a solution containing 3% NDS with 0.25% TBX. Sections were coverslipped with 4', 6-diamidino-2-phenylindole (DAPI)-conjugated mounting media (Vector Laboratories, Burlington, ON). The immunofluorescence was viewed and photographed with a Zeiss microscope. Images were captured using a Zeiss AxioCam high resolution scanning digital camera with Axiovision software (version 4.2). After

adjusting the images for brightness and contrast, these images were converted to .tif files and used to generate figures with Adobe Illustrator CS5.

### ***Nissl staining***

Nissl staining was performed on the cell culture wells for the experiment involving the application of an agarose biomatrix on top of cultured OECs. First, culture wells were fixed with 4% paraformaldehyde for 48 hours. Thionin solution (Sigma-Aldrich) was then added to each well three times. The wells were then dehydrated with a graded series of ethanols and then viewed under bright-field optics with a Zeiss microscope.

## **RESULTS**

In this study, three variations of methacrylated glycol chitosan (MGC) biomatrices were examined to determine their potential to support survival of cultured olfactory ensheathing cells (OECs) for a period of 4, 5, or 6 days. In addition to these three variations of MGC, we also tested the ability of agarose gels (at three different concentrations) to support the survival of OECs. Finally, strips of olfactory mucosa isolated from the rodent olfactory system were cultured for 3, 4, 5, 8, 10, or 15 days and stained with markers for olfactory axon growth as well as to examine cell viability.

Rodent OECs that were expanded for two weeks *in vitro* were seeded on the surface of the 2% MGC gel and cultured for 4 days. The gels were fixed, frozen, sectioned, and then stained with 4', 6-diamidino-2-phenylindole (DAPI) to reveal

individual cell nuclei. Under the fluorescent microscope, no individual cells were observed (data not shown).

The second variation of MGC examined in this study was MGC with methacrylated chondroitin sulfate (MGC-CS). We speculated that the negatively-charged chondroitin sulfate will promote cell adherence to the biomatrix. This polymer was constructed by dissolving and mixing methacrylated chondroitin sulfate with the MGC polymer in deionized water to result in a final concentration of 2%. After addition of the photoinitiator cross-linker and irradiation of the mixture with ultraviolet light, the 2% MGC-CS mixture became a viscous gel. Rat OECs that were expanded for two weeks *in vitro* were seeded on the surface of the 2% MGC-CS gel and cultured for 4 days. The gels were fixed, frozen, sectioned, and then stained with DAPI to reveal individual cell nuclei. Under the fluorescent microscope, no individual cells were observed (data not shown).

The third variation of MGC investigated in this study was MGC with an arginine-glycine-aspartic acid (RGD) ligand group grafted into the MGC backbone (MGC-RGD). As speculated by Sukarto and colleagues (2012), grafting of a peptide containing the cell ligand binding motif RGD onto the MGC backbone may optimize the viability of rodent OECs. To construct this polymer, a Michael-type addition reaction was employed between the MGC and a thiol on a cysteine within the peptide Ac-GCGYGRGDSPG-NH<sub>2</sub>. The resulting MGC-RGD mixture was then cured with the addition of the photoinitiator cross-linker and ultraviolet irradiation. The resulting product was a viscous gel with a concentration of 2%. Rodent OECs that were expanded for two weeks *in vitro*

were seeded on the surface of the 2% MGC-RGD gel and cultured for 5 days. The gels were fixed, frozen, sectioned, and then stained with DAPI to reveal individual cell nuclei. Under the fluorescent microscope, only a scarce population of cells were observed around the perimeter of the gels (data not shown). In an effort to promote cell growth further, we photoencapsulated OECs within a MGC-RGD polymer, with the rationale that the RGD peptide groups would be more accessible to cells encapsulated within the polymer (as opposed to cells seeded on the surface). To accomplish this cell encapsulation, MGC-RGD polymers were dissolved in either a solution of cell media or phosphate buffer saline (PBS). These two solutions were then mixed with the photoinitiator cross-linker and rat OECs which have been expanded for two weeks and then lifted for this experiment. The resulting MGC-RGD/ photoinitiator/ OEC solutions were then cured with ultraviolet irradiation, yielding 2% viscous gels (either 2% MGC-RGD in cell media or 2% MGC-RGD in PBS). The gels were cultured for 5 days and were then fixed, frozen, sectioned and then stained for DAPI to reveal individual cell nuclei, as well as stained for S100 $\beta$  and glial fibrillary acidic protein (GFAP) to reveal the cytoplasm and cytoplasmic extensions (Figure 12). The MGC-RGD gel that was made in cell media had consistent cell survival throughout the gel at all sections. The MGC-RGD gel that was made in PBS also had consistent cell survival throughout the gel at all sections; however, it had an even greater cell consistency than the MGC-RGD gel made in cell media. Immunostaining for S100 $\beta$  and GFAP was performed on the MGC-RGD gels made in PBS as there was greater cell viability on these gels. Though DAPI-staining yielded consistent cell viability throughout the gels, staining for S100 $\beta$  and GFAP was sparse in comparison. In a cluster of about ten to twenty cell nuclei, only one

or two cells stained positively for S100 $\beta$  and GFAP; the cells which did stain positively for both markers did not appear very healthy. These cells appeared shriveled and condensed, atypical of the healthy cultured OEC that usually extends many cytoplasmic processes.

In an effort to determine whether OEC survival can be promoted in another type of biomatrix, we investigated agarose gels at concentrations of 1%, 2%, and 4%. Rodent OECs that were expanded for two weeks *in vitro* were encapsulated within the agarose gels during the gelation process and cultured for 4 or 6 days. The gels were fixed, frozen, sectioned, and then stained with DAPI to reveal individual cell nuclei. Under the fluorescent microscope, no individual cells were observed (data not shown). To determine whether stressful conditions will promote cell migration and survival in the agarose gel, rat OECs were seeded in 6-well culture plates and fed cell media for 1 week. Agarose gels that were 4% in concentration were then constructed and placed in each of the 6 wells containing OECs. After 6 days of culturing, the gels were fixed, frozen, sectioned, and then stained with DAPI to reveal individual nuclei. The wells were also Nissl-stained to examine viability of cells that did not migrate into the agarose gel. Under the light microscope, no Nissl-stained cells were observed (data not shown). Furthermore, under the fluorescent microscope, no individual cells were observed within the gels (data not shown).

Given the previous use of olfactory mucosal strips for spinal cord implantation (Lu et al., 2001, 2002; Lima et al., 2006, 2010), we sought to determine whether strips of olfactory mucosa isolated from the rodent olfactory system would be able to sustain

OECs in culture for 3, 4, 5, 8, 10, and 15 days in culture. The structural integrity of the rodent olfactory mucosal strips remained relatively intact after 3 and 4 days in culture compared to mucosal strips that were cultured for 5-15 days. In the mucosal strips that were cultured for 3 and 4 days, the olfactory fascicles were very defined, with a prominent layer of perineurial fibroblasts surrounding each fascicle. In the mucosal strips that were cultured for 5 days or more, however, it became less obvious as to identifying individual fascicles, as the mucosal tissue seemed to be looser and not as organized.

After 3, 4, and 5 days in culture, numerous growth associated protein-43 (GAP-43)-expressing olfactory axons were present in the lamina propria fascicles (Figures 13, 14, and 15). In addition to the GAP-43 immunoreactivity seen in the fascicles, there was positive GFAP immunostaining, indicating the presence of GFAP-immunopositive OECs. S100 $\beta$  immunostaining was prominent within the fascicles as well. Though positive immunostaining for  $\alpha$ SMA was seen in the perineurial fibroblasts surrounding the olfactory fascicles, there was a pronounced lack of  $\alpha$ SMA immunostaining in the OECs. Microglia cells stained positive for Iba-1 in both the olfactory fascicles as well as the olfactory epithelium. Similarly to  $\alpha$ SMA, calponin-positive perineurial fibroblasts were observed, but not OECs.

After 8 and 10 days in culture, OECs displayed positive immunostaining for both GFAP and S100 $\beta$  (Figure 16). Though the fascicles were somewhat observable, they were not as intact as the fascicles present in the strips cultured for 3 and 4 days. Positive immunostaining for GFAP was not as pronounced in the mucosal strips cultured for 10

days as it was for the mucosal strips cultured for 3, 4, 5, and 8 days. As seen in the mucosal strips cultured for 3, 4, and 5 days,  $\alpha$ SMA-immunopositive perineurial fibroblasts, but not  $\alpha$ SMA-immunopositive OECs, were observed surrounding the fascicles of mucosal strips cultured for 8 and 10 days.

In olfactory mucosal strips cultured for 15 days, the structural integrity of the lamina propria was lost, making it difficult to identify individual olfactory nerve fascicles (data not shown). In addition, positive immunostaining for GFAP, S100 $\beta$ , and  $\alpha$ SMA was not present.

## **FIGURES**

**Figure 12:** Immunostaining assay for survival of olfactory ensheathing cells (OECs) encapsulated in methacrylated glycol chitosan - with an arginine-glycine-aspartic acid group attached – (MGC-RGD) biomatrices mixed with cell media or phosphate buffer saline (PBS). Cells were cultured for 5 days and biomatrices were fixed and stained with DAPI, S100 $\beta$ , and glial fibrillary acidic protein (GFAP). All sections are in cross-sectional view. **A, B.** OECs (blue) are found distributed consistently throughout MGC-RGD biomatrices mixed in cell media (**A**) and PBS (**B**). **C, D.** One S100 $\beta$ -immunopositive OEC (green) is found amongst a cluster of OECs in a MGC-RGD biomatrix mixed with PBS at low magnification (**C**) and at high magnification (**D**). **E, F.** One GFAP-immunopositive OEC (green) is found amongst a group of OECs in a MGC-RGD biomatrix mixed with PBS at low magnification (**E**) and at high magnification (**F**). Staining for GFAP and S100 $\beta$  is shown in green. Scale bars = 100  $\mu$ m (**A, B, C, E**), and 50  $\mu$ m (**D, F**).

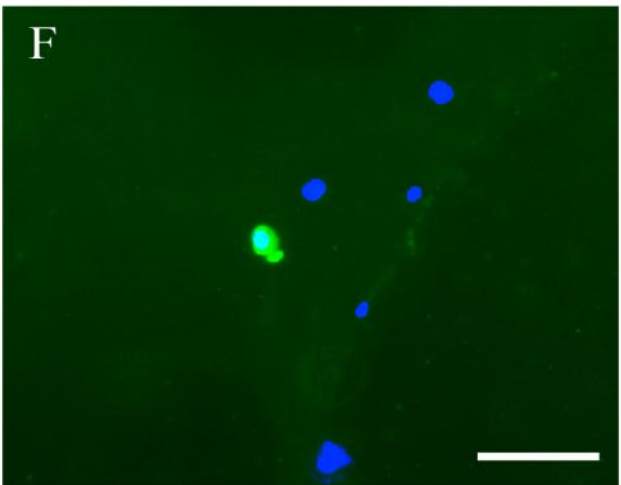
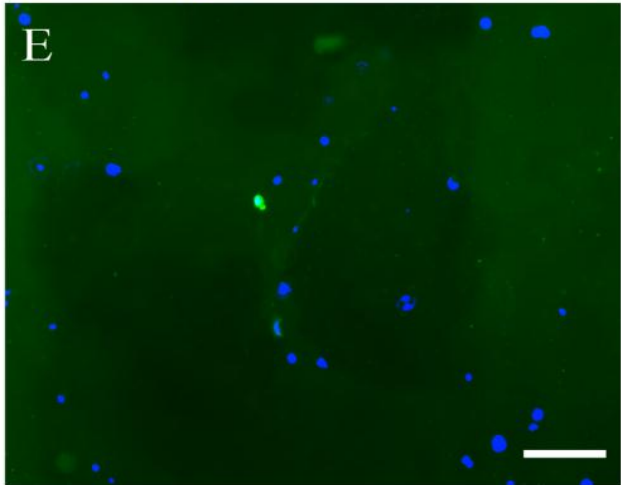
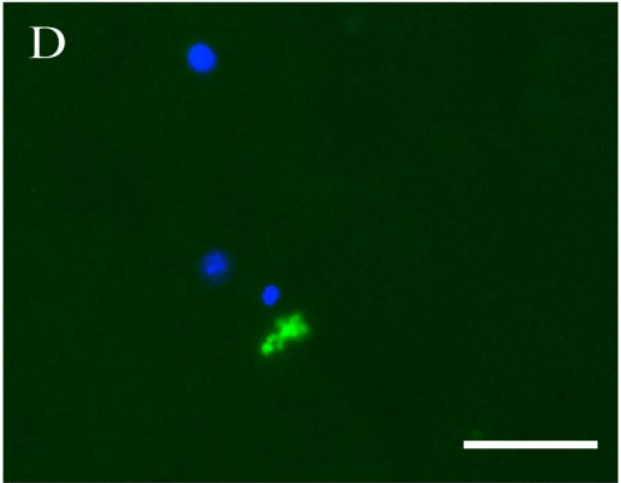
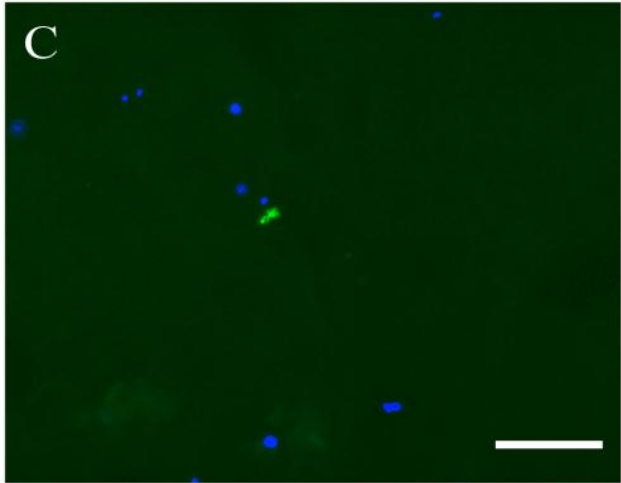
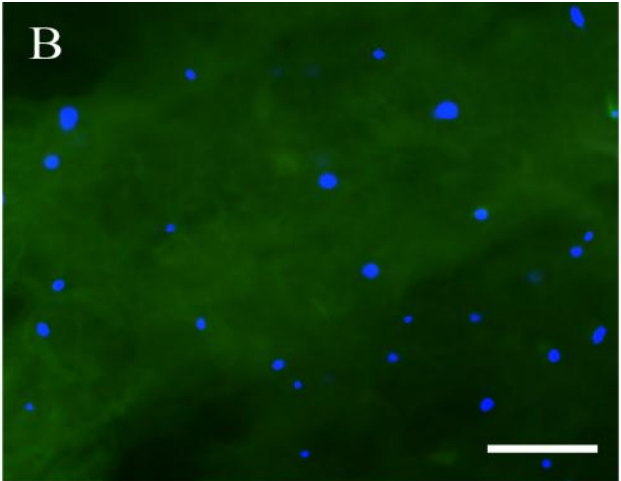
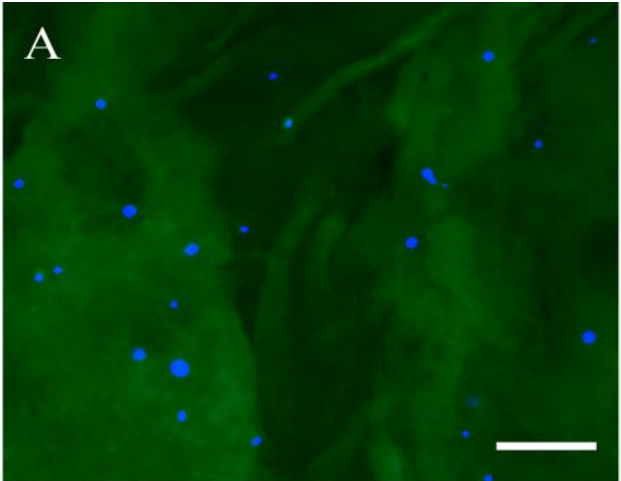


**Figure 13:** Immunostaining of rat lamina propria sections cultured for 3 days for growth associated protein-43 (GAP-43), glial fibrillary acidic protein (GFAP), S100 $\beta$ ,  $\alpha$ -smooth muscle actin ( $\alpha$ SMA), Iba1, and calponin. **A.** GAP-43-immunopositive olfactory axons are found within the olfactory nerve fascicles (FAS). **B.** Populations of GFAP-immunopositive olfactory ensheathing cells (OECs) are found inside the olfactory nerve fascicles. **C.** Populations of S100 $\beta$ -immunopositive OECs are seen in the olfactory nerve fascicles. **D.**  $\alpha$ SMA-immunopositive perineurial fibroblasts, but not  $\alpha$ SMA-immunopositive OECs, are evident surrounding the olfactory nerve fascicles. **E.** Positive staining for Iba1 (marker for microglia) is seen within an olfactory nerve fascicle as well as within the olfactory epithelium (OE). **F.** Though calponin-immunopositive OECs are not evident in an olfactory nerve fascicle, calponin-immunopositive perineurial fibroblasts are seen surrounding the fascicles. All sections have DAPI staining (blue) to reveal the individual nuclei. Staining for GAP-43, GFAP, S100 $\beta$ ,  $\alpha$ SMA, Iba1, and calponin is shown in green. Sections **A-C**, and **E** are longitudinal views whereas sections **D** and **F** are cross-sectional views. Scale bars = 50  $\mu$ m (**A-D, F**), and 100  $\mu$ m (**E**).

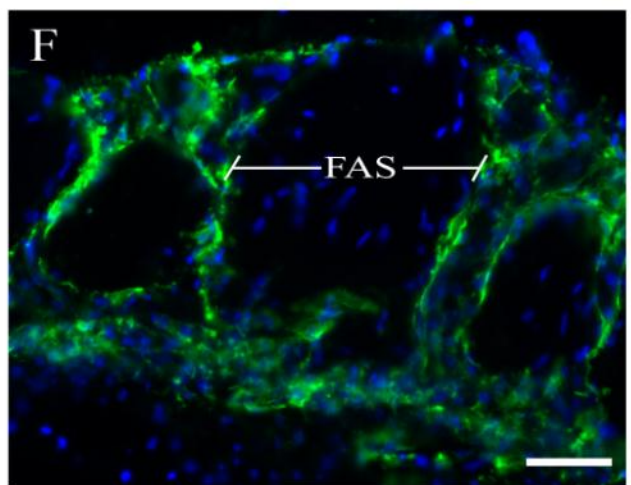
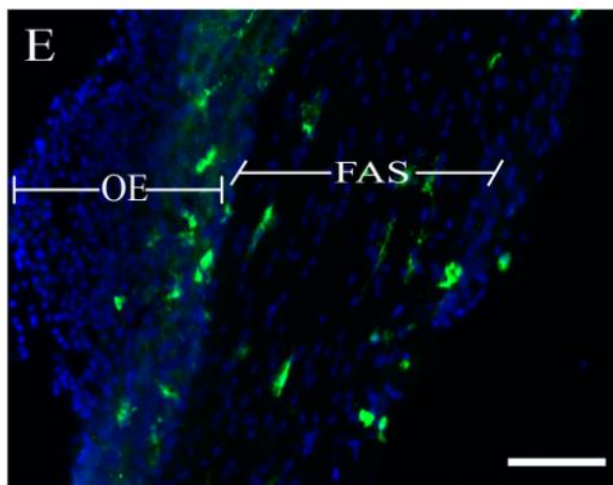
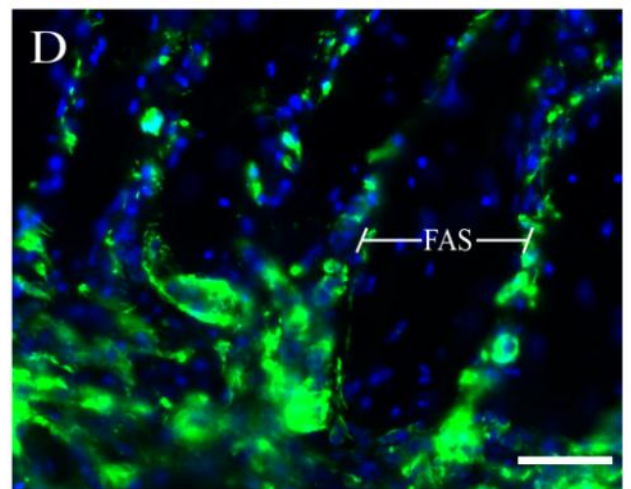
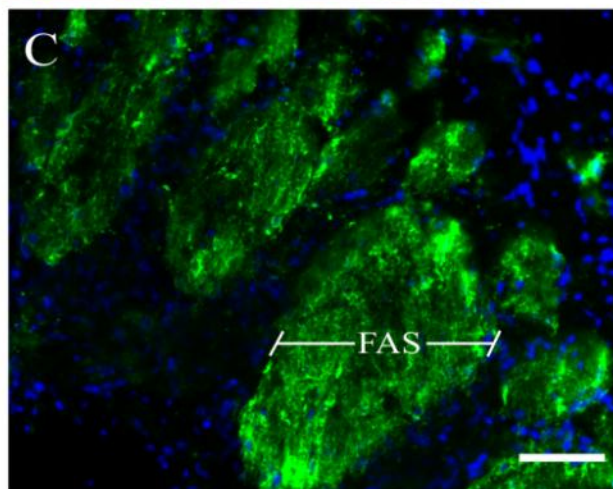
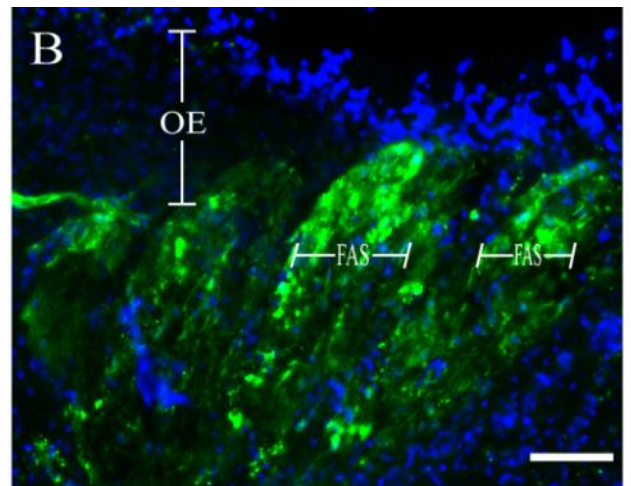
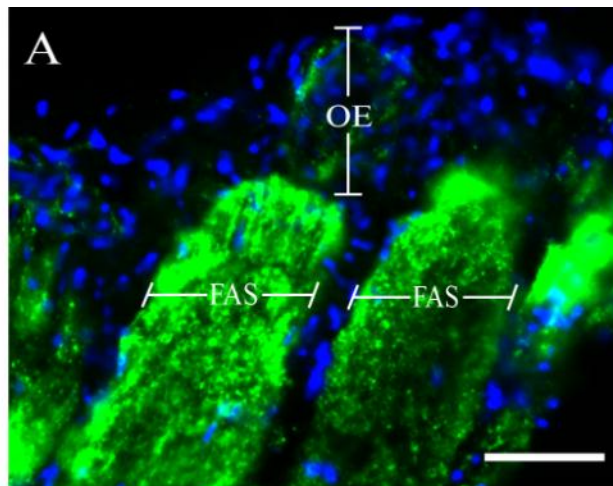


**Figure 14:** Immunostaining of rat lamina propria sections cultured for 4 days for growth associated protein-43 (GAP-43), glial fibrillary acidic protein (GFAP), S100 $\beta$ ,  $\alpha$ -smooth muscle actin ( $\alpha$ SMA), Iba1, and calponin. **A.** GAP-43-immunopositive olfactory axons are found within the olfactory nerve fascicles (FAS). **B.** Populations of GFAP-immunopositive olfactory ensheathing cells (OECs) are found inside the olfactory nerve fascicles. **C.** Populations of S100 $\beta$ -immunopositive OECs are seen in the olfactory nerve fascicles. **D.**  $\alpha$ SMA-immunopositive perineurial fibroblasts, but not  $\alpha$ SMA-immunopositive OECs, are evident surrounding the olfactory nerve fascicles. **E.** Positive staining for Iba1 (marker for microglia) is seen. **F.** Though calponin-immunopositive OECs are not evident in the olfactory nerve fascicles, calponin-immunopositive perineurial fibroblasts are seen surrounding the fascicles. All sections have DAPI staining (blue) to reveal the individual nuclei. Staining for GAP-43, GFAP, S100 $\beta$ ,  $\alpha$ SMA, Iba1, and calponin is shown in green. Sections **A-C**, **E**, and **F** are in longitudinal views whereas section **D** is in cross-sectional view. Scale bars = 50  $\mu$ m (**A-C**, **E**, **F**), and 25  $\mu$ m (**D**).

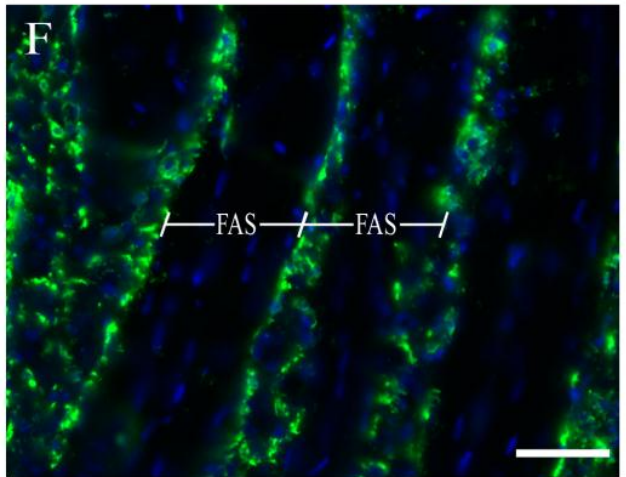
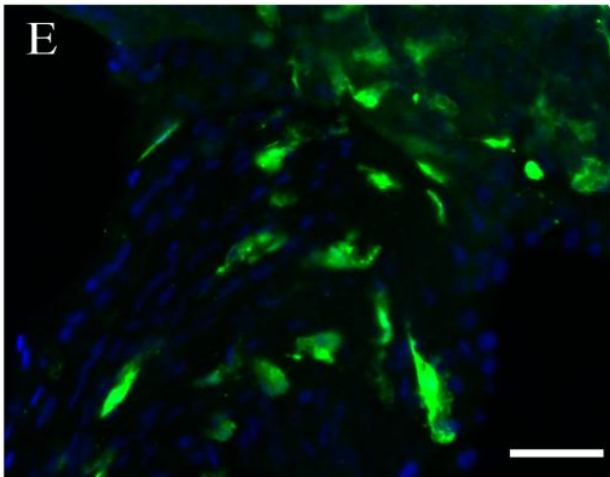
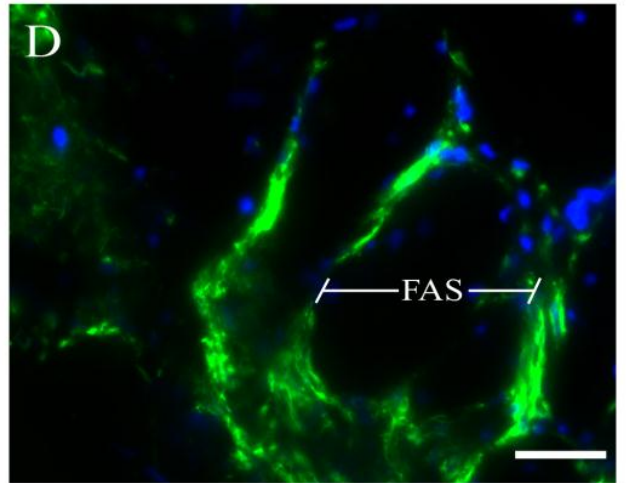
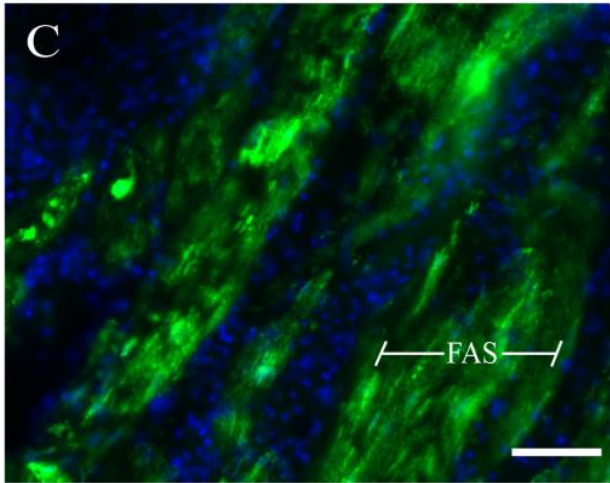
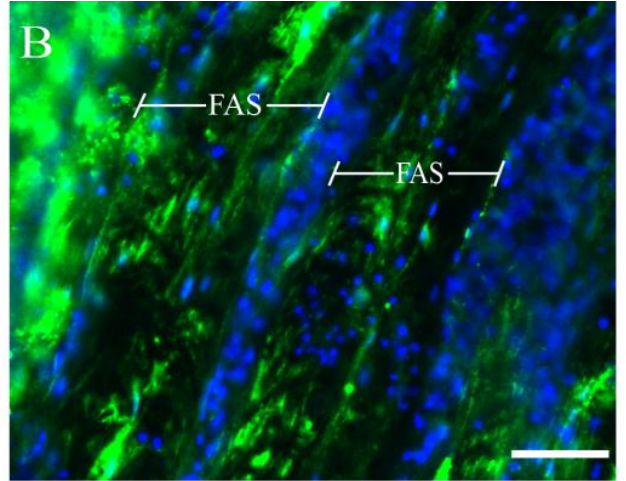
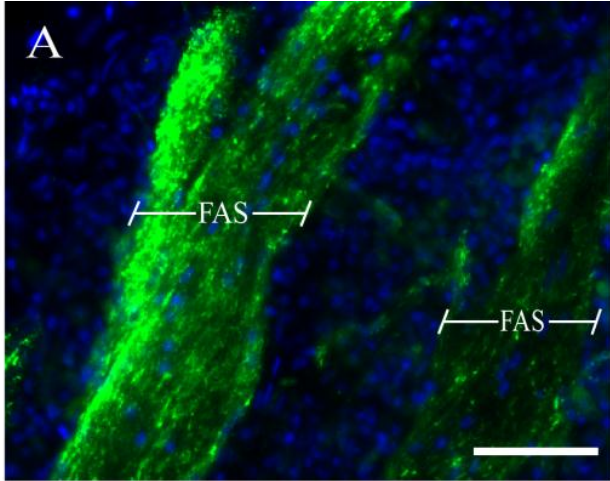


**Figure 15:** Immunostaining of rat lamina propria sections cultured for 5 days for growth associated protein-43 (GAP-43), glial fibrillary acidic protein (GFAP), S100 $\beta$ ,  $\alpha$ -smooth muscle actin ( $\alpha$ SMA), Iba1, and calponin. **A.** GAP-43-immunopositive olfactory axons are found within an olfactory nerve fascicle (FAS). **B.** Populations of GFAP-immunopositive olfactory ensheathing cells (OECs) are found inside an olfactory nerve fascicle. **C.** Populations of S100 $\beta$ -immunopositive OECs are seen in the olfactory nerve fascicles. **D.**  $\alpha$ SMA-immunopositive perineurial fibroblasts, but not  $\alpha$ SMA-immunopositive OECs, are evident surrounding an olfactory nerve fascicle. **E.** Positive staining for Iba1 (marker for microglia) is seen within an olfactory nerve fascicle. **F.** Though calponin-immunopositive OECs are not evident within olfactory nerve fascicles, calponin-immunopositive perineurial fibroblasts are seen surrounding the fascicles. All sections have DAPI staining (blue) to reveal the individual nuclei. Staining for GAP-43, GFAP, S100 $\beta$ ,  $\alpha$ SMA, Iba1, and calponin is shown in green. All sections are in longitudinal views. Scale bars = 50  $\mu$ m.

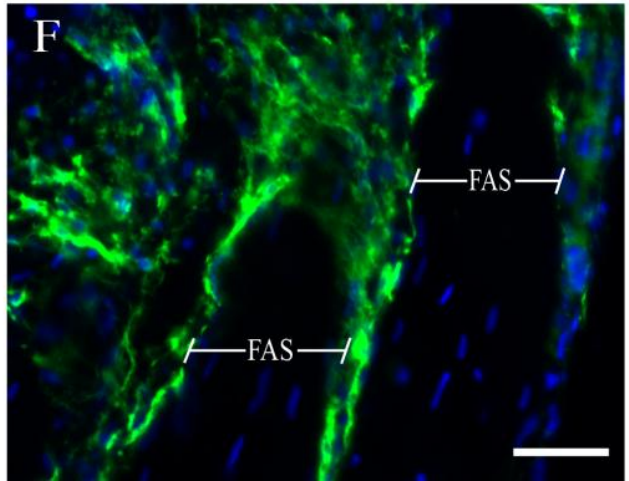
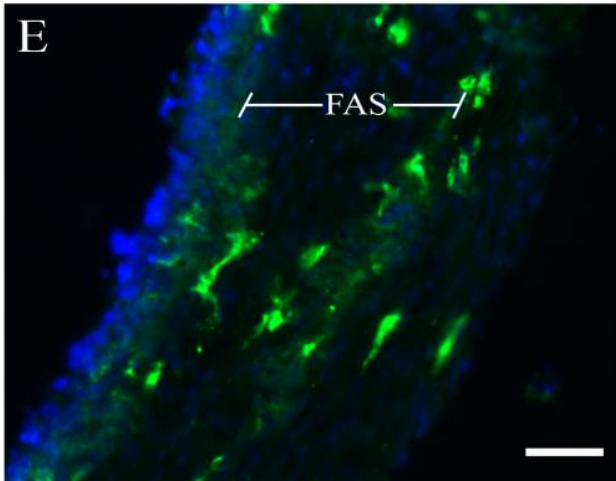
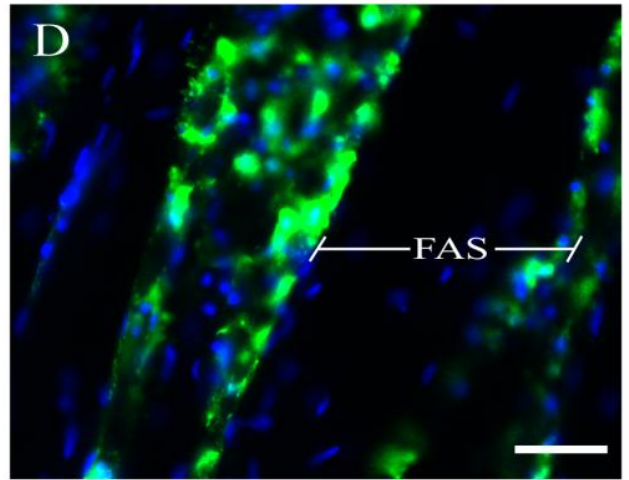
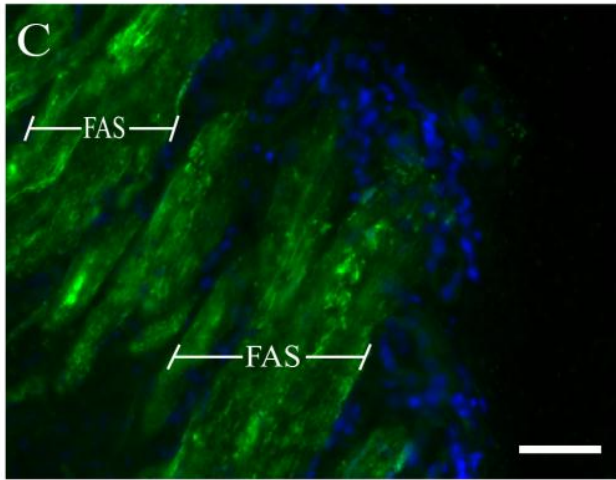
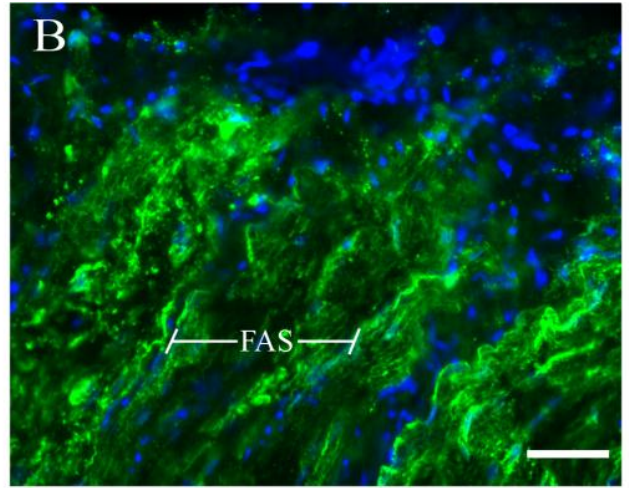
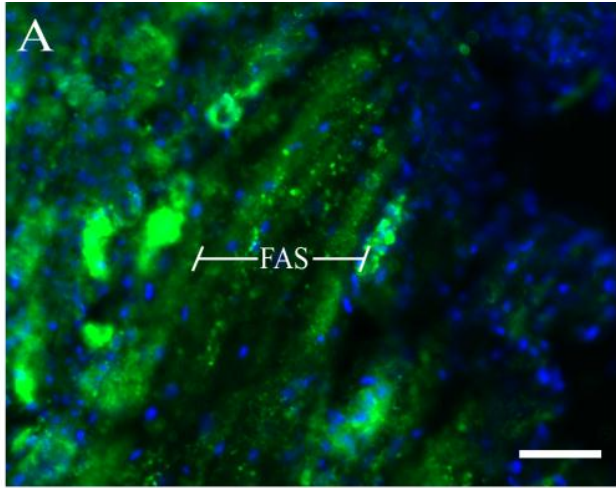
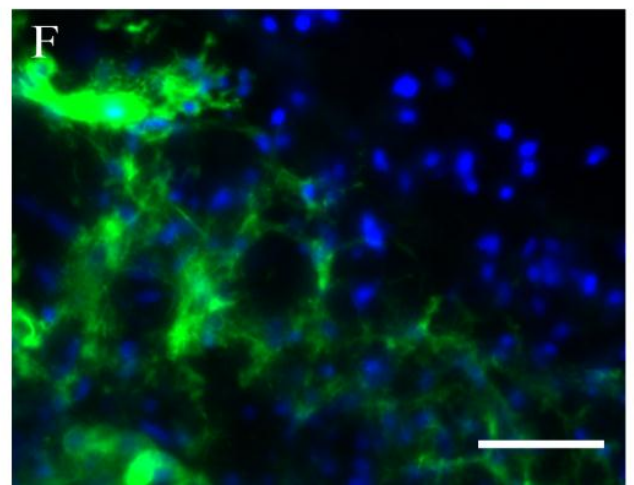
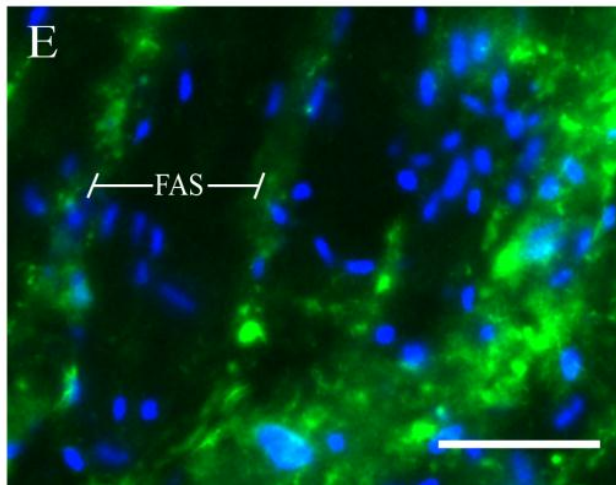
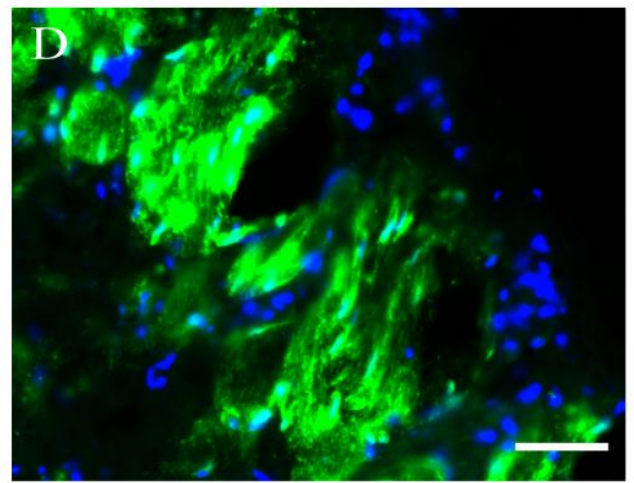
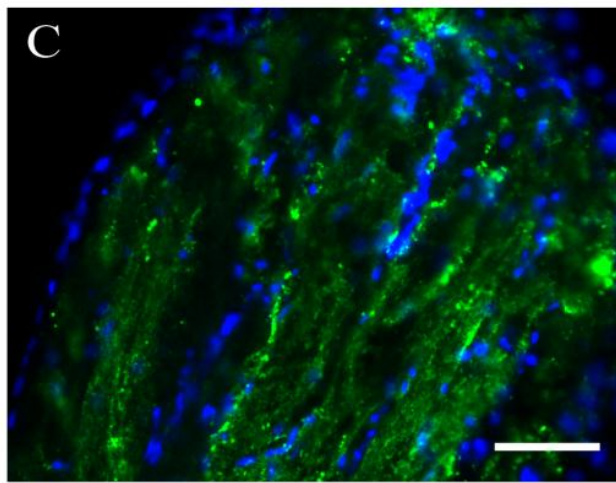
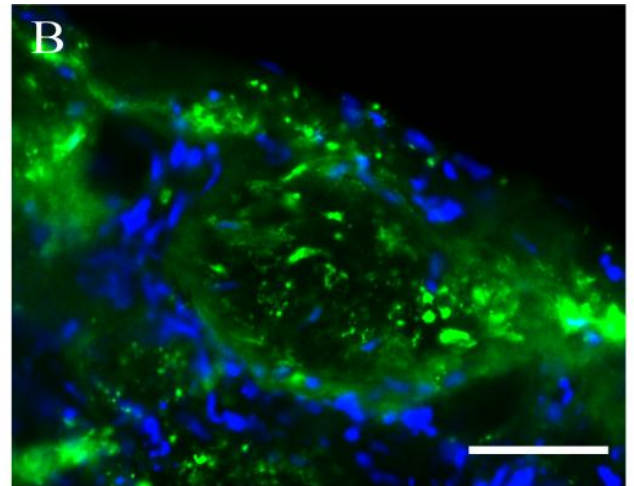
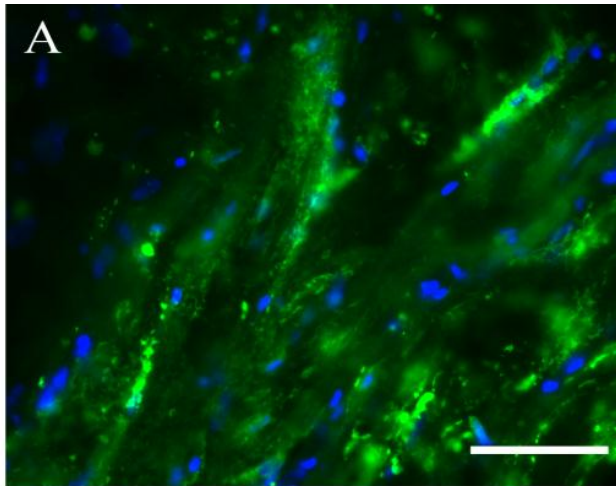


**Figure 16:** Immunostaining of rat lamina propria sections cultured for 8 (**A, C, E**) and 10 (**B, E, F**) days for glial fibrillary acidic protein (GFAP), S100 $\beta$ ,  $\alpha$ -smooth muscle actin ( $\alpha$ SMA). **A, B.** Populations of GFAP-immunopositive olfactory ensheathing cells (OECs) are found in cultures for 8 days (**A**) and for 10 days (**B**). **C, D.** Populations of S100 $\beta$ -immunopositive OECs are seen in cultures for 8 days (**C**) and for 10 days (**D**). **E, F.** In cultures for 8 days (**E**) and 10 days (**F**),  $\alpha$ SMA-immunopositive perineurial fibroblasts, but not  $\alpha$ SMA-immunopositive OECs, are evident. All sections have DAPI staining (blue) to reveal the individual nuclei. Staining for GFAP, S100 $\beta$ , and  $\alpha$ SMA is shown in green. Sections **A-E** are in longitudinal views whereas section **F** is in cross-sectional view. Scale bars = 50  $\mu$ m.



## DISCUSSION

In this study, we examined the ability of various biomatrices to promote and sustain growth and survival of cultured rodent OECs. In addition to analysing these biomatrices, we also investigated the potential of OECs to survive in olfactory mucosal strips isolated from the rodent olfactory system and cultured between 3 to 15 days. Though methacrylated glycol chitosan (MGC) and its variations (chondroitin-sulfate [MGC-CS] and arginine-glycine-aspartic acid [MGC-RGD] groups attached), as well as the agarose-based biomatrix did not sustain or promote healthy OEC survival, this observation provides new insight into developing biomatrices with properties which may encourage OEC survival. When isolated olfactory mucosal strips from the rodent olfactory system were cultured, OECs remained viable for 10 days in culture. Positive immunostaining for GFAP and S100 $\beta$  was seen, indicating the presence of viable OECs in the mucosal strips. In addition,  $\alpha$ SMA immunostaining and calponin immunostaining displayed healthy survival of perineurial fibroblasts as well as intact olfactory nerve fascicles. Immunostaining for Iba-1 displayed a healthy population of microglia and immunostaining for GAP-43 indicated many regenerating olfactory axons in the isolated olfactory mucosal strips. These results suggest that olfactory mucosal transplants are viable in culture for a short period of time, providing more flexibility prior to intraspinal transplantation. Despite these results, there is potential in developing biomatrices and using autologous olfactory mucosal strips for spinal cord transplantation.

MGC has been demonstrated to provide consistent cell attachment and proliferation of cultured chondrocytes, promoting uniform tissue growth (Amsden et al., 2007). In addition, the relatively mild gelation conditions of this gel allow effective

encapsulation of cells under physiological temperature and pH (Bryant and Anseth, 2002). Despite these promising attributes of this biomatrix, we did not observe any cell attachment or proliferation when OECs were seeded directly on top of MGC, MGC-CS, or MGC-RGD. When cells were photoencapsulated within the MGC-RGD polymer, however, cell attachment and survival was seen after five days *in vitro*. The incorporation of the RGD peptide group may have promoted cell adherence, allowing the cells to remain attached. Though the cells seemed to attach and remain viable, GFAP and S100 $\beta$  immunostaining was weak, indicating that the cells were not healthy in these biomatrices. It has been shown that cultured OECs under typical growth conditions consistently express GFAP and S100 $\beta$  (Au and Roskams, 2003; Jahed et al., 2007; Krudewig et al., 2006; Radtke et al., 2004; Techangamsuwan et al., 2009). To potentially improve the ability of this biopolymer to provide the necessary support for OECs to successfully grow and proliferate during spinal cord transplantation, growth factors may be supplemented to the factors already present in the serum-containing cell media. Growth factors shown to induce OEC survival and proliferation *in vitro* are basic fibroblast growth factor, glial growth factor 2, as well as forskolin (Chuah et al., 2000; Chuah and Teague, 1999 Yan et al., 2001). Supplementing cell media with these growth factors or delivering these growth factors through MGC-embedded microspheres may encourage OEC proliferation in this particular biomatrix (Sukarto and Amsden, 2012).

Another factor contributing to the lack of OEC proliferation in this biogel may be due to the intensity of UV light used during photopolymerization. During this polymerization process, UV light homolytically (i.e. breaking of a single bond in which one electron stays with each atom from the electron pair) cleaves photoinitiator molecules

to free radical species which then initiate the polymerization reaction. These free radical species, however, may also subsequently react with phospholipids of cell membranes and form oxygen reactive species. These oxygen reactive species may then lead to lipid peroxidation, protein damage, as well as DNA damage (Cerutti, 1985; Terakado et al., 1984). The photopolymerization performed in this study used UV light at an intensity of 10 mW/cm<sup>2</sup> for 4 minutes, which may have caused some damage to the OECs present in the gel solution. Though some studies have shown that goat bone marrow mesenchymal stem cells were viable under UV intensities of 4 and 6 mW/cm<sup>2</sup>, different cell types may have variable responses (Fedorovich et al., 2009; Williams et al., 2005). Reducing the intensity and duration of UV irradiation may also help to promote OEC proliferation within this biomatrix.

In addition to investigating the properties of MGC and its variations, we also examined the ability of agarose to sustain and promote OEC proliferation. Agarose is a polysaccharide that is easily prepared and has been shown to stimulate neurite extension from cultured dorsal root ganglia (Balgude et al., 2001; Bellamkonda et al., 1995). Here we show that OECs are not able to attach to and grow in an agarose construct. When OECs were encapsulated within agarose gels at concentrations of 1%, 2%, and 4%, no cells were observed after 4 or 6 days of culturing. This pronounced lack of survival may be due to agarose not having sufficient chemical moieties for the cells to attach to and proliferate. In addition to not observing OEC survival when these cells were encapsulated in agarose gels, we did not see any OEC survival when agarose gels were placed on top of the cells in culture wells (after allowing the cells to proliferate for 1 week). This result indicates that agarose may be cytotoxic to OECs. In addition to the

poor outcome of OEC survival with agarose gels seen in this study, it has also been shown that agarose has a poor degradation rate *in vivo*, limiting the potential of this polymer to be useful in intraspinal transplantation (Hunziker, 2002).

To date, only two groups have used isolated strips of olfactory mucosa in spinal cord transplantations studies (Lu et al., 2001, 2002; Lima et al., 2006, 2010). Lu and colleagues (2001, 2002) used autografts from rats and observed a significant recovery in locomotor movement. Lima and colleagues (2006, 2010) performed pilot studies on human patients with complete spinal cord injury using autologous olfactory mucosal grafts and observed motor improvements in most of the patients. In this study, we isolated olfactory mucosal strips from rats and cultured them for 3 to 15 days, investigating their structural integrity as well as OEC viability. For mucosal strips cultured for 3 to 10 days, the anatomical structure remained fairly intact, with the individual olfactory nerve fascicles still being readily identifiable with  $\alpha$ SMA-expressing and calponin-expressing perineurial fibroblasts surrounding them (more so for mucosal strips cultured for 3 to 4 days than for mucosal strips cultured for 5 to 10 days). In addition, regenerating olfactory axons expressing GAP-43, as well as GFAP- and S100 $\beta$ -expressing OECs were observed, indicating survival of the cultured tissue. Though these results are encouraging, mucosal strips cultured for 15 days showed no positive OEC or fibroblast immunostaining, indicating that 15 days *in vitro* is too long in duration for these tissues to survive. These results suggest that 3 to 10 days is the optimal length of time that these mucosal strips can be sustained *in vitro* with these culture conditions. Future directions with this approach may be to transplant these cultured mucosal strips into the injured spinal cord. None of the four studies that used this approach for

intraspinal implantation commented on how the mucosal strips were aligned inside the spinal cord lesion. Aligning the olfactory nerve fascicles with the severed descending and ascending nerve tracts may promote directional neural growth across the lesion cavity, possibly improving functional outcome further than was seen in the other four studies.

In conclusion, we have investigated the potential of various transplantation methods to support and promote OEC viability and proliferation *in vitro*. Though OECs photoencapsulated in MGC-RGD gels showed viability, there was a paucity in the expression of two common OEC biomarkers as well as a pronounced lack in proliferation. Addition of growth factors to the biomatrix, increasing RGD concentration, or reducing the intensity and duration of the UV light during photopolymerization may all be methods to improve cellular viability and proliferation with this gel. In this study, we also showed no cell growth using agarose as a biomatrix. Finally, culturing olfactory mucosal strips isolated from the rodent olfactory system showed some survival when cultured for 3 to 10 days. Future directions would be to employ these cultured mucosal strips in a spinal cord transplantation model.

## **ACKNOWLEDGEMENTS**

This work was supported by a grant from the Botterell Foundation at Queen's University. Khalil S. Rawji is supported by an Ontario Graduate Scholarship. We would like to thank Dr. Brian Amsden for the methacrylated glycol chitosan hydrogels, as well as Dr. Dale Marecak for the preparation of the methacrylated glycol chitosan hydrogels. We would also like to thank Ms. Verna Norkum for the preparation of tissues and sections for fluorescent microscopic assessments.

## **CHAPTER 4: CONCLUSION**

Spinal cord injury is an incapacitating event which affects many people every year. Most spinal cord injuries result in a loss of sensorimotor conduction below the level of the lesion, mainly due to cellular injury, nerve demyelination, and axon retraction. Currently, spinal cord repair results in limited recovery. One promising approach for spinal cord injury is cellular transplantation.

In animal models of spinal cord injury, as well as to a degree in some clinical trials, the use of olfactory ensheathing cells (OECs) for spinal cord transplantation has been investigated. OECs are the main glial cell in the olfactory nervous system and are thought to be responsible for the successful directional growth of new olfactory axons from the olfactory mucosa (peripheral nervous system) to the olfactory bulb (central nervous system). Due to this unique capability of promoting neurogenesis as well as being able to thrive both peripherally and centrally, OECs have been targeted as a promising approach for spinal cord injury.

Despite these favourable features of OECs, there are a few challenges associated with this cellular transplantation strategy: i.) It is difficult to accurately identify and isolate OECs from their native olfactory environment due to the phenotypic biomarkers of these cells being very similar to those of Schwann cells, astrocytes, and fibroblasts; ii.) Once transplanted into the injured spinal cord, the exact function of OECs is unknown as it is difficult to distinguish them from other glial cells (such as myelinating Schwann cells); iii.) OECs transplanted into the spinal cord usually have low survival; iv.) Regenerating axons after intraspinal transplantation of OECs have difficulty innervating the appropriate targets.

To address the former two challenges, we investigated the neurochemical features of OECs in five mammalian species (including hamsters, rabbits, monkeys, mice, and pigs) using three biomarkers, glial fibrillary acidic protein (GFAP), S100 $\beta$ , and  $\alpha$ -smooth muscle actin ( $\alpha$ SMA). We found that both mucosal and bulbar OECs of all five mammalian species express S100 $\beta$ ; mucosal OECs, but not bulbar OECs, express GFAP in adult hamsters and monkeys (adult mice only have a sparse population of OECs expressing GFAP); both mucosal and bulbar OECs of monkeys as well as bulbar OECs of hamsters and mucosal OECs of rabbits express  $\alpha$ SMA. This comparative neurochemical analysis of OECs highlights the efficacy of S100 $\beta$  and  $\alpha$ SMA as biomarkers for mammalian OECs *in vivo*, providing more knowledge to aid in phenotypically distinguishing these cells from other types of cells.

To address the latter two challenges, we investigated the capacity of a few synthetic polymers as well as isolated strips of olfactory lamina propria to sustain and promote OEC growth and proliferation. In this study, we found that MGC, methacrylated chondroitin sulfate-MGC, and agarose failed to promote proliferation of rodent OECs *in vitro*. Only when OECs were photoencapsulated within RGD-MGC did they survive for 5 days (despite lacking positive immunostaining for GFAP and S100 $\beta$ ). Future studies using these biogels for OECs should consider the following three points: i.) The intensity and length of time used for ultraviolet irradiation in this study may have been too strong and may have contributed to cell damage; ii.) The degree of RGD-grafting to the MGC backbone may have not been high enough to promote sufficient cell adherence; iii.) The incorporation of growth factors such as glial growth factor 2 and basic fibroblast growth factor may promote cell survival.

In this study, we also found that isolated strips of olfactory lamina propria from the rodent olfactory system maintain their histological architecture between three and ten days of culturing. In addition, positive immunostaining for GFAP, S100 $\beta$ ,  $\alpha$ SMA, calponin (for perineurial fibroblasts), growth associated protein (GAP)-43 (for regenerating axons), and Iba1 (for microglia) is retained, suggesting that OECs, fibroblasts, and microglia are able to survive and that neurogenesis can occur in these culture conditions. These results show promise for the idea of transplanting autologous olfactory lamina propria tissue in spinal cord injuries. Future studies should examine the efficacy of these isolated lamina propria strips in spinal cord injury models.

In conclusion, OECs present an exciting cellular therapy for spinal cord injury. Though positive findings for spinal cord transplantation have been reported in the literature, there is much to learn about this unique glial population. Investigating the neurochemical properties of OECs will allow us to better distinguish these cells from other cell populations, leading to more accurate isolation prior to, and enhanced identification after, intraspinal implantation. In addition, by finding biopolymers which are biocompatible with these cells, the regenerative potential of these cells may be enhanced by providing a supportive, protective matrix, ultimately, with hope, advancing this therapy to help alleviate the burden experienced by thousands of patients currently suffering with spinal cord injury.

## REFERENCES

Acheson A, Barker PA, Alderson RF, Miller FD, Murphy RA. 1991. Detection of brain-derived neurotrophic factor-like activity in fibroblasts and Schwann cells: inhibition by antibodies to NGF. *Neuron* 7:265-275.

Adegboyega PA, Mifflin RC, DiMari JF, Saada JI, Powell DW. 2002. Immunohistochemical study of myofibroblasts in normal colonic mucosa, hyperplastic polyps, and adenomatous colorectal polyps. *Arch Pathol Lab Med* 126:829-836.

Aebischer P, Guenard V, Valentini RF. 1990. The morphology of regenerating peripheral nerves is modulated by the surface microgeometry of polymeric guidance channels. *Brain Res* 531:211-218.

Akiyama Y, Lankford K, Radtke C, Greer CA, Kocsis JD. 2004. Remyelination of spinal cord axons by olfactory ensheathing cells and Schwann cells derived from a transgenic rat expressing alkaline phosphatase marker gene. *Neuron Glia Biol* 1:47-55.

Amsden BG, Sukarto A, Knight DK, Shapka SN. 2007. Methacrylated glycol chitosan as a photopolymerizable biomaterial. *Biomacromolecules* 8:3758-3766.

Au E, Roskams AJ. 2003. Olfactory ensheathing cells of the lamina propria in vivo and in vitro. *Glia* 41:224-236.

Balgude AP, Yu X, Szymanski A, Bellamkonda RV. 2001. Agarose gel stiffness determines rate of DRG neurite extension in 3D cultures. *Biomaterials* 22:1077-1084.

Barakat DJ, Gaglani SM, Neravetla SR, Sanchez AR, Andrade CM, Pressman Y, Puzis R, Garg MS, Bunge MB, Pearse DD. 2005. Survival, integration, and axon growth support of glia transplanted into the chronically contused spinal cord. *Cell Transplant* 14:225-240.

Barber PC, Lindsay RM. 1982. Schwann cells of the olfactory nerves contain glial fibrillary acidic protein and resemble astrocytes. *Neuroscience* 7:3077-3090.

Barber PC. 1982. Neurogenesis and regeneration in the primary olfactory pathway of mammals. *Bibl Anat* 1:12-25.

Barnett SC, Alexander CL, Iwashita Y, Gilson JM, Crowther J, Clark L, Dunn LT, Papanastassiou V, Kennedy PG, Franklin RJ. 2000. Identification of a human olfactory ensheathing cell that can effect transplant-mediated remyelination of demyelinated CNS axons. *Brain* 123:1581-1588.

Barnett SC, Hutchins AM, Noble M. 1993. Purification of olfactory nerve ensheathing cells from the olfactory bulb. *Dev Biol* 155:337-350.

- Barraud P, Seferiadis AA, Tyson LD, Zwart MF, Szabo-Rogers HL, Ruhrberg C, Liu KJ, Baker CV. 2010. Neural crest origin of olfactory ensheathing glia. *Proc Natl Acad Sci USA* 107:21040-21045.
- Beharier O, Kahn J, Shusterman E, Sheiner E. 2012. S100B - A potential biomarker for early detection of neonatal brain damage following asphyxia. *J Matern Fetal Neonatal Med* [Epub ahead of print].
- Bellamkonda R, Ranieri JP, Bouche N, Aebischer P. 1995. Hydrogel-based three-dimensional matrix for neural cells. *J Biomed Mater Res* 29:663-671.
- Bjorklund A, Dunnett SB, Brundin P, Stoessl AJ, Freed CR, Breeze RE, Levivier M, Peschanski M, Studer L, Barker R. 2003. Neural transplantation for the treatment of Parkinson's disease. *Lancet Neurol* 2:437-445.
- Blits B, Boer GJ, Verhaagen J. 2002. Pharmacological, cell, and gene therapy strategies to promote spinal cord regeneration. *Cell Transplant* 11:593-613.
- Bock P, Beineke A, Techangamsuwan S, Baumgartner W, Wewetzer K. 2007. Differential expression of HNK-1 and p75(NTR) in adult canine Schwann cells and olfactory ensheathing cells in situ but not in vitro. *J Comp Neurol* 505:572-585.
- Boruch AV, Connors JJ, Pipitone M, Deadwyler G, Storer PD, Devries GH, Jones KJ. 2001. Neurotrophic and migratory properties of an olfactory ensheathing cell line. *Glia* 33:225-229.
- Boyd JG, Jahed A, McDonald TG, Krol KM, Van Eyk JE, Doucette R, Kawaja MD. 2006. Proteomic evaluation reveals that olfactory ensheathing cells but not Schwann cells express calponin. *Glia* 53:434-440.
- Boyd JG, Lee J, Skihar V, Doucette R, Kawaja MD. 2004. LacZ-expressing olfactory ensheathing cells do not associate with myelinated axons after implantation into the compressed spinal cord. *Proc Natl Acad Sci USA* 101:2162-2166.
- Boyd JG, Skihar V, Kawaja M, Doucette R. 2003. Olfactory ensheathing cells: historical perspective and therapeutic potential. *Anat Rec B New Anat* 271:49-60.
- Bretzner F, Liu J, Currie E, Roskams AJ, Tetzlaff W. 2008. Undesired effects of a combinatorial treatment for spinal cord injury - transplantation of olfactory ensheathing cells and BDNF infusion to the red nucleus. *Eur J Neurosci* 28:1795-1807.
- Bryant SJ, Anseth KS. 2002. Hydrogel properties influence ECM production by chondrocytes photoencapsulated in poly(ethylene glycol) hydrogels. *J Biomed Mater Res* 59:63-72.

- Bryant SJ, Nuttelman CR, Anseth KS. 2000. Cytocompatibility of UV and visible light photoinitiating systems on cultured NIH/3T3 fibroblasts in vitro. *J Biomater Sci Polym Ed* 11:439-457.
- Bunge MB, Pearse DD. 2003. Transplantation strategies to promote repair of the injured spinal cord. *J Rehabil Res Dev* 40:55-62.
- Burden S, Yarden Y. 1997. Neuregulins and their receptors: a versatile signaling module in organogenesis and oncogenesis. *Neuron* 18:847-855.
- Burdick JA, Anseth KS. 2002. Photoencapsulation of osteoblasts in injectable RGD-modified PEG hydrogels for bone tissue engineering. *Biomaterials* 23:4315-4323.
- Carr VM, Farbman AI. 1993. The dynamics of cell death in the olfactory epithelium. *Exp Neurol* 124:308-314.
- Cerutti PA. 1985. Prooxidant states and tumor promotion. *Science* 227:375-381.
- Cheng H, Cao Y, Olson L. 1996. Spinal cord repair in adult paraplegic rats: partial restoration of hind limb function. *Science* 273:510-513.
- Chuah MI, Au C. 1991. Olfactory Schwann cells are derived from precursor cells in the olfactory epithelium. *J Neurosci Res* 29:172-180.
- Chuah MI, Cossins J, Woodhall E, Tennent R, Nash G, West AK. 2000. Glial growth factor 2 induces proliferation and structural changes in ensheathing cells. *Brain Res* 857:265-274.
- Chuah MI, Teague R. 1999. Basic fibroblast growth factor in the primary olfactory pathway: mitogenic effect on ensheathing cells. *Neuroscience* 88:1043-1050.
- Chuah MI, Tennent R, Jacobs I. 1995. Response of olfactory Schwann cells to intranasal zinc sulfate irrigation. *J Neurosci Res* 42:470-478.
- Davis KA, Burdick JA, Anseth KS. 2003. Photoinitiated crosslinked degradable copolymer networks for tissue engineering applications. *Biomaterials* 24:2485-2495.
- Deumens R, Koopmans GC, Honig WM, Maquet V, Jerome R, Steinbusch HW, Joosten EA. 2006. Chronically injured corticospinal axons do not cross large spinal lesion gaps after a multifactorial transplantation strategy using olfactory ensheathing cell/olfactory nerve fibroblast-biomatrix bridges. *J Neurosci Res* 83:811-820.
- Devon R, Doucette R. 1992. Olfactory ensheathing cells myelinate dorsal root ganglion neurites. *Brain Res* 589:175-179.

- Donato. 1999. Functional roles of S100 proteins, calcium-binding proteins of the EF-hand type. *Biochim Biophys Acta* 1450:191-231.
- Doucette JR, Kiernan JA, Flumerfelt BA. 1983. The re-innervation of olfactory glomeruli following transection of primary olfactory axons in the central or peripheral nervous system. *J Anat* 137:1-19.
- Doucette R, Devon R. 1995. Elevated intracellular levels of cAMP induce olfactory ensheathing cells to express GAL-C and GFAP but not MBP. *Glia* 13:130-140.
- Doucette R. 1990. Glial influences on axonal growth in the primary olfactory system. *Glia* 3:433-449.
- Doucette R. 1991. PNS-CNS transitional zone of the first cranial nerve. *J Comp Neurol* 312:451-466.
- Doucette R. 1993. Glial cells in the nerve fiber layer of the main olfactory bulb of embryonic and adult mammals. *Microsc Res Tech* 24:113-130.
- Doucette R. 1993. Glial progenitor cells of the nerve fiber layer of the olfactory bulb: effect of astrocyte growth media. *J Neurosci Res* 35:274-287.
- Doucette R. 1996. Immunohistochemical localization of laminin, fibronectin and collagen type IV in the nerve fiber layer of the olfactory bulb. *Int J Dev Neurosci* 14:945-959.
- Duncan ID, Hammang JP, Jackson KF, Wood PM, Bunge RP, Langford L. 1988. Transplantation of oligodendrocytes and Schwann cells into the spinal cord of the myelin-deficient rat. *J Neurocytol* 17:351-360.
- Dunning MD, Lakatos A, Loizou L, Kettunen M, French-Constant C, Brindle KM, Franklin RJ. 2004. Superparamagnetic iron oxide-labeled Schwann cells and olfactory ensheathing cells can be traced in vivo by magnetic resonance imaging and retain functional properties after transplantation into the CNS. *J Neurosci* 24:9799-9810.
- Farbman AI. 1994. The cellular basis of olfaction. *Endeavour* 18:2-8.
- Fedorovich NE, Oudshoorn MH, van Geemen D, Hennink WE, Alblas J, Dhert WJ. 2009. The effect of photopolymerization on stem cells embedded in hydrogels. *Biomaterials* 30:344-353.
- Franklin RJ, Gilson JM, Franceschini IA, Barnett SC. 1996. Schwann cell-like myelination following transplantation of an olfactory bulb-ensheathing cell line into areas of demyelination in the adult CNS. *Glia* 17:217-224.

- Franssen EH, de Bree FM, Verhaagen J. 2007. Olfactory ensheathing glia: their contribution to primary olfactory nervous system regeneration and their regenerative potential following transplantation into the injured spinal cord. *Brain Res Rev* 56:236-258.
- Gall CM, Berschauer R, Isackson PJ. 1994. Seizures increase basic fibroblast growth factor mRNA in adult rat forebrain neurons and glia. *Brain Res Mol Brain Res* 21:190-205.
- Gan Q, Yoshida T, Li J, Owens GK. 2007. Smooth muscle cells and myofibroblasts use distinct transcriptional mechanisms for smooth muscle alpha-actin expression. *Circ Res* 101:883-892.
- Gautier SE, Oudega M, Frago M, Chapon P, Plant GW, Bunge MB, Parel JM. 1998. Poly(alpha-hydroxyacids) for application in the spinal cord: resorbability and biocompatibility with adult rat Schwann cells and spinal cord. *J Biomed Mater Res* 42:642-654.
- Gong Q, Bailey MS, Pixley SK, Ennis M, Liu W, Shipley MT. 1994. Localization and regulation of low affinity nerve growth factor receptor expression in the rat olfactory system during development and regeneration. *J Comp Neurol* 344:336-348.
- Graziadei GA, Graziadei PP. 1979b. Neurogenesis and neuron regeneration in the olfactory system of mammals. II. Degeneration and reconstitution of the olfactory sensory neurons after axotomy. *J Neurocytol* 8:197-213.
- Graziadei PP, Graziadei GA. 1979a. Neurogenesis and neuron regeneration in the olfactory system of mammals. I. Morphological aspects of differentiation and structural organization of the olfactory sensory neurons. *J Neurocytol* 8:1-18.
- Hulsebosch CE. 2002. Recent advances in pathophysiology and treatment of spinal cord injury. *Adv Physiol Educ* 26:238-255.
- Hunziker EB. 2002. Articular cartilage repair: basic science and clinical progress. A review of the current status and prospects. *Osteoarthritis Cartilage* 10:432-463.
- Imaizumi T, Lankford KL, Burton WV, Fodor WL, Kocsis JD. 2000. Xenotransplantation of transgenic pig olfactory ensheathing cells promotes axonal regeneration in rat spinal cord. *Nat Biotechnol* 18:949-953.
- Imaizumi T, Lankford KL, Waxman SG, Greer CA, Kocsis JD. 1998. Transplanted olfactory ensheathing cells remyelinate and enhance axonal conduction in the demyelinated dorsal columns of the rat spinal cord. *J Neurosci* 18:6176-6185.

Jahed A, Rowland JW, McDonald T, Boyd JG, Doucette R, Kawaja MD. 2007. Olfactory ensheathing cells express smooth muscle alpha-actin in vitro and in vivo. *J Comp Neurol* 503:209-223.

Kawaja MD, Boyd JG, Smithson LJ, Jahed A, Doucette R. 2009. Technical strategies to isolate olfactory ensheathing cells for intraspinal implantation. *J Neurotrauma* 26:155-177.

Key B, Treloar HB, Wangerek L, Ford MD, Nurcombe V. 1996. Expression and localization of FGF-1 in the developing rat olfactory system. *J Comp Neurol* 366:197-206.

Kliot M, Smith GM, Siegal JD, Silver J. 1990. Astrocyte-polymer implants promote regeneration of dorsal root fibers into the adult mammalian spinal cord. *Exp Neurol* 109:57-69.

Kott JN, Westrum LE, Raines EW, Sasahara M, Ross R. 1994. Olfactory ensheathing glia and platelet-derived growth factor B-chain reactivity in the transplanted rat olfactory bulb. *Int J Dev Neurosci* 12:315-323.

Krudewig C, Deschl U, Wewetzer K. 2006. Purification and in vitro characterization of adult canine olfactory ensheathing cells. *Cell Tissue Res* 326:687-696.

Lakatos A, Barnett SC, Franklin RJ. 2003. Olfactory ensheathing cells induce less host astrocyte response and chondroitin sulphate proteoglycan expression than Schwann cells following transplantation into adult CNS white matter. *Exp Neurol* 184:237-246.

Lecain E, Alliot F, Laine MC, Calas B, Pessac B. 1991. Alpha isoform of smooth muscle actin is expressed in astrocytes in vitro and in vivo. *J Neurosci Res* 28:601-606.

Lee MJ, Calle E, Brennan A, Ahmed S, Sviderskaya E, Jessen KR, Mirsky R. 2001. In early development of the rat mRNA for the major myelin protein P(0) is expressed in nonsensory areas of the embryonic inner ear, notochord, enteric nervous system, and olfactory ensheathing cells. *Dev Dyn* 222:40-51.

Lemmon V, Farr KL, Lagenaur C. 1989. L1-mediated axon outgrowth occurs via a hemophilic binding mechanism. *Neuron* 2:1597-1603.

Li Y, Field PM, Raisman G. 2005. Olfactory ensheathing cells and olfactory nerve fibroblasts maintain continuous open channels for regrowth of olfactory nerve fibres. *Glia* 52:245-251.

Lima C, Escada P, Pratas-Vital J, Branco C, Arcangeli CA, Lazzeri G, Maia CA, Capucho C, Hasse-Ferreira A, Peduzzi JD. 2010. Olfactory mucosal autografts and

rehabilitation for chronic traumatic spinal cord injury. *Neurorehabil Neural Repair* 24:10-22.

Lima C, Pratas-Vital J, Escada P, Hasse-Ferreira A, Capucho C, Peduzzi JD. 2006. Olfactory mucosa autografts in human spinal cord injury: a pilot clinical study. *J Spinal Cord Med* 29:191-206.

Lipson AC, Widenfalk J, Lindqvist E, Ebendal T, Olson L. 2003. Neurotrophic properties of olfactory ensheathing glia. *Exp Neurol* 180:167-171.

Lu J, Feron F, Ho SM, Mackay-Sim A, Waite PM. 2001. Transplantation of nasal olfactory tissue promotes partial recovery in paraplegic adult rats. *Brain Res* 889:344-357.

Lu J, Feron F, Mackay-Sim A, Waite PM. 2002. Olfactory ensheathing cells promote locomotor recovery after delayed transplantation into transected spinal cord. *Brain* 125:14-21.

Lu P, Yang H, Culbertson M, Graham L, Roskams AJ, Tuszynski MH. 2006. Olfactory ensheathing cells do not exhibit unique migratory or axonal growth-promoting properties after spinal cord injury. *J Neurosci* 26:11120-11130.

Mahanthappa NK, Cooper DN, Barondes SH, Schwarting GA. 1994. Rat olfactory neurons can utilize the endogenous lectin, L-14, in a novel adhesion mechanism. *Development* 120:1373-1384.

Martin D, Robe P, Franzen R, Delree P, Schoenen J, Stevenaert A, Moonen G. 1996. Effects of Schwann cell transplantation in a contusion model of rat spinal cord injury. *J Neurosci Res* 45:588-597.

Miragall F, Kadmon G, Husmann M, Schachner M. 1988. Expression of cell adhesion molecules in the olfactory system of the adult mouse: presence of the embryonic form of N-CAM. *Dev Biol* 129:516-531.

Miragall F, Kadmon G, Schachner M. 1989. Expression of L1 and N-CAM cell adhesion molecules during development of the mouse olfactory system. *Dev Biol* 135:272-286.

Monard D, Solomon F, Rentsch M, Gysin R. 1973. Glia-induced morphological differentiation in neuroblastoma cells. *Proc Natl Acad Sci USA* 70:1894-1897.

Montgomery CT, Tenaglia EA, Robson JA. 1996. Axonal growth into tubes implanted within lesions in the spinal cords of adult rats. *Exp Neurol* 137:277-290.

- Monti Graziadei GA, Graziadei PPC. 1978. Neurogenesis and neuron regeneration in the olfactory system of mammals. II. Degeneration and reconstitution of the olfactory sensory neurons after axotomy. *J Neurocytol* 8:197-213.
- Nguyen KT, West JL. 2002. Photopolymerizable hydrogels for tissue engineering applications. *Biomaterials* 23:4307-4314.
- Nieke J, Schachner M. 1985. Expression of the neural cell adhesion molecules L1 and N-CAM and their common carbohydrate epitope L2/HNK-1 during development and after transection of the mouse sciatic nerve. *Differentiation* 30:141-151.
- Oudega M, Gautier SE, Chapon P, Fragoso M, Bates ML, Parel JM, Bunge MB. 2001. Axonal regeneration into Schwann cell grafts within resorbable poly(alpha-hydroxyacid) guidance channels in the adult rat spinal cord. *Biomaterials* 22:1125-1136.
- Pearse DD, Barakat DJ. 2006. Cellular repair strategies for spinal cord injury. *Expert Opin Biol Ther* 6:639-652.
- Pearse DD, Pereira FC, Marcillo AE, Bates ML, Berrocal YA, Filbin MT, Bunge MB. 2004. cAMP and Schwann cells promote axonal growth and functional recovery after spinal cord injury. *Nat Med* 10:610-616.
- Pearse DD, Sanchez AR, Pereira FC, Andrade CM, Puzis R, Pressman Y, Golden K, Kitay BM, Blits B, Wood PM, Bunge MB. 2007. Transplantation of Schwann cells and/or olfactory ensheathing glia into the contused spinal cord: Survival, migration, axon association, and functional recovery. *Glia* 55:976-1000.
- Perroteau I, Oberto M, Ieraci A, Bovolin P, Fasolo A. 1998. ErbB-3 and ErbB-4 expression in the mouse olfactory system. *Ann N Y Acad Sci* 855:255-259.
- Plant GW, Christensen CL, Oudega M, Bunge MB. 2003. Delayed transplantation of olfactory ensheathing glia promotes sparing/regeneration of supraspinal axons in the contused adult rat spinal cord. *J Neurotrauma* 20:1-16.
- Pollock GS, Franceschini IA, Graham G, Marchionni MA, Barnett SC. 1999. Neuregulin is a mitogen and survival factor for olfactory bulb ensheathing cells and an isoform is produced by astrocytes. *Eur J Neurosci* 11:769-780.
- Radtke C, Akiyama Y, Brokaw J, Lankford KL, Wewetzer K, Fodor WL, Kocsis JD. 2004. Remyelination of the nonhuman primate spinal cord by transplantation of H-transferase transgenic adult pig olfactory ensheathing cells. *FASEB J* 18:335-337.
- Radtke C, Lankford KL, Wewetzer K, Imaizumi T, Fodor WL, Kocsis JD. 2010. Impaired spinal cord remyelination by long-term cultured adult porcine olfactory

ensheathing cells correlates with altered in vitro phenotypic properties. *Xenotransplantation* 17:71-80.

Ramon-Cueto A, Cordero MI, Santos-Benito FF, Avila J. 2000. Functional recovery of paraplegic rats and motor axon regeneration in their spinal cords by olfactory ensheathing glia. *Neuron* 25:425-435.

Ramon-Cueto A, Perez J, Nieto-Sampedro M. 1993. In vitro enfolding of olfactory neurites by p75 NGF receptor positive ensheathing cells from adult rat olfactory bulb. *Eur J Neurosci* 5:1172-1180.

Ramon-Cueto A, Plant GW, Avila J, Bunge MB. 1998. Long-distance axonal regeneration in the transected adult rat spinal cord is promoted by olfactory ensheathing glia transplants. *J Neurosci* 18:3803-3815.

Reier PJ, Houle JD, Jakeman L, Winialski D, Tessler A. 1988. Transplantation of fetal spinal cord tissue into acute and chronic hemisection and contusion lesions of the adult rat spinal cord. *Prog Brain Res* 78:173-179.

Reier PJ. 2004. Cellular transplantation strategies for spinal cord injury and translational neurobiology. *NeuroRx* 1:424-451.

Reinhard E, Meier R, Halfter W, Rovelli G, Monard D. 1988. Detection of glia-derived nexin in the olfactory system of the rat. *Neuron* 1:387-394.

Richter M, Westendorf K, Roskams AJ. 2008. Culturing olfactory ensheathing cells from the mouse olfactory epithelium. *Methods Mol Biol* 438:95-102.

Rizek PN, Kawaja MD. 2006. Cultures of rat olfactory ensheathing cells are contaminated with Schwann cells. *Neuroreport* 17:459-462.

Rohm B, Ottemeyer A, Lohrum M, Puschel AW. 2000. Plexin/neuropilin complexes mediate repulsion by the axonal guidance signal semaphorin 3A. *Mech Dev* 93:95-104.

Rubio MP, Munoz-Quiles C, Ramon-Cueto A. 2008. Adult olfactory bulbs from primates provide reliable ensheathing glia for cell therapy. *Glia* 56:539-551.

Ruitenbergh MJ, Plant GW, Hamers FP, Wortel J, Blits B, Dijkhuizen PA, Gispen WH, Boer GJ, Verhaagen J. 2003. Ex vivo adenoviral vector-mediated neurotrophin gene transfer to olfactory ensheathing glia: effects on rubrospinal tract regeneration, lesion size, and functional recovery after implantation in the injured rat spinal cord. *J Neurosci* 23:7045-7058.

- Sasaki M, Honmou O, Akiyama Y, Uede T, Hashi K, Kocsis JD. 2001. Transplantation of an acutely isolated bone marrow fraction repairs demyelinated adult rat spinal cord axons. *Glia* 35:26-34.
- Sasaki M, Lankford KL, Zemedkun M, Kocsis JD. 2004. Identified olfactory ensheathing cells transplanted into the transected dorsal funiculus bridge the lesion and form myelin. *J Neurosci* 24:8485-8493.
- Schildmeyer LA, Braun R, Taffet G, Debiase M, Burns AE, Bradley A, Schwartz RJ. 2000. Impaired vascular contractility and blood pressure homeostasis in the smooth muscle alpha-actin null mouse. *FASEB J* 14:2213-2220.
- Schwartz GA, Kostek C, Ahmad N, Dibble C, Pays L, Puschel AW. 2000. Semaphorin 3A is required for guidance of olfactory axons in mice. *J Neurosci* 20:7691-7697.
- Seiger A. 1989. Collection and use of fetal central nervous system tissue. *Fetal Ther* 4:104-107.
- Silver J, Ogawa MY. 1983. Postnatally induced formation of the corpus callosum in acallosal mice on glia-coated cellulose bridges. *Science* 220:1067-1069.
- Smith PM, Sim FJ, Barnett SC, Franklin RJ. 2001. SCIP/Oct-6, Krox-20, and desert hedgehog mRNA expression during CNS remyelination by transplanted olfactory ensheathing cells. *Glia* 36:342-353.
- Smithson LJ, Kawaja MD. 2009. A comparative examination of biomarkers for olfactory ensheathing cells in cats and guinea pigs. *Brain Res* 1284:41-53.
- Sommer I, Schachner M. 1981. Monoclonal antibodies (O1 to O4) to oligodendrocyte cell surfaces: an immunocytological study in the central nervous system. *Dev Biol* 83:311-327.
- Sukarto A, Amsden BG. 2012. Low melting point amphiphilic microspheres for delivery of bone morphogenetic protein-6 and transforming growth factor- $\beta$ 3 in a hydrogel matrix. *J Control Release* 158:53-62.
- Takahashi S, Iwanaga T, Takahashi Y, Nakano Y, Fujita T. 1984. Neuron-specific enolase, neurofilament protein and S-100 protein in the olfactory mucosa of human fetuses. An immunohistochemical study. *238:231-234*.
- Takami T, Oudega M, Bates ML, Wood PM, Kleitman N, Bunge MB. 2002. Schwann cell but not olfactory ensheathing glia transplants improve hindlimb locomotor performance in the moderately contused adult rat thoracic spinal cord. *J Neurosci* 22:6670-6681.

- Techangamsuwan S, Imbschweiler I, Kreutzer R, Kreutzer M, Baumgartner W, Wewetzer K. 2008. Similar behaviour and primate-like properties of adult canine Schwann cells and olfactory ensheathing cells in long-term culture. *Brain Res* 1240:31-38.
- Techangamsuwan S, Kreutzer R, Kreutzer M, Imbschweiler I, Rohn K, Wewetzer K, Baumgartner W. 2009. Transfection of adult canine Schwann cells and olfactory ensheathing cells at early and late passage with human TERT differentially affects growth factor responsiveness and in vitro growth. *J Neurosci Methods* 176:112-120.
- Tennent R, Chuah MI. 1996. Ultrastructural study of ensheathing cells in early development of olfactory axons. *Brain Res Dev Brain Res* 95:135-139.
- Terakado M, Yamazaki M, Tsujimoto Y, Kawashima T, Nagashima K, Ogawa J, Fujita Y, Sugiya H, Sakai T, Furuyama S. 1984. Lipid peroxidation as a possible cause of benzoyl peroxide toxicity in rabbit dental pulp – a microsomal lipid peroxidation in vitro. *J Dent Res* 63:901-905.
- Tomasek JJ, Haaksma CJ, Schwartz RJ, Vuong DT, Zhang SX, Ash JD, Ma JX, Al-Ubaidi MR. 2006. Deletion of smooth muscle alpha-actin alters blood-retina barrier permeability and retinal function. *Invest Ophthalmol Vis Sci* 47:2693-2700.
- Turner CP, Perez-Polo JR. 1992. Regulation of the low affinity receptor for nerve growth factor, p75NGFR, in the olfactory system of neonatal and adult rat. *Int J Dev Neurosci* 10:343-359.
- Ubink R, Halasz N, Zhang X, Dagerlind A, Hokfelt T. 1994. Neuropeptide tyrosine is expressed in ensheathing cells around the olfactory nerves in the rat olfactory bulb. *Neuroscience* 60:709-726.
- Ubink R, Hokfelt T. 2000. Expression of neuropeptide Y in olfactory ensheathing cells during prenatal development. *J Comp Neurol* 423:13-25.
- Valverde F, Santacana M, Heredia M. 1992. Formation of an olfactory glomerulus: morphological aspects of development and organization. *Neuroscience* 49:255-275.
- Vartanian T, Fischbach G, Miller R. 1999. Failure of spinal cord oligodendrocyte development in mice lacking neuregulin. *Proc Natl Acad Sci USA* 96:731-735.
- Vickland H, Westrum LE, Kott JN, Patterson SL, Bothwell MA. 1991. Nerve growth factor receptor expression in the young and adult rat olfactory system. *Brain Res* 565:269-279.
- Vincent AJ, West AK, Chuah MI. 2003. Morphological plasticity of olfactory ensheathing cells is regulated by cAMP and endothelin-1. *Glia* 41:393-403.

Vincent AJ, West AK, Chuah MI. 2005. Morphological and functional plasticity of olfactory ensheathing cells. *J Neurocytol* 34:65-80.

Vracko R. 1974. Basal lamina scaffold-anatomy and significance for maintenance of orderly tissue structure. *Am J Pathol* 77:314-346.

Wewetzer K, Kern N, Ebel C, Radtke C, Brandes G. 2005. Phagocytosis of O4+ axonal fragments in vitro by p75-neonatal rat olfactory ensheathing cells. *Glia* 49:577-587.

Williams CG, Malik AN, Kim TK, Manson PN, Elisseeff JH. 2005. Variable cytocompatibility of six cell lines with photoinitiators used for polymerizing hydrogels and cell encapsulation. *Biomaterials* 26:1211-1218.

Woerly S. 2000. Restorative surgery of the central nervous system by means of tissue engineering using NeuroGel implants. *Neurosurg Rev* 23:59-79.

Woodhall E, West AK, Chuah MI. 2001. Cultured olfactory ensheathing cells express nerve growth factor, brain-derived neurotrophic factor, glia cell line-derived neurotrophic factor and their receptors. *Brain Res Mol Brain Res* 88:203-213.

Xu XM, Guenard V, Kleitman N, Bunge MB. 1995. Axonal regeneration into Schwann cell-seeded guidance channels grafted into transected adult rat spinal cord. *J Comp Neurol* 351:145-160.

Xu XM, Zhang SX, Li H, Aebischer P, Bunge MB. 1999. Regrowth of axons into the distal spinal cord through a Schwann-cell-seeded mini-channel implanted into hemisectioned adult rat spinal cord. *Eur J Neurosci* 11:1723-1740.

Yamasaki M, Yamada K, Furuya S, Mitoma J, Hirabayashi Y, Watanabe M. 2001. 3-Phosphoglycerate dehydrogenase, a key enzyme for L-serine biosynthesis, is preferentially expressed in the radial glia/astrocyte lineage and olfactory ensheathing glia in the mouse brain. *J Neurosci* 21:7691-7704.

Yan H, Bunge MB, Wood PM, Plant GW. 2001. Mitogenic response of adult rat olfactory ensheathing glia to four growth factors. *Glia* 33:334-342.

Zhou Q, Cummings RD. 1993. L-14 lectin recognition of laminin and its promotion of in vitro cell adhesion. *Arch Biochem Biophys* 300:6-17.